SERPINA3N ACCELERATES WOUND CLOSURE IN A MURINE MODEL OF DIABETIC WOUND HEALING

by

Chiao-Wen Ivy Hsu

B.Sc. (Honours), The University of Toronto, 2012

A THESIS SUBMITTED IN PARTIAL FULFILLMENT OF

THE REQUIREMENTS FOR THE DEGREE OF

MASTER OF SCIENCE

in

THE FACULTY OF GRADUATE AND POSTDOCTORAL STUDIES

(Pathology and Laboratory Medicine)

THE UNIVERSITY OF BRITISH COLUMBIA

(Vancouver)

September 2014

Abstract

Chronic, non-healing wounds are a major complication of diabetes and are characterized by chronic inflammation and excessive protease activity. While once thought to function primarily as a pro-apoptotic serine protease, granzyme B (GzmB) can also accumulate in the extracellular matrix during chronic inflammation and cleave extracellular matrix (ECM) proteins that are essential for proper wound healing, including fibronectin. We hypothesized that GzmB contributes to the pathogenesis of impaired diabetic wound healing through excessive degradation of the ECM.

In the first part of the thesis, we demonstrated that the majority of GzmB was secreted by mast cells and localized in the wound edges and granulation tissues of completely reepithelialized diabetic mouse wounds at higher levels. Subsequently, we observed that GzmB induced detachment of mouse embryonic fibroblasts and also showed that co-incubation with a mouse serine protease inhibitor, serpina3n (SA3N), abrogated this effect. Finally, we administered SA3N to diabetic mouse wounds and found that wound closure including both reepithelialization and contraction were significantly increased in wounds treated with SA3N. Histological and immunohistochemical analyses of the SA3N-treated wounds revealed a more mature, proliferative granulation tissue phenotype as indicated by increased cells with proliferative activity, vascularization, contractile myofibroblasts, as well as collagen deposition in remodeling tissues. Skin homogenates from SA3N-treated wounds also exhibited greater levels of full-length intact fibronectin when compared to control wounds.

In summary, our findings suggested that GzmB contributes to the pathogenesis of diabetic wound healing through the proteolytic cleavage of fibronectin that are essential for normal wound closure, and that inhibition of GzmB can promote granulation tissue maturation

and collagen deposition. These results offer preliminary evidence that a GzmB inhibitor may be a relevant therapeutic target in wound management therapy.

Preface

- Ivy Hsu and Dr. David J Granville were responsible for identifying and designing the hypothesis and specific aims of this thesis.
- Ivy Hsu performed all the animal studies (including wound healing surgeries and tissue collections), histological and immunohistochemical stainings, fibronectin cleavage assays, skin homogenizations and western blots.
- Kathryn Westendorf assisted with mouse granzyme B activity assays.
- Leigh Parkinson assisted with mouse embryonic fibroblast detachment assays.
- Amrit Samra assisted with Masson's trichrome histology stainings.
- Hongyan Zhao assisted with tissue processing and histological and immunohistochemical stainings.
- Ivy Hsu performed all the wound pictures, histological and immunohistochemical analyses, and statistical analyses.
- Tyler Brown assisted with wound picture analyses and Ki67 positive counts.
- All the writing was done by Ivy Hsu.
- In chapter 1:

  1) Figure 1A (the hematoxylin and eosin staining of human skin) was obtained with permission from the David F. Hardwick Pathology Learning Centre 'The Virtual Collections.'

  2) Figures 2, 3, 4 and Table 1 were adapted with permission from "Granzyme B in injury, inflammation and repair" by Hiebert PR and Granville DJ (*Trends Mol Med*. 2012 Dec;18(12):732-41).

3) Figure 5 was adapted from permission from “Intracellular versus extracellular granzyme B in immunity and disease: challenging the dogma” by Boivin WA, Cooper DM, Hiebert PR and Granville DJ (*Lab Invest*. 2009 Nov;89(11):1195-220).

- For all chapters, portions of the text contain contents from a manuscript titled “Serpina3n accelerates tissue repair in a diabetic mouse model of delayed wound healing” and numbered CDDIS-14-0084 that has been accepted for publication by *Cell Death and Disease* on August 28, 2014.
- The animal studies were conducted in accordance with the procedure guidelines approved by the University of British Columbia Animal Care Committee under protocol and certificate number A13-0001.

Table of Contents

List of Tables

List of Figures

List of Abbreviations

α-SMA	alpha smooth muscle actin
AAA	abdominal aortic aneurysm
COPD	chronic obstructive pulmonary disease
CTL	cytotoxic T lymphocyte
D	dermis
DNA	deoxyribonucleic acid
E	epidermis
ECM	extracellular matrix
ED	extra domain
EGF	epidermal growth factor
FGFR-1	fibroblast growth factor receptor-1
FN	fibronectin
GAG	glycosaminoglycan
GAPDH	glyceraldehyde 3-phosphate dehydrogenase
gtBid	granzyme B-truncated product
Gzm	granzyme
H	hypodermis
H&E	hematoxylin and eosin
HF	hair follicles
IL	interleukin
MCL-1	myeloid cell leukemia sequence-1
MMP	matrix metalloproteinase

NAR	nicotinic acetylcholine receptor
NGR	neuronal glutamate receptor
NK	natural killer
PBS	phosphate buffered saline
PC	panniculus carnosus
PDGF	platelet derived growth factor
PG	proteoglycans
PI-9	protease inhibitor-9
RA	rheumatoid arthritis
RGD	Arginine-Glycine-Aspartic Acid
RR	rete ridges
SA3N	serpina3n
SDS	sodium dodecyl sulphate
SFM	serum free media
SG	sebaceous glands
SMC	smooth muscle cells
TBS	Tris-buffered saline
TBST	Tris-buffered saline-Tween 20
TGF	transforming growth factor
TIMP	tissue inhibitors of metalloproteinase
VEGF	vascular endothelial growth factor
vWf	von Willebrand factor

Acknowledgements

Thank you to everyone who shared this experience as a graduate student with me.

Firstly, I would like to thank my supervisor, Dr. David Granville, for being such a supportive mentor. I am fortunate to have worked under his tutelage and to have had the opportunity to tackle this interesting project. Without the company of all the past and present members of the Granville Lab, my days in the lab could not have been more enjoyable. It has been an honor to work alongside all of you. In particular, thank you to Dr. Leigh Parkinson, Dr. Steve Shen and Hongyan Zhao for their patience and encouragement, especially during times when I struggled and needed the most motivation.

I would also like to thank my committee members, Dr. Tillie Hackett, Dr. Honglin Luo and Dr. Decheng Yang for all of their advice and constructive feedback. All of the animal work in this project would not have been possible without the assistance of the personnel from the Genetically Engineered Models facility, including Tatjana Bozin, Lynne Carter, Lubos Bohunek and Claire Smits as well as the help from Dean English. I would like to also take the opportunity to acknowledge the extensive training I received from the CIHR Skin Research Training Centre, and to thank Dr. Harvey Lui and Leanne Li for their constant guidance during my role as the Chief Scholar there.

I would like to acknowledge all the friends that cheered me on through the ups and downs of graduate school. A special thank you to Tracee Wee who, despite her busy schedule, always found time to munch on some hearty Thai food with me.

Lastly, thank you Nicholas, for being there, always. You are my rock and my inspiration. It is a blessing to be sharing this special journey with you.

Dedication

I dedicate this work to my family – my parents, siblings (Wendy, Annie, Amy, Peter) and grandparents. This degree could not have been completed without the unconditional support and words of wisdom from all of you. A special dedication to Amy who have been so patient with me throughout the entire process.

Chapter 1: Introduction

1.1 Skin

The skin is the largest organ of the human body and is composed of three layers – the epidermis, dermis and hypodermis (1). The primary function of the skin is to act as a physical protective barrier to a hostile external environment. However, additional functions include regulating body temperature, synthesizing vitamin D and relaying sensory information. Therefore, any injury to the skin should be repaired.

1.1.1 Anatomy of the skin

The epidermis is the outermost layer of the skin and contains mostly keratinocytes with a scattering of Langerhans cells, melanocytes and Merkel cells in between (1). The epidermis can be described as being a multi-layer of keratinocytes. Specifically, the deepest layer of the epidermis or otherwise known as the stratum basale, contains basal keratinocytes, which are highly proliferative stem cells of the epidermis (1). As these stem cells divide, their daughter cells are pushed upward, enabling maturing keratinocytes to make up the middle layers of the epidermis including the stratum spinosum, stratum granulosum and stratum lucidum. As the keratinocytes migrate through the epidermal layers, they start to lose, structurally, their nuclei and organelles, and functionally, their proliferative potential (1). Finally, dead keratinocytes end up forming the most superficial layer, the stratum corneum, where they are eventually shed off (1).

The basement membrane divides the epidermis and dermis making up the so called dermal-epidermal junction. In particular, it tightly anchors the epidermis to the dermis below through type IV collagen, various glycoproteins and proteoglycans (PGs) such as laminin, fibronectin (FN), perlecan, and cell adhesion protein complexes (2). The dermis lies below the

epidermis and consists of connective tissues. It is largely supported by three main cell types, namely fibroblasts, macrophages and adipocytes, and various extracellular matrix (ECM) components including collagen, fibrous proteins and PGs (1). In addition, the dermis also contains accessory structures such as hair follicles, sebaceous and sweat glands, blood and lymphatic vessels and sensory nerves (1). The primary function of the dermis is to provide nourishment and support for the epidermis. Although the division is only subtle, the hypodermis is the subcutaneous layer of adipose tissues underneath the dermis, and mainly serves as an energy reservoir and body temperature regulator.

There are some differences between human and mouse skin and these are illustrated in Figure 1. As mice are considered to be loosely-skinned animals, they have an additional layer of striated muscles below the hypodermis known as the panniculus carnosus (PC) (3). This layer enables loosely-skinned animals to move their skin independent of attached muscle layers deeper below. In addition, in contrast to human skin, mouse skin does not have an obvious feature known as rete ridges (3). These rete ridges are epidermal invaginations arising from the stratum basale that extend deep into the dermis to increase the overall surface area of the dermal-epidermal junction.

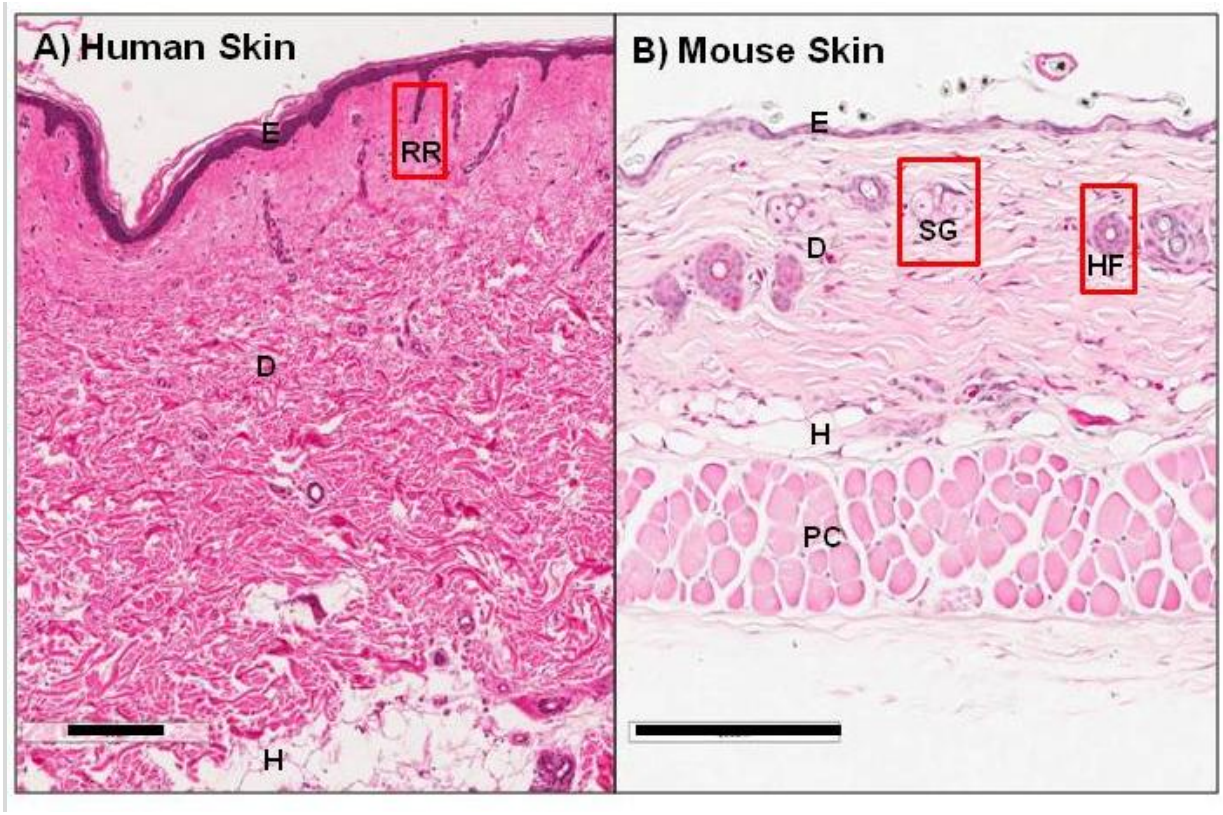

Figure 1 Anatomy of human and mouse skin. (A) Cross section of human abdomen stained with hematoxylin and eosin showing the three layers of skin: epidermis [E], dermis [D] and hypodermis [H]. The epidermis is largely made up of multi-layers of keratinocytes. The dermis is made up of mainly collagen supported by cell types including fibroblasts and macrophages. The dermis also contains accessory structures including sebaceous glands [SG] and hair follicles [HF] not shown here, but in the mouse skin. The hypodermis is the subcutaneous layer of adipose tissues. The human skin has obvious rete ridges [RR] that increase the surface area of the dermal-epidermal junction. **(B)** Cross section of mouse skin stained with hematoxylin and eosin showing again the three layers of skin: epidermis [E], dermis [D] with accessory structures and the hypodermis [H]. In addition to the three basic layers, mouse skin has an additional striated muscle layer known as the panniculus carnosus [PC] below the hypodermis. In addition, mouse skin has no obvious rete ridges. *[Scale bars = 200 μm]*

Note: The stained human skin section was obtained with permission from the David F. Hardwick Pathology Learning Centre 'The Virtual Collections.'

1.1.2 Extracellular matrix of the skin

Although the ECM was once believed to be a rather metabolically inert, non-cellular and purely structural part of skin tissue, this perception has been overturned (4). Instead, the ECM is now considered to be a metabolically active and dynamic component that is integral for proper tissue function (4). Specifically, the ECM of the skin not only provides the structural organizational framework for proper stability and elasticity, but also acts as a scaffold medium for cellular counterparts to perform their functions properly and effectively.

The ECM of the skin is largely composed of two classes of macromolecules, namely the fibrous proteins including collagen, elastic fiber, and cellular FN, and PGs including three main families of small leucine-rich PGs, modular PGs and cell-surface PGs (4,5).

The main fibrous protein in the skin is collagen, which is largely synthesized by surrounding fibroblasts. Although there are six main types of collagen, the major fiber-forming collagens of the skin are types I and III collagen (4). In addition to providing tensile strength, types I and III collagen also regulate cell adhesion, support cell migration and direct tissue remodeling (5). The collagen fibrils interact with elastin fibers to determine the extent of skin elasticity (4,5). The integrity of elastin fibers is supported by elastin, and covered with an acidic, cysteine-rich glycoprotein microfibrillar complex made up of fibrillins (6). Finally, cellular FN is a multi-functional glycoprotein that facilitates cell-matrix interactions, thus regulating cell attachment, differentiation, migration and signaling (5). FN can bind to many ECM components and cell-surface receptors such as collagen, fibrin, soluble heparin and integrin receptors (7).

The PGs are made from glycosaminoglycan (GAG) chains covalently linked to a protein core backbone (8). Specifically, the GAG chains are unbranched polysaccharide units with repeating disaccharide units that can be sulfated (8). The sulfated GAGs include chondroitin

sulfate, heparan sulfate and keratan sulfate, whereas the non-sulfated GAGs include hyaluronic acid (8). The GAGs are extremely hydrophilic, thus can absorb water to provide proper hydration and enable the skin to withstand high compressive forces (5). The small-leucine rich PGs such as decorin, biglycan and betaglycan are mostly involved in cell signaling pathways through binding to growth factor receptors (9,10). The modular PGs, such as serglycin, modulate cell adhesion, migration and proliferation (11). The cell-surface PGs, such as syndecan, mainly act as co-receptors and have also been shown to facilitate cell adhesion, migration and proliferation (12).

The ECM also acts as a storage reservoir for various cytokines and growth factors, including interleukin-1 beta (IL-1β), epidermal growth factor (EGF) and transforming growth factor beta (TGF-β) (13-15). The local cytokines and growth factors can be released and activated when the ECM is altered by proteases and much research has focused on the large family of metalloendopeptidases known as the matrix metalloproteinases (MMPs) (13-15). There are 23 human MMPs that have been identified and these are divided into collagenases, gelatinases, stromelysins, matrilysins and membrane-type MMPs based on structural similarity and functional specificity (13,16). As MMPs are considered to be the major mediator of the ECM, their activities are strictly regulated. The tissue inhibitors of metalloproteinases (TIMPs) and plasma protease inhibitors, such as α1-antitrypsin and α2-macroglobulin, are all capable of inhibiting MMPs, thus ensuring that there is a perfect dynamic reciprocity between the cell, ECM and everything in between for tissue homeostasis (16,17).

1.2 Cutaneous wound healing

When adult skin sustains an injury, any physical and functional damages are repaired through a process known as cutaneous wound healing. This process is complex and dynamic, and

involves four overlapping sequential phases: hemostasis, inflammation, granulation tissue formation and tissue remodeling. However, due to the formation of scars as an end result, cutaneous wound healing does not fully restore the adult skin's original structure and function. In contrast, fetal skin regenerates itself when injured, rather than repairing itself as adult skin does (18). Since regeneration does not leave scars, it restores the normal structure and function of fetal skin back to its original state (18).

1.2.1 Physiology of acute wound healing

As soon as the skin is wounded and blood vessels are damaged, platelets begin to aggregate and the intrinsic coagulation cascade is activated to restore hemostasis. A fibrin plug predominantly consisting of polymerized fibrinogen and plasma FN is formed for immediate wound coverage to temporarily halt blood loss, trap foreign pathogens and provide structural support for invading cells (19). During this phase of hemostasis, platelets release pro-inflammatory growth factors, such as EGF, platelet-derived growth factor (PDGF) and transforming growth factor alpha (TGF-α), that all act as chemoattractants to recruit inflammatory cells (20,21).

In the inflammatory phase, neutrophils and macrophages sequentially infiltrate the wound site by chemotaxis, transmigration and diapedesis (22). Neutrophils are mainly involved in wound debridement through phagocytosing foreign particles, debris and damaged ECM components. In addition to general wound debridement of foreign particles, debris, damaged ECM components and neutrophils, macrophages also secrete various cytokines and growth factors, such as IL-1, TGF-β and vascular endothelial growth factor (VEGF), to promote fibroplasias, angiogenesis and ECM deposition for granulation tissue formation (23).

As the inflammatory response dampens, the fibrin plug is eventually replaced with provisional matrix that forms the majority of the granulation tissue. The composition of granulation tissue includes cells such as fibroblasts, macrophages, endothelial cells and neovessels, as well as a structural provisional matrix made of collagen, glycoproteins and PGs. In particular, macrophages and granules of mast cells provide signals, including PDGF, TGF-β and VEGF, required for fibroblasts to proliferate and deposit type III collagen and ECM proteins including FN, and for endothelial cells to stimulate angiogenesis (23,24). Specifically, fibroblasts are the most common cell type in the granulation tissue and are derived from mesenchymal stem cells (5,25). These mesenchymal cells can be from bone marrows or epithelial cells when they dedifferentiate during epithelial-mesenchymal transition (25). The shape of the secreting, non-contractile fibroblasts is spindle-like as the cells are actively producing collagen, ECM proteins and PGs (25).

The formation of granulation tissue promotes wound closure through reepithelialization and contraction. Specifically, during reepithelialization, basal keratinocytes from either side of the wound edges begin to migrate and proliferate across the granulation tissue until the epithelial layer of the wounded skin is restored. The reepithelialization process is coordinated by various growth factors and chemokines, such as IGF-1, EGF and adiponectin, during which IGF-1 facilitates spreading, EGF induces contraction and adiponectin induces proliferation and migration of keratinocytes (26,27). As the granulation tissue matures, the secreting, non-contractile fibroblasts differentiate into contractile myofibroblasts, which then attach themselves to the wound edges to enable the pulling and contracting of the wound. The contraction process is coordinated mainly by TGF-β, and the differentiation of fibroblasts to contractile myofibroblasts

features more organized fibers that have higher expression levels of α-smooth muscle actin (α-SMA) (28).

During the final phase of tissue remodeling, also mediated by TGF-β signaling, the thinner type III collagen bundles in the granulation tissue that were previously deposited by fibroblasts are eventually replaced by thicker type I collagen bundles to restore the tensile strength of the skin (29,30). Eventually, once the collagen has been deposited, the myofibroblasts undergo apoptosis for resolution (31). However, it is worthwhile to note that although cutaneous wound healing can repair skin damage, it cannot restore full tensile strength to the skin and the scarred tissues have been shown to have, at most, upward 80% of original tensile strength (32).

In order for wounds to heal timely and properly, there must be a fine balance of interaction between various cell types, cytokines, growth factors and ECM components at every stage of cutaneous wound healing. Usually, wounds heal without issues - such a wound is described to be an acute wound. However, in some individuals with underlying clinical pathological conditions such as diabetes mellitus, venous insufficiency, pressure necrosis and vasculitis, the normal continuum of wound healing is disrupted and wounds enter a chronic non-healing state (33). This is particularly detrimental as chronic wounds can affect the ability of the skin to perform its many primary functions.

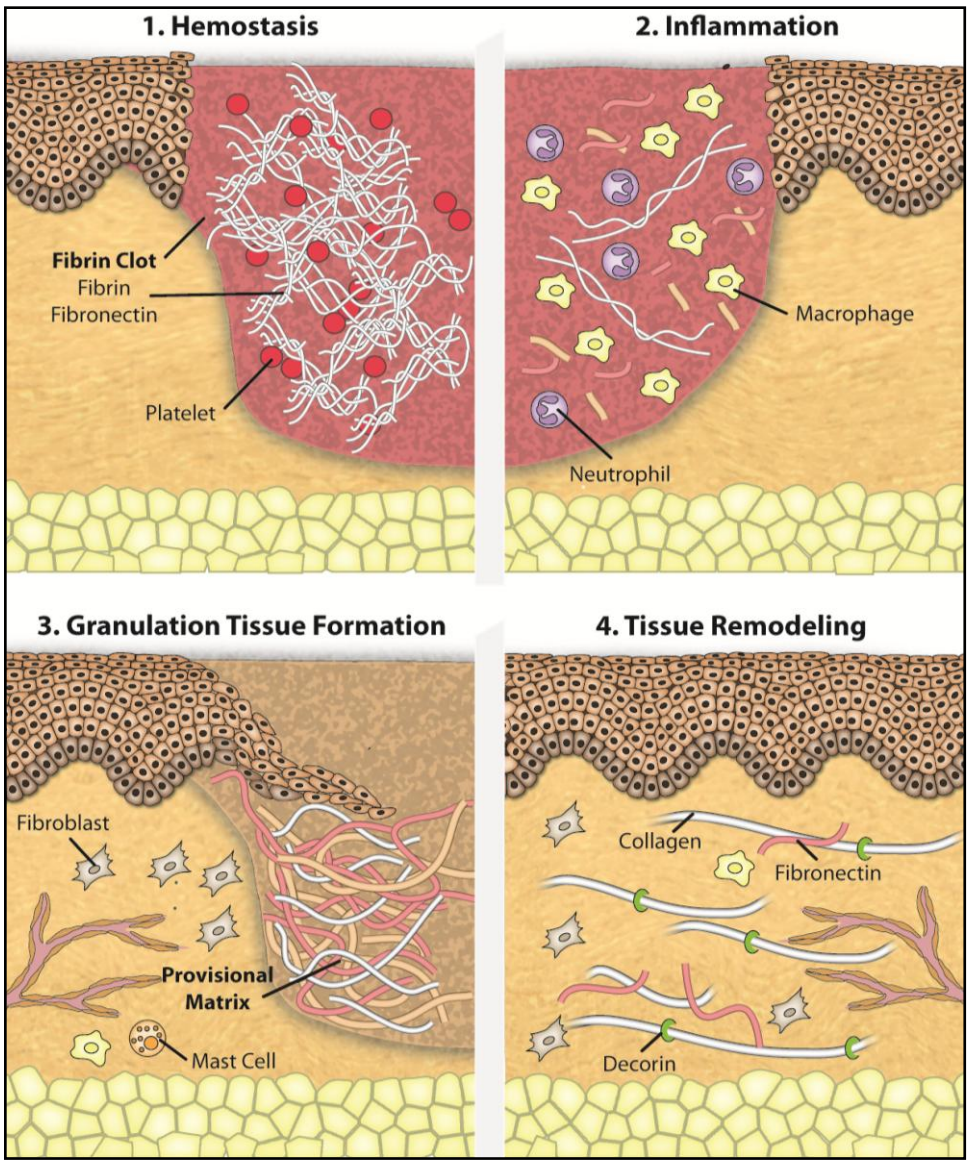

Figure 2 The four phases of acute wound healing. (A) During hemostasis, a fibrin plug made of polymerized fibrinogen and plasma fibronectin is formed to temporarily halt blood loss, trap foreign particles and provide structural support for invading cells. **(B)** During inflammation, neutrophils and macrophages sequentially infiltrate the wound site. They respectively phagocytose foreign particles, debris and damaged extracellular matrix components, and secrete various cytokines and growth factors to promote formation of granulation tissue. **(C)** During granulation tissue formation, macrophages and mast cells provide signals required for collagen synthesis, angiogenesis and provisional matrix deposition by fibroblasts, myofibroblasts and endothelial cells, which enable wound closure through reepithelialization and contraction. **(D)** During tissue remodeling, type III collagen is replaced by type I collagen. The interaction with decorin and fibronectin allow for restoration of tensile strength.

Note: The figure was obtained and reproduced with permission from "Granzyme B in injury, inflammation and repair" by Hiebert PR and Granville DJ (*Trends Mol Med*. 2012 Dec;18(12):732-41).

1.2.1.1 Role of fibronectin in acute wound healing

FN is a multi-domain glycoprotein that is made up of twelve type I, two type II and fifteen to seventeen type III repeats depending on alternative splicing (7,34). Together, these repeats make up the functional domains of the glycoprotein including the 70 kDa N-terminal domain, the 120 kDa central binding domain and the C-terminal heparin-binding domain (34). There are two forms of FN, namely the plasma and cellular FN. Plasma FN differs structurally in that it has only fifteen type III repeats as opposed to cellular FN which has seventeen (7,34). The two additional domains that plasma FN lacks are the extra-domain-A (ED-A) and ED-B (7,34).

Plasma FN is synthesized and secreted by hepatocytes into the plasma as a soluble protein (7). Plasma FN is one of the main components of the fibrin plug that is initially recruited and formed as part of the temporary scaffolding medium during the early hemostasis stage in wound healing (19). Specifically, plasma FN cross-links with fibrins either covalently through glutamine residues in the N-terminus of plasma FN interacting with the alpha chains of fibrin, or non-covalently through binding to type I repeats (34). The presence of plasma FN in the fibrin plug is also essential for platelet adhesion, spreading and aggregation (35).

Cellular FN is synthesized largely by fibroblasts, but also by endothelial cells, during the granulation tissue formation phase. The N-terminal region of cellular FN has been shown to bind types I and III collagen, fibrin, fibrillin-1 and 2, fibulin, laminin and tenascin-C, thus regulating and maintaining the functionalities of these ECM components (7,34). In addition, cellular FN is also capable of sequestering growth factors and related binding proteins in the ECM (7,34). This includes VEGF and TGF-β binding proteins which largely bind to the C-terminal region of cellular FN and regulate downstream cell-signaling pathways (7,34). The central binding domain of cellular FN contains a sequence of Arginine-Glycine-Aspartic Acid (RGD) that is denoted as

the RGD domain. The RGD site binds to integrins such as α5β1and αvβ3 integrins, and facilitates cell-matrix interactions including cellular adhesion (7,34). The two additional domains, ED-A and ED-B, are vital for neovascularization and capillary sprouting as binding to endothelial cells promotes cellular migration and proliferation (7,34). The differentiation of fibroblasts to myofibroblasts is largely dependent on three cues, namely TGFβ-1, the ED-A domain of cellular FN and mechanical tension, and as a result, cellular FN is also involved in wound contraction and tissue remodeling (36).

1.2.2 Pathophysiology of chronic wound healing

Although the clinical etiologies leading to the development of chronic wounds may be wide-ranging, all chronic wounds feature increased proteolytic activity and chronic inflammation. As the ECM is integral for proper wound healing, degradation of ECM components by proteases inevitably creates a physiologically imbalanced local environment that disrupts the functionalities of cellular and non-cellular components; in such an environment, chronic wounds can persist.

There have been various studies showing elevated levels and increased proteolytic activity of proteases in chronic wounds. In particular, increased activity of collagenases (MMP-1 and MMP-8), gelatinases (MMP-2 and MMP-9) and serine proteases (plasmin, neutrophil elastase and cathepsin G) have been reported in human chronic wound fluid samples (37-44). Conversely, protease inhibitors, such as TIMP-1, α1-antitrypsin and α2-macroglobulin are degraded and non-functional in human chronic wound fluid samples (40,41,44,45). As many ECM components can be cleaved, abnormal levels of proteases are capable of disrupting the overall ECM integrity. In addition, since the ECM is a reservoir for pro-inflammatory cytokines, elevated proteolytic activity can subsequently lead to the release of sequestered cytokines such as IL-1β and TGF-β,

both of which have been reported to be elevated in human chronic wound fluid samples (46-48). The chronic inflammatory state adopted by chronic wounds can also be attributed to reduced levels and functionalities of neutrophils and macrophages (22). Specifically, neutrophils in chronic wounds release more reactive oxygen species, such as superoxide anion, hydroxyl radicals, singlet oxygen and hydrogen peroxide, which renders the wound environment extremely oxidative (49,50). Macrophages in chronic wounds are no longer actively secreting growth factors and cytokines involved in inflammation resolution (22).

Altogether, persistent inflammation and elevated proteolytic activity disrupt the physiological harmony between cells and the ECM. As such, fibroblasts, keratinocytes and endothelial cells are unable to function properly. Specifically, fibroblasts isolated from diabetic mice exhibited decreased cellular migration and VEGF production, whereas fibroblasts isolated from human chronic wound samples displayed reduced mitogenic and proliferative responses, which indicated that many of these cells are in a senescent state (51-55). Interestingly, keratinocytes from human chronic wound skin biopsies did not show reduced proliferation; instead, delayed reepithelialization may be due to impaired differentiation and migration of keratinocytes (56-59). Since cells are not able to properly attach, proliferate and migrate in the hostile wound microenvironment, wounds stay open and become chronic wounds.

Besides delayed healing, excessive healing can also occur when the skin fails to respond to signals indicating the resolution of cutaneous wound healing. This usually is the result of the inability of myofibroblasts to undergo apoptosis during the final tissue remodeling phase (29,30,60). Since myofibroblasts are involved in collagen deposition, their persistence in the wound environment can result in excessive collagen production and contraction, thus leading to fibrosis. In the skin, excessive collagen growth can lead to the development of keloid or systemic

scleroderma (25,60). Specifically, one of the cellular abnormalities that contribute to keloid formation is the altered response of fibroblasts to apoptotic signals due to overexpression of growth factor receptors, including IGF-1 growth receptors (61). In addition, fibroblasts and myofibroblasts cultured from patients with systemic scleroderma exhibited a phenotype that is more resistant to anti-Fas-induced apoptosis (62).

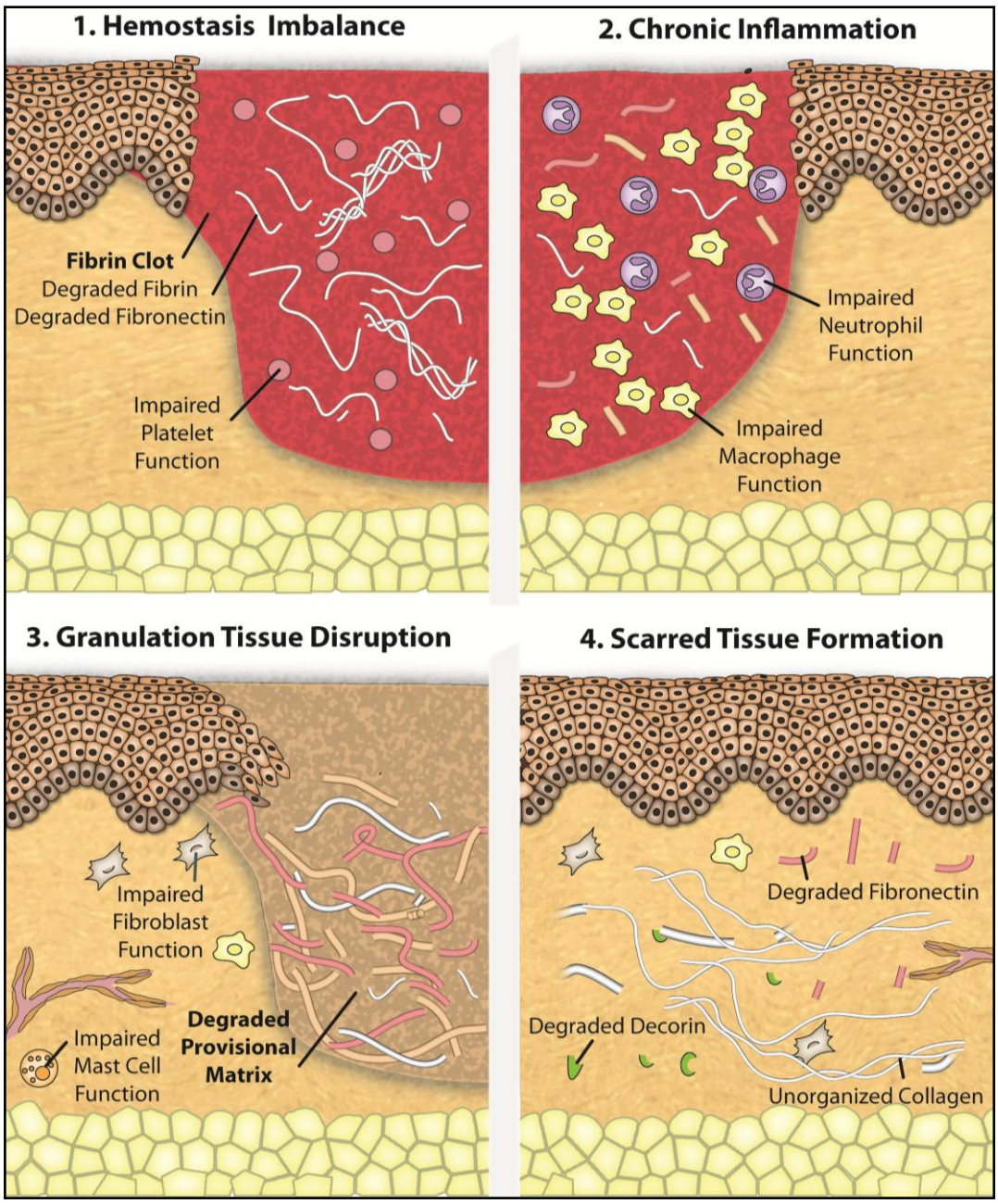

Figure 3 Features of chronic wound healing: (A) hemostasis imbalance due to the cleavage of factors involved in the clotting cascade, **(B)** chronic inflammation due to the infiltration of impaired immune cells and the release of pro-inflammatory cytokines, **(C)** disruption of granulation tissue formation due to the degradation of extracellular matrix proteins and an increase in the number of senescent fibroblasts and **(D)** improper tissue remodeling due to degradation of decorin and fibronectin which leads to the formation of unorganized collagen fibers and scarred tissues.

Note: The figure was obtained and reproduced with permission from "Granzyme B in injury, inflammation and repair" by Hiebert PR and Granville DJ (*Trends Mol Med*. 2012 Dec;18(12):732-41).

1.3 Diabetic skin ulcers

Diabetes mellitus is a group of metabolic diseases characterized by hyperglycemia. This results from either the body's inability to produce insulin as in type I diabetes, or failure to respond to insulin as in type II diabetes. There are many major complications associated with diabetes, including cardiovascular diseases, renal failure, retinopathy and skin ulcers. In particular, diabetic skin ulcers are non-healing chronic wounds and have been noted to be a significant public health burden in many countries (63). It is estimated that up to a quarter of diabetic patients will develop these ulcers in their lifetime (64). As a result of their lesions, nearly a fifth of these diabetic patients will require non-traumatic lower limb amputations (64). To put the problem into context, it is believed that a lower limb is lost to diabetes every thirty seconds (65).

The main causes of diabetic skin ulcers are neuropathy, ischemia or a combination of both. People with diabetes usually suffer from a loss of motor, sensory and autonomic nerve fibers, and the nerve deficits cause most patients to overlook initial symptoms during the development of the ulceration (66). As such, repeating trauma and wrong pressure loading to the foot can exacerbate the problem. Furthermore, as diabetes is both a microvascular and macrovascular disease, nutrient and oxygen sources to the already ulcerated wound site are diminished and capacity of the skin to self-restore is compromised.

1.3.1 Treatments

Numerous treatment options for the management of diabetic ulcers have been explored, and they can be divided into several categories including bioengineered skin substitutes, growth factors enhancement, pressure offloading and hyperbaric oxygen therapy (67-73). The use of skin

substitutes and growth factors allow for the addition of cells and growth factors, which are largely impaired in chronic wounds. The most common skin substitute that has been utilized is Dermagraft where human neonatal fibroblasts are cultured onto an absorbable matrix that enables them to produce endogenous ECM proteins, PG and growth factors (67,68) . The efficacy of Dermagraft has been demonstrated in prospective randomized clinical trials (67,68). The main growth factor that has largely been engineered into gels or dressings is PDGF and its efficacy has been demonstrated in randomized, double blind and place-controlled studies (69,70,74). As diabetic skin ulcers usually develop in the lower limbs of diabetic patients, therapy that allows for mechanical relief, such as negative pressure dressings and pressure offloading devices, have also been explored. Finally, as ischemia is one of the main causes of diabetic skin ulcers, the use of hyperbaric oxygen therapy delivers pure oxygen intermittently to the local wound to restore adequate tissue reperfusion (73). However, even though many of these treatments have gone onto clinical trials, they have largely been unsuccessful, and a combination of local surgical or larval debridement and infection control to remove dead and contaminated tissues continue to be the standard recommended treatment strategy (66). As such, there is a need for establishing novel therapeutic targets for managing chronic diabetic wounds.

1.4 Granzymes

The granule-secreted enzymes or otherwise known as granzymes, are a family of serine proteases that have both intracellular and extracellular functions. All the granzymes share three conserved features, namely a triad of residues at the catalytic site (aspartic acid, histidine and serine), an Isoleucine-Isoleucine-Glycine-Glycine amino acid sequence at the N-terminus and the presence of disulphide bridges (75). However, despite the structural similarities, the five

granzymes that are present in humans differ in terms of their substrate specificity: granzyme A (GzmA; tryptase), granzyme B (GzmB; aspartase), granzyme H (GzmH; chymase), granzyme K (GzmK; tryptase) and granzyme M (GzmM; metase) (76,77). All the granzymes were first identified in the granules of cytotoxic T lymphocytes (CTLs) and natural killer (NK) cells (78-83). Upon secretion, they can readily be taken up by target cells and are the primary mediator of apoptosis in allogenic, transformed and/or virally-infected cells through both caspases-dependent and -independent pathways (84,85).

Since their characterizations in the 1980s, GzmA and GzmB have been extensively studied whereas GzmH, GzmK and GzmM are still largely considered to be orphan granzymes. In particular, recent studies have challenged the traditional intracellular pro-apoptotic role of GzmA and proposed that the primary role of GzmA may instead be regulating immune responses through mediating the production and release of pro-inflammatory cytokines (86-88). Subsequently, through *in vitro* cleavage assays and *in vivo* mouse studies, there has been emerging evidence that GzmB can also accumulate in the extracellular milieu during chronic inflammation and cleave many ECM proteins and PGs, suggesting an additional extracellular proteolytic role of GzmB in addition to an already well-established role in inducing cytotoxicity (89-93).

1.5 Granzyme B

In 1978, Hatcher *et al.* isolated a cytotoxic protease from human peripheral blood lymphocytes that was later identified to be GzmB (94). In humans, the GzmB gene corresponds to a locus on chromosome 14D that encodes for the GzmB gene product, which is approximately 3500 bp long and comprises of four introns and 5 exons (95). GzmB is a 32 kDa chymotrypsin-like serine protease that is also known as cytotoxic T lymphocyte-associated serine esterase-1, or

granzyme 2. The binding pocket of GzmB contains an arginine residue at position 226 that confers enzyme-substrate specificity, and enables the enzyme to interact with and cleave aspartic acid residues at the P1 position of the substrate (96).

Although GzmB was once thought to be exclusively expressed in the granules of CTLs and NK cells, many studies have refuted this claim and GzmB has been shown to be expressed by both immune and non-immune cells. The other immune sources of GzmB include activated macrophages, B lymphocytes, basophils, CD4+ T lymphocytes, dendritic cells, mast cells, neutrophils and regulatory T cells (97-105). In addition, the non-immune sources of GzmB include chondrocytes, granulosa cells, keratinocytes, primary spermatocytes, Sertoli cells, syncytial trophoblasts, smooth muscle cells (SMCs) and type II pneumocytes (106-111). Altogether, the diversity of cell types which express GzmB accounts for the diverse range of functions, both intracellular and extracellular, that the enzyme performs.

In many of these cell sources, the expression profile of GzmB can also be altered. As the transcription of GzmB is dependent on the binding of four transcription factors to their binding sites at the upstream promoter region of GzmB, mutations in any one of them can negate GzmB expression (112,113). The transcription factors involved include activating transcription factor/cyclic adenosine monophosphate-responsive element-binding protein-1, activator protein-1, Ikaros and core-binding factor (112-115). Although lymphocytes constitutively express GzmB, transcription can further be induced when CTLs and NK cells are activated through T cell receptor activation and co-stimulation with cytokines (116). Upon ultraviolet stimulation, GzmB expression in keratinocytes is elevated through stimulation of the mitogen activated protein kinase signaling pathways (108,115). Furthermore, recent studies have revealed that upon activation, protein expression of GzmB in dendritic cells and mast cells is elevated without a corresponding

increase in messenger ribonucleic acid levels; this indicates that GzmB may be regulated through translational mechanisms although specifics currently remain unknown (101,102).

1.5.1 Intracellular role of granzyme B

There are two main apoptotic pathways that CTLs use to eradicate virally-infected and malignant cells, namely the receptor-mediated pathway involving Fas ligand and the granule-mediated pathway involving granzymes (117). In CTLs and NK cells, GzmB is synthesized as a pro-peptide tagged with mannose-6-phosphate (118). Specifically, this tag enables the inactive GzmB zymogen to be trafficked to the granules (118). Once the inactive GzmB enters the granules, a Glycine-Glutamic Acid domain at the N-terminus is removed by cathepsin C (119). Although GzmB is activated once cleaved, its proteolytic activity is still suppressed because of the acidic pH environment inside the granules, as well as the storage of active GzmB on a scaffold that is associated with serglycin, a chondroitin sulfate modular PG (116,120).

As CTLs and NK cells initiate target cell engagement, the contents of the granules including GzmB are released into the immunological synapse, which is the space between CTLs and NK cells, and target cells (121). Although the exact mechanism is still debatable, it is generally accepted that GzmB is able to gain entry into the target cells with the assistance of perforin, a pore-forming, membrane-disrupting protein (122,123). Specifically, perforin, a 66 kDa calcium-dependent protein, can polymerize and form a pore in the plasma membrane of the target cells, enabling GzmB to be endocytosed into the cytoplasm of the target cells (123,124).

Once inside the target cell, GzmB is capable of cleaving many different intracellular substrates involved in apoptosis, including caspase 3, Bid and myeloid cell leukemia sequence-1 (MCL-1) (125-129). In particular, activation of caspases 3 through GzmB cleavage subsequently

activates downstream caspase-3 targets, such as caspase-activated deoxyribonuclease and nuclear laminin, and ultimately leads to deoxyribonucleic acid (DNA) fragmentation and nuclear membrane disruption (125). In addition, GzmB cleavage of Bid results in the formation and translocation of the GzmB-truncated product (gtBid) to the mitochondria, thus leading to mitochondrial membrane disruption and apoptosome formation through the release of cytochrome c, apoptosis-inducing factor and caspase 9 (126-128,130,131). Furthermore, cleavage of the anti-apoptotic protein, MCL-1, can promote apoptosis through the stimulation of mitochondrial permeabilization and further cytochrome c release (129).

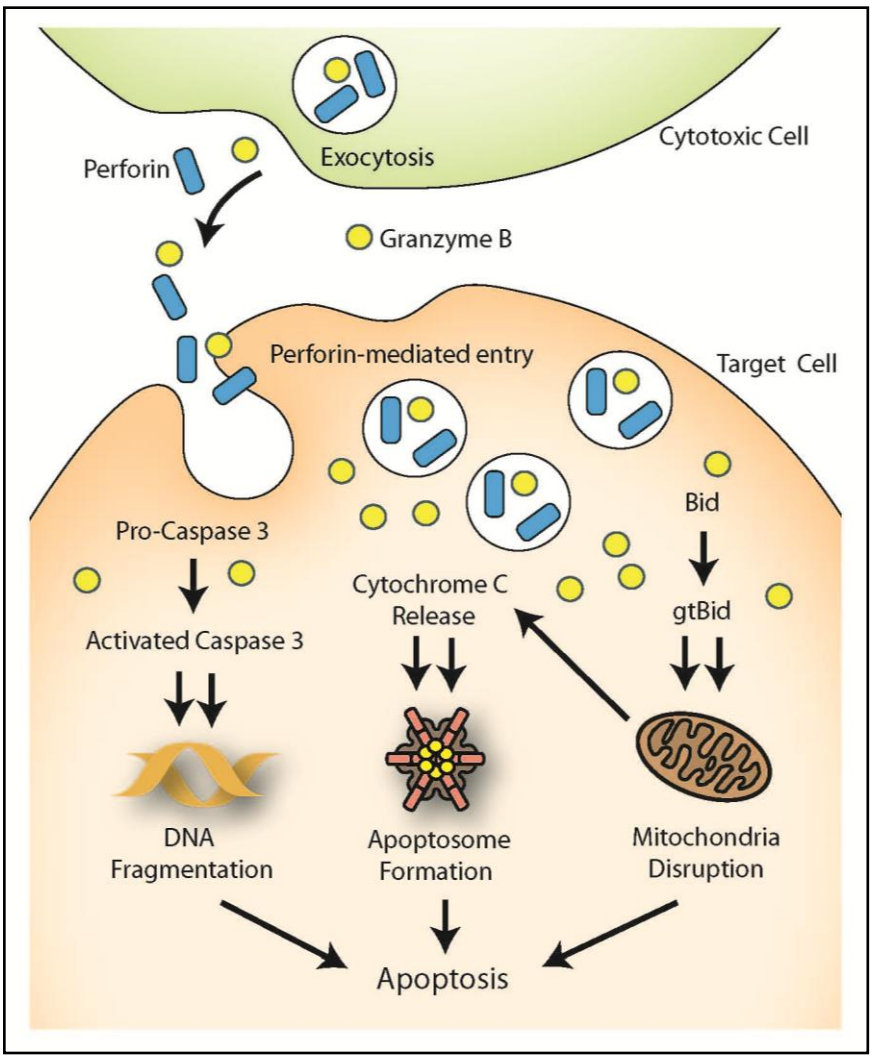

Figure 4 Intracellular role of granzyme B in apoptosis. Granzyme B can be released into the immunological synapse by cytotoxic lymphocytes and internalized into the target cell by perforin, a pore-forming and membrane disrupting protein. In the target cell, granzyme B can cleave pro-caspase 3 and Bid into active caspase 3 and granzyme B-truncated product known as gtBid, and induce apoptosis through DNA fragmentation, mitochondrial disruption and apoptosome formation.

Note: The figure was obtained and reproduced with permission from "Granzyme B in injury, inflammation and repair" by Hiebert PR and Granville DJ (*Trends Mol Med*. 2012 Dec;18(12):732-41).

1.5.2 Extracellular role of granzyme B

Since its discovery over a quarter of a century ago, the understanding of GzmB biology has been limited to its intracellular apoptotic role in inducing cell death in virally-infected and malignant target cells (78,132,133). However, in recent years, there has been emerging evidence challenging the dogma that GzmB only acts intracellularly and this controversy has been the subject of many recent reviews (77,86,134,135).

In particular, as many sources of GzmB have come to be identified, it is imperative to highlight that many of these cell types such as basophils, mast cells, keratinocytes and chondrocytes, do not express perforin (102,105,106,108). As perforin is essential for GzmB's entry into target cells and thus for it to perform its intracellular function, the expression of GzmB in the absence of perforin is indicative of an entirely extracellular function of GzmB in these cell types. In addition, it is also possible that GzmB can escape the immunological synapse and leak into the extracellular space during degranulation of CTLs (136). As previously mentioned, lymphocytes constitutively express GzmB (116). It has been reported that up to a third of GzmB is non-specifically released from CTLs and NK cells after prolonged T-cell receptor and interleukin-2 activation (137). In the absence of target cell engagement, NK cells are capable of releasing active GzmB via the granule-dependent pathway, whereas CTLs can secrete inactive GzmB via a granule-independent mechanism (138). As such, it is now generally accepted that GzmB also has an additional extracellular role and its accumulation in the extracellular milieu has been implicated in many diseases featuring chronic inflammation included in mouse models of skin aging, atherosclerosis and abdominal aortic aneurysm (AAA) (139-141).

In the plasma of healthy individuals, median reported levels of GzmB range from 20 to 40 pg/mL (142,143). The serum levels of GzmB are reported to be elevated in patients with diseases,

including Epstein Barr virus infection, human immunodeficiency virus-1 infection and rheumatoid arthritis (RA) (142,144-146). In addition, GzmB levels are also elevated in bodily fluids, including the synovial fluid of RA patients, the cerebrospinal fluid of multiple sclerosis and Rasmussen encephalitis patients and the bronchoalveolar lavage of patients with chronic obstructive pulmonary disease (COPD) and atopic asthma (144,145,147-151).

1.5.3 Granzyme B inhibitors

The serine protease inhibitors, or also known as serpins, are the largest protease inhibitor super family and are divided into sixteen clades (152). As their name implies, serpins inhibit proteases, and more specifically, the majority of serpins inhibit either serine or cysteine proteases (153). The structure of serpins is highly conserved in that all of the members contain three α-sheets and at least seven β-helices (152). The reactive centre loop containing the protease recognition site is inserted between the secondary structure containing the α-sheets and β-helices (152). Specifically, the reactive centre loop enables serpins to act as pseudo-substrates and form a covalent complex with their target enzymes, thereby inhibiting their enzymatic activities (154).

Since GzmB is a potent inducer of apoptosis, it is important for GzmB-expressing cells to protect themselves from accidental leakage of GzmB into the cytoplasm, which can cause self-induced cytotoxicity. Currently, protease inhibitor-9 (PI-9), which is part of the SERPINB clade, is the only known endogenous inhibitor of human GzmB (152). Specifically, the reactive centre loop of PI-9 contains acidic residues in the P1 and P4-P4’ positions that subsequently interact and promote irreversible conformational changes to inhibit GzmB (155). Many immune cells including CTLs and NK cells express high levels of PI-9 (152,156,157). Interestingly, non-immune cells, such as endothelial cells and vascular SMCs, have also been shown to have high

PI-9 expression levels, possibly to protect these bystander cells from targeted cytotoxicity induced by GzmB during chronic inflammation (158,159).

In contrast to intracellular GzmB, extracellular GzmB level is largely unregulated. PI-9 has been shown to be non-functional in the highly oxidative extracellular environment, and as such, is only considered to be an endogenous intracellular GzmB inhibitor in humans (155). Specifically, GzmB retains up to 70% of its activity despite PI-9 being present in the plasma of healthy individuals (135,160). Currently, there have been no reports of any other endogenous GzmB inhibitor, and lack of evidence of any extracellular GzmB inhibitors in humans. As such, excessive GzmB in the ECM and subsequent degradation of ECM components may have important manifestations.

1.5.3.1 Serpina3n

In addition to PI-9, the serine protease inhibitor, serpina3n (SA3N), which is part of the serpina clade, has also been identified as a potent inhibitor of both human and mouse GzmB (161,162). SA3N is only present in mice and is widely expressed in the brain, liver, lung, spleen, testis and thymus of mice (154). However, the physiological role of SA3N in these tissues is still unknown (162). Specifically, SA3N is the mouse orthologue of the human anti-chymotrypsin (154). The human anti-chymotrypsin is encoded by only one gene; however, extensive diversification and duplication in mice have resulted in fourteen related serpina3 genes clustered at chromosome 12F1 (153). Specifically, the two genes for SA3N and human anti-chymotrypsin share 61% homology at the amino acid level (154). Each serpina3 gene encodes for a protease inhibitor with its own tissue distribution and substrate specificity. In particular, the inhibitory activity of SA3N against GzmB was first identified in cultured Sertoli cells (162). However,

SA3N has broad substrate specificity and in addition to GzmB, can also bind and inhibit chymotrypsin, trypsin, cathepsin G and elastase (162). Specifically, a methionine residue in the P1 position and various acidic residues in the P4-P4' positions have all been implicated in the binding of SA3N to GzmB to render the enzyme inactive (154)

The administration of SA3N enables researchers to study the extracellular role of GzmB instead of using a systemic knockout approach. The *in vivo* efficacy of SA3N has been validated using a mouse model of AAA (161). In particular, SA3N was largely shown to reduce AAA rupture and ECM remodeling through the inhibition of the cleavage of decorin, and these findings are consistent with results from a previous GzmB-knockout study (141,161).

1.5.4 Extracellular granzyme B substrates

The list of extracellular substrates of GzmB that have so far been identified is extensive and includes coagulation mediators, cytokines, glycoproteins, PGs and cell surface receptors (91). The possible consequences of cleavage of these substrates are summarized in Figure 5. Many of them are ECM proteins that are important in wound healing and they are outlined in Table 1 (90).

There are a number of factors important in the coagulation cascade that are cleaved by GzmB, including von Willebrand factor (vWF), fibrinogen, plasminogen and plasmin (163,164). GzmB cleaves vWF at two sites in the A1-3 domains that are critical for interaction with platelets (164). As a result of GzmB-mediated vWF cleavage, ristocetin-induced platelet aggregation, tethering, adhesion and spreading are impaired (164). Usually, fibrinogen is found in either a soluble form or an ECM-bound form, and both interact with activated platelets for platelet adhesion and thrombus growth (165). However, fibrinogen that is bound to the ECM is susceptible to GzmB cleavage, likewise impairing platelet aggregation (164). Normally,

conversion of plasminogen by enzymes, such as tissue plasminogen activator and urokinase plasminogen activator, forms plasmin (166). However, GzmB is capable of cleaving both plasminogen and plasmin, and such cleavage leads to the further formation of a 38 kDa anti-angiogenic fragment, angiostatin, that has been shown to contribute to impaired angiogenesis and delayed wound healing through apoptosis of endothelial cells in patients with scleroderma (163,167).

GzmB can also promote inflammation through the cleavage of pro-inflammatory cytokines. Normally, IL-18 is sequestered in its inactive precursor form in monocytes and keratinocytes. However, GzmB can cleave IL-18 to its biologically active form and further stimulate inflammation through interferon-gamma production (149). GzmB and IL-18 have together been shown to be important in protection against herpes simplex virus-1 in mice through regulating the activity of NK cells (168). The synovial fluid of RA patients, which have been shown to contain elevated GzmB levels, also showed increased levels of IL-18 (144,169). In addition, GzmB can also cleave IL-1α to an even more active form (170). This was supported by *in vivo* results showing that the immune response to ovalbumin was enhanced in mice injected with cleaved IL-1α fragments (170). In particular, IL-1α levels are elevated in chronic wound fluid and GzmB-mediated IL-α cleavage fragments are also observed in the bronchoalveolar lavage of patients with COPD, cystic fibrosis and brochiectasis (170) .

There are many glycoproteins and PGs in the ECM that have been identified as GzmB substrates. The provisional matrix forming part of the granulation tissue contains FN and vitronectin, both of which are cleaved by GzmB (171-173). GzmB preferentially cleaves after Asp residues at the RGD integrin binding site of vitronectin (171). Although the site of cleavage of FN by GzmB has not yet been identified, it is possible that the cleavage may also occur at the same

RGD site in the central binding domain of the glycoprotein. Since FN and vitronectin are important for cell attachment, differentiation and migration during wound healing, cleavage of these two glycoproteins can possibly impair keratinocytes and fibroblasts as groups reported anoikis and detachment when cultured SMCs and endothelial cells were incubated with GzmB (171,172,174). When apolipoprotein-knockout mice were fed a high fat diet for 37 weeks, the animals exhibited delayed wound closure that was attributed to GzmB-mediated degradation of FN and vitronectin (173).

In addition, GzmB knockout mice have increased vascular permeability that may be due to the inhibition of FN cleavage in comparison to wildtype mice when challenged with oxalazone in an animal model of contact dermatitis (175). Another important protein in the dermal-epidermal junction that is cleaved by GzmB is laminin (171). As laminin level is reduced in the dermal-epidermal junction of chronic diabetic wounds in comparison to acute excisional wounds, it is possible that GzmB-mediated laminin cleavage disrupts keratinocyte migration and the reepithelialization process as the integrity of basal lamina is hindered (59).

GzmB can also cleave small leucine-rich PGs including decorin, betaglycan and biglycan (176). Normally, active TGF-β1 is sequestered in the ECM in the inactive form by binding to the aforementioned PGs (9,10,176). However, upon GzmB cleavage of these PGs, active TGF-β1 can subsequently be released, contributing to phosphorylation and the activation of Smad-3 in human coronary artery SMC, and possibly also contributing to fibrosis as TGF-β1 is important during tissue remodeling (176). In addition, decorin binds to collagen fibrils and orchestrates proper collagen organization and spacing, thus regulating tensile strength of the tissues (177). Using animal models, GzmB-cleavage of decorin has been implicated in the pathogenesis of mouse skin

aging and AAA as reduced collagen density was prevented in both GzmB knockout mice and upon administration of SA3N, the mouse GzmB inhibitor (139,161).

There are numerous cell surface receptors that are cleaved by GzmB, including nicotinic acetylcholine receptor (NAR), neuronal glutamate receptor (NGR), Notch-1 and fibroblast growth factor receptor-1 (FGFR-1) (178-180). The cleavage of NAR and NGR subsequently generates autoantigen that can mount a host autoimmune response, whereas the cleavage of Notch-1 and FGFR-1 generates pro-apoptotic fragments involved in tumor survival and viral protection (178-180).

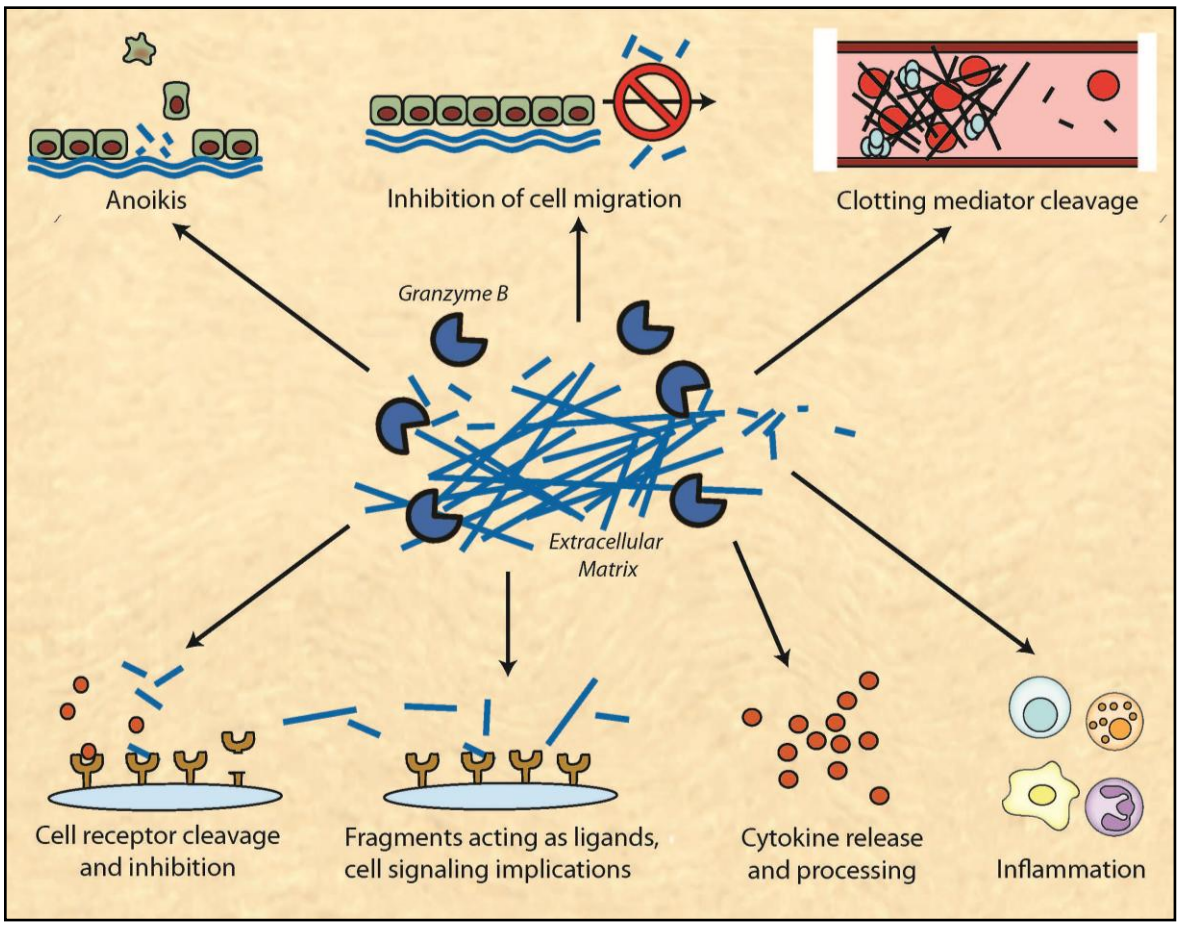

Figure 5 Possible consequences of the cleavage of extracellular granzyme B. Granzyme B can act extracellularly when it is not internalized into target cells or when it has escaped the immunological synapse. It is capable of cleaving various receptors leading to the activation or inhibition of cell signaling pathways. It can also induce detachment-mediated cell death (anoikis) and inhibit cell migration. In addition, GzmB-mediated cleavage fragments can promote pro-inflammatory cytokine release, which leads to chronic inflammation.

Note: The figure was obtained and reproduced with permission from "Intracellular versus extracellular granzyme B in immunity and disease: challenging the dogma" by Boivin WA, Cooper DM, Hiebert PR and Granville DJ (*Lab Invest.* 2009 Nov;89(11):1195-220).

GzmB Substrate	Role in Wound Healing	Consequences of GzmB Cleavage
Phase 1: Hemostasis		
von Willebrand factor	platelet aggregation, tethering, adhesion and spreading	impaired platelet aggregation, tethering, adhesion and spreading (164)
fibrinogen	platelet adhesion and thrombus growth	impaired platelet aggregation (164)
plasminogen, plasmin	activation of fibrinolytic system	impaired angiogenesis (163,167)
Phase 2: Inflammation		
interleukin-18	pro-inflammatory cytokine	stimulate production of interferon-gamma (149)
interleukin-1α	pro-inflammatory cytokine	formation of a potent form of IL-1α (170)
Phase 3 & Phase 4: Granulation Tissue Formation & Tissue Remodeling		
fibronectin	attachment, differentiation and migration of keratinocytes and fibroblasts	impaired functions of keratinocytes and fibroblasts (171,172,174)
vitronectin	attachment, differentiation and migration of keratinocytes and fibroblasts	impaired functions of keratinocytes and fibroblasts (171,172,174)
laminin	dermal-epidermal junction	disrupts keratinocytes migration (59)
decorin	orchestrate proper collagen organization and spacing	reduced collagen density (139,161)

Table 1 Extracellular granzyme B substrates and their consequences when cleaved during wound healing.

Chapter 2: Rationale, Hypothesis and Specific Aims

Since the discovery of GzmB over a quarter of a century ago, most research has only focused on its intracellular role in inducing apoptotic cell death even though GzmB was originally proposed to be a protease that could function both intracellularly and extracellularly (78,132). However, because GzmB can be induced in other types of immune and non-immune cells that often do not express perforin and/or do not form immunological synapses with target cells, there is emerging evidence supporting the paradigm that GzmB can accumulate in the extracellular milieu (102,105,106,108). Specifically, many of the proteins in the ECM are subject to cleavage by GzmB and the consequences of cleavage by extracellular GzmB are implicated in many diseases featuring chronic inflammation, as shown in mouse models of AAA, skin aging, atherosclerosis and wound healing using GzmB knockout mice (139-141,173). Currently, no known human endogenous extracellular GzmB inhibitor exists, so the proteolytic activity of GzmB can persist, as evident by high activity levels retained in bodily fluids (144,145,147-149,149-151).

Wound healing is a complex process that involves overlapping and sequential phases involving hemostasis, inflammation, granulation tissue formation and tissue remodeling. For wounds to heal, there must be a fine balance of interaction between various cell types, cytokines, growth factors, proteases and ECM components at every stage. Since non-healing wounds feature persistent inflammation and enhanced proteolytic activity, we speculated that GzmB may be contributing to the pathogenesis of chronic wound healing, especially as many substrates of GzmB are ECM proteins essential for proper wound healing.

Due to aging demographics and an increasing diabetic patient population, the incidence of chronic non-healing wounds is on the rise (181) . Of relevance to the possible role of GzmB in

age-related chronic wounds, a previous study by our group demonstrated that apolipoprotein-knockout mice fed a high fat diet for 37 weeks exhibited delayed wound closure that was not present in apolipoprotein-GzmB double knockout mice (173). To our knowledge, it was the first study implicating GzmB's pathogenic role in chronic wound healing and suggested that GzmB inhibition may be a viable therapeutic target for chronic wounds.

The purpose of my thesis was to determine whether local inhibition of extracellular GzmB could accelerate wound closure in a genetically-induced type II diabetic mouse model of delayed wound healing. Specifically, many of the proteins in the ECM involved in wound healing are subject to cleavage by GzmB, including FN. As there are currently no GzmB inhibitors commercially available, mice were treated with SA3N, a mouse GzmB inhibitor, which was previously utilized in an animal model of AAA that demonstrated its efficacy (161).

I hypothesized that GzmB contributes to the pathogenesis of diabetic wound healing through excessive degradation of ECM proteins essential for proper wound healing.

The specific aims for this thesis are:

(1) To identify the expression and source(s) of GzmB in type II diabetic mouse wounds

(2) To determine whether local inhibition of GzmB can accelerate wound closure in a genetically-induced type II murine model of diabetic wound healing

(3) To investigate the mechanism by which GzmB contributes to the pathogenesis of diabetic wound healing in a genetically-induced type II murine model of diabetic wound healing

Chapter 3: Materials and Methods

3.1 Animals

The animal studies were conducted in accordance with the procedure guidelines approved by the University of British Columbia Animal Care Committee. All mice used in the studies were purchased from the Jackson Laboratories (stock number 000642; Bar Harbor, Maine) at 7 weeks old. All mice used were from a C57BLKS/J background strain, male and either homozygous or heterozygous for the spontaneous mutation in the leptin receptor. The mice homozygous for the leptin receptor mutation were considered to be diabetic. The mice heterozygous for the leptin receptor mutation were considered to be the non-diabetic littermates. All mice were fed standard laboratory chow (equal parts of PicoLab Mouse Diet 20 #5058 and PicoLab Rodent Diet 20 #5053 from LabDiet, Richmond, Indiana) and water *ad libitum*.

Two days before the wound healing surgery, all mice were fasted for 4 hours and fasting blood glucose levels of the mice were determined with OneTouch Ultra Blood Glucose Meter (LifeScan, New Brunswick, New Jersey). Only mice with fasting blood glucose levels greater than 200 mg/dL were considered diabetic. The hair on the backs of the animals were removed by shaving with hair clippers followed by treatment with Nair™ (Church and Dwight, Ewing, New Jersey) for 90 seconds. Finally, only mice with no visible active hair follicles were subjected to surgery.

3.1.1 Wound healing surgery

The wound healing surgery was modified using procedures reported in a previous paper (182). All mice were anesthetized using a mixture of isoflurane and oxygen on a warm heating pad to prevent hypothermia. Once the mice had reached proper anesthetic depth, eye lube was

applied and buprenorphine (0.05 mg/kg; McGill University, Montreal, Quebec) was administered subcutaneously. The skin area to be wounded was then prepared by swabbing with betadine and two washes of 70% ethanol. After prepping, a 10 mm diameter punch biopsy (Acuderm, Fort Lauderdale, Florida) was used to outline a wound pattern and a full thickness skin excision (including the PC muscle layer) was created on the mid-lower back of the mice using sterilized surgical scissors. Once wounded, digital pictures of the wound area were captured at a fixed distance and the angle and wound area were covered by a transparent Tegaderm™ dressing (3M, Minneapolis, Minnesota). All surgical animals were allowed to recover and were housed individually to prevent the removal of dressings by other animals.

Figure 6 Representative image of mouse that underwent wound healing surgery. After removal of hair by shaving and depilatory cream, a 10 mm excisional wound was created on the back of the mice and covered with a transparent Tegaderm™ dressing.

3.1.1.1 Time course studies

Wound areas were cleaned by washing with sterile saline and replaced with new Tegaderm™ every 3 days, and on each of these days, digital pictures of the wound area were captured, with ruler placed below, for planimetry measurements. In summary, wound pictures

were taken at days 0, 3, 6, 9, 12, 15 and 18 post-wounding. The non-diabetic animals were sacrificed at either day 12, 16 or 31 post-wounding.

3.1.1.2 Treatment studies

Wound areas were cleaned by washing with sterile saline and replaced with new Tegaderm™ every 3 days. At this time, digital pictures of the wound area were captured, with ruler placed below, for planimetry measurements and taken also every 3 days until day of sacrifice (either day 12, 18 or 35 post-wounding). In addition, all mice were treated immediately after wounding and every 3 days until day of sacrifice (either day 12, 18 or 35 post-wounding). The mice were divided into two treatment groups and received either sterile saline control or SA3N (at a concentration of 35 ng/µL diluted with sterile saline; generous gift from Dr. Chris R Bleackley of University of Alberta, Edmonton, Alberta) in a 100 µL volume. On days 0, 3, 6 and 9, the treatment was administered topically by injecting directly underneath the Tegaderm™ with an insulin syringe. Starting from day 12 and every treatment day onwards, saline or SA3N was administered subcutaneously by injecting into surrounding wound areas, either top and bottom or right and left.

3.2 Tissue collection and processing

On the day of sacrifice, mice were euthanized by carbon dioxide asphyxiation. A 7 mm by 7 mm representative piece of wounded tissue was harvested and cut in half, bisecting the wound centre. The left half was immediately flask frozen in liquid nitrogen and stored at -80°C. The right half was fixed in 10% phosphate-buffered formalin overnight, and transferred to 70% ethanol, before paraffin embedding for histological and immunohistochemical analyses.

3.3 Histology and immunohistochemistry

Five micron sections were deparaffinized and rehydrated in the following order for histological and immunohistochemical stainings: 3 washes of xylene, 100% ethanol, 90% ethanol, 70% ethanol and 2 washes of Tris-buffered saline (TBS).

For hematoxylin and eosin staining to evaluate morphology, slides were dipped in hematoxylin for 5 minutes, washed with water, dipped in 1% acid alcohol for 10 seconds, washed with water, dipped in lithium carbonate for 30 seconds, 70% ethanol for an additional 30 seconds and finally into 1% eosin prepared in 80% ethanol for 15 seconds. For toluidine blue staining to detect mast cells, slides were immersed in toluidine blue working solution (prepared by dissolving toluidine blue powder in 70% ethanol and further diluted in 1% sodium chloride with pH 2.3) for 3 minutes. For Masson's trichrome staining to detect collagen, slides were dipped in saturated picric red solution for 10 minutes, washed in water, dipped in Weigert's iron hematoxylin working solution for another 10 minutes, washed in water, differentiated in 1% acid alcohol for 3 seconds, washed in water again, stained with Biebrich scarlet-acid fuchsin solution for 1 minute, washed in water, differentiated in fresh 1% phosphotungstic acid for 5 minutes, washed in water again, dipped in 0.5% light green for 5 minutes, rinsed in water and finally in 1% acetic acid for 30 seconds. For picrosirius red staining to detect fibrillar collagen, slides were immersed in picrosirius red working solution (prepared by dissolving Sirus red F3BA in a saturated solution of picric acid) for 1 hour and rinsed with acetic acid water solution 3 times.

For immunohistochemistry, slides were heated in 80°C citrate buffer (pH 6.0) for 10 minutes, cooled at room temperature for 30 minutes and quenched in 3% hydrogen peroxide for 10 minutes. These slides were then blocked with either a mixture of 10% goat serum and 2% mouse serum (for F4/80 primary antibody) or a 10% goat serum (for all other primary antibodies)

for 1 hour at room temperature to reduce non-specific background staining. Subsequently, the slides were incubated with primary antibody prepared in either a mixture of 10% goat serum and 2% mouse serum (for F4/80 primary antibody) or a 10% goat serum (for all other primary antibodies) overnight at 4°C. The primary antibodies used were as follows (Abcam, Cambridge, Massachusetts; Cell Signaling Technology, Danvers, Massachusetts; AbD Serotec, Raleigh, North Carolina):

Primary Antibody	Vendor	Catalogue Number	Dilution
rabbit-anti-mouse **α-SMA**	Abcam	ab5694	1:2000
rabbit-anti-mouse **CD3**	Abcam	ab5690	1:800
rabbit-anti-mouse **CD31**	Abcam	ab28364	1:200
rat-anti-mouse **F4/80**	AbD Serotec	MCA497R	1:100
rabbit-anti-mouse **granzyme B**	Abcam	ab4059	1:100
rabbit-anti-mouse **Ki67**	Cell Signaling	12202	1:500
rabbit-anti-mouse **vimentin**	Cell Signaling	5741	1:500

Table 2 Details of primary antibodies used for immunohistochemistry.

The following day, slides were incubated with biotinylated goat-anti rabbit secondary antibody (1:350; Vector Laboratories, Burlingame, California) prepared in either a mixture of 5% goat serum and 1% mouse serum (for F4/80 primary antibody) or a 5% goat serum (for all other primary antibodies) for 30 minutes at room temperature, washed twice in TBS and incubated with Vectastain® Elite ABC reagent (Vector Laboratories) for 30 minutes. Subsequently, the slides were washed twice in TBS-Tween 20 (TBST) and incubated with Vector® DAB substrate (Vector Laboratories) for 5 minutes. Finally, the slides were then counterstained with hematoxylin for 30 seconds for visualization and quantification.

3.4 Wound pictures analyses

Digital pictures of the wound area were captured, with ruler placed below, were captured on the day of wound healing surgery and every 3 days until day of sacrifice. For all wounds, the open wound was normalized to wound size at day 0 and expressed as a percentage.

3.5 Histological analyses

All quantification associated with hematoxylin and eosin-stained slides were assessed by Aperio ImageScope version 11.1.2.760 (Aperio, Vista, California) and normalized to the percentage of original wound area. For analysis of epithelial and PC margins, the two ends of each layer were identified and the distance between the two ends was measured. For measurement of epithelial thickness, the thickest distance between top to bottom of the epithelium was measured. For measurement of granulation tissue thickness, the thickest distance from top to bottom of the granulation tissue was used. For measurement of granulation tissue area, the whole granulation tissue area was traced. For quantification of collagen in Masson's trichrome-stained slides, all images were taken at 20X magnification from the middle and/or the two edges of the wound. Using Image Pro Plus version 4.5.0.29 (Media Cybernetics, Rockville, Maryland), the intensity RGB threshold was set for the blue-green positive colour of collagen and the number of positive pixels was counted and expressed as a percentage collagen per traced representative area. Specifically, for analyses of wounded tissues from days 12, 16 and 18, the set RGB threshold was R: 20000 to 50000, G: 40000 to 52000 and B: 37000 to 50000, and for days 31 and 35, the set RGB threshold was R: 20000 to 50000, G: 40000 to 55000 and B: 2000 to 55000. For quantification of collagen in picrosirius-red stained slides, all images were taken at 20X from the middle of the wound. Using Image Pro Plus version 4.5.0.29, the intensity RGB threshold was set

for the red colour of collagen and the number of positive pixels was counted and expressed as a percentage collagen per traced representative area. Specifically, the set RGB threshold was R: 50 to 255, G: 20 to 100 and B: 15 to 30.

3.6 Immunohistochemical analyses

For quantification of all immunohistochemical staining, all images were taken either at 20X or 40X magnification from the middle and/or both edges of the wound. For Ki67 counting, representative areas from each image were defined and numbers of positive brown-staining cells per area were counted. For all the rest of the immunohistochemical analyses for GzmB, α-SMA, CD31 and vimentin, an intensity threshold was set for the brown colour and the number of positive pixels was counted and expressed as a percentage positive staining per traced representative area using Image Pro Plus version 4.5.0.29. For GzmB, the set RGB threshold was R: 0 to 55000, G: 0 to 50000 and B: 0 to 47000 for all tissues. For α-SMA, the set RGB threshold was R: 0 to 55000, G: 0 to 50000 and B: 0 to 35000 for day 12 tissues of non-diabetic wounds and R: 0 to 40000, G: 0 to 50000 and B: 0 to 30000 for all other tissues. For CD31, the set RGB threshold was R: 0 to 50000, G: 0 to 50000 and B: 0 to 42000 for day 12 tissues of non-diabetic wounds and R: 0 to 50000, G: 0 to 50000 and B: 0 to 27000 for all other tissues. For vimentin, the set RGB threshold was R: 0 to 47000, G: 0 to 50000 and B: 0 to 40000 for day 12 tissues of non-diabetic wounds and R: 0 to 40000, G: 0 to 50000 and B: 0 to 40000 for all other tissues.

3.7 Mouse granzyme B activity assay

The mouse granzyme B activity assay was modified using procedures reported in a previous paper (161). Increasing concentrations of SA3N (0.004 nM to 665 nM) was incubated

with 12 nM recombinant mouse GzmB (Beryllium, Bedford, Massachusetts) in a reaction buffer (50 mM HEPES, 0.1% CHAPS and 5 mM dithiothreitol mixed in distilled water) at room temperature and shaking for 5 minutes, room temperature incubation for 20 minutes and 30°C incubation for 5 minutes. Subsequently, the fluorogenic mouse GzmB substrate, 50 µM Ac-IEPD-AMC (California Peptide, Salt Lake City, Utah), was added. Cleavage of the substrate was monitored by measuring excitation and emission signals at wavelengths of 380 nm and 460 nm at 30°C with a Magellan Tecan SaFire 2 plate reader (Tecan Group Ltd., Männedorf, Switzerland) in kinetic mode for 15 cycles in duplicates. The average slope of the relative fluorescence units per second for every minute between cycles 2 to 14 was obtained. The percentage activity was calculated from the slope after normalized to positive controls containing just mouse GzmB and Ac-IEPD-AMC.

3.8 Fibronectin cleavage assay

The fibronectin cleavage assay was modified using procedures reported in a previous paper (172). The 48 well plates were coated with 3µg of mouse FN (#92784, Abcam) per well diluted in PBS at 37°C for 2 hours and subsequently blocked with 1% bovine serum albumin for 30 minutes at 37°C. The wells were treated with 50 nM mouse GzmB (Sigma-Aldrich, St. Louis, Missouri) in the absence or presence of 100 nM SA3N at 37 °C overnight. The next day, supernatants were collected from each well and cleavage fragments were analyzed by western blot.

3.9 Mouse embryonic fibroblasts detachment assay

The mouse embryonic fibroblast detachment assay was modified using procedures reported in a previous paper (171). 3T3 mouse embryonic fibroblasts were plated to wells of a 96 well tissue culture plate (1.25×10^4 /well) in Dulbecco's Modified Eagle's Medium containing 10% fetal bovine serum and 1% penicillin streptomycin, and allowed to adhere overnight in an 37°C incubator with 5% carbon dioxide. Cells were washed with phosphate buffered saline (PBS) and incubated in 100 µL of serum free media (SFM) containing 50 nM, 100 nM or 200 nM GzmB in the presence or absence of 100 nM SA3N. Cells were incubated at 37°C for 7 hours, after which images of the cells in the plate were captured under phase contrast using a microscope camera. The media was aspirated and cells were washed once with PBS to remove non-adherent cells. Fresh SFM was replaced, and for quantification of remaining adherent cells, CellTiter® AQueous One Solution MTS Cell Proliferation Assays (Promega, Madison, Wisconsin) were performed by the addition of 20 µL of MTS reagent and incubation for 3 hours. Absorbance was read at 490 nm with a Magellan Tecan SaFire 2 plate reader.

3.10 Skin homogenization

Frozen skin sections were cut to 5 mm by 5 mm pieces and placed in a centrifuge tube containing a cold 5 mm stainless steel bead and 300 µL of urea lysis buffer (50 mM Tris pH 7.4, 7 M urea, 150 mM sodium chloride, 1% Triton) with 4 µL of protease inhibitor cocktail (Sigma-Aldrich). The skin sections were homogenized in TissueLyser LT (Qiagen, Venlo, Netherlands) at 50 Hz for 4 minutes, 3 times in total. In between each cycle, tubes were placed on ice for 30 seconds to prevent over-heating of the samples. After homogenization, samples were incubated on ice for 15 minutes and centrifuged at 4°C for 10 minutes at 15000 rpm to separate proteins from

pelleted cell debris. The supernatant was then transferred to a new tube containing 250 µL PBS with 0.1% sodium dodecyl sulphate (SDS) and centrifuged at 4°C again for 10 minutes at 15000 rpm to separate proteins from pelleted cell debris. The supernatant was transferred to Amicon® Ultra Filter (Millipore, Billerica, Massachusetts) and spun at 14000 rpm at 4°C for 12 minutes, 3 times in total. The filtrate was discarded and 400 µL PBS with 0.1% SDS was added after each spin to exchange the buffer. Total protein concentration of homogenized samples was measured and calculated using standard Bradford protein assays (Biorad, Hercules, California) such that samples were adjusted to ensure equivalent amounts of total protein for western blot.

3.11 Western blots

For preparation of samples for western blot, either 25 µL of supernatant (for FN cleavage assay) or 16.5 µg of homogenized protein (for FN detection in wounded tissues) was added to 6X Laemmli buffer (300 nM Tris-hydrogen chloride pH 6.8, 600 mM dithiothreitol 12% w/v SDS, 40% w/v glycerol, 0.25% w/v bromophenol blue) and denatured at 100°C for 5 minutes. Boiled samples were run on a 10% SDS-polyacrylamide gel at 85 V for 15 minutes and 125 V for 90 minutes, and were subsequently transferred to a nitrocellulose membrane. Membranes were blocked with 5% TBST in skim milk for 1 hour and incubated with anti-FN antibody (#2413, Abcam) and/or anti-SA3N antibody (AF4709, R&D Systems, Minneapolis, Minnesota) at respectively, a 1:1500 dilution and/or 1:700 dilution prepared in 5% TBST in skim milk and gently rocking overnight at 4°C. Membranes were washed with TBST for 5 minutes, 3 times in total. After washes, membranes were incubated for 1 hour with IRDye 800 conjugated anti-mouse and/or IRDye 700 conjugated anti-goat secondary immunoglobulin G antibody (both from Rockland Inc., Gilbertsville, Pennsylvania) at 1:5000 and/or 1:2000 dilutions and washed again

with TBS for 5 minutes, 3 times in total. Subsequently, membranes were visualized with the Odyssey Infrared Imaging System (LI-COR Biotechnology, Lincoln, New England). Bands were detected and quantification of FN densitometry was normalized to glyceraldehyde 3-phosphate dehydrogenase (GAPDH) when required.

3.12 Statistical analyses

For the fibroblast detachment *in vitro* assays, one-way ANOVA with Dunnett's multiple comparison test was used for statistical analysis. For all other experiments, unpaired Student t-test was used for statistical analyses. All statistical tests were performed using GraphPad Prism version 5.04 (GraphPad Software, San Diego, California). In all cases, p-values less than 0.05 were considered significant.

Chapter 4: Results

4.1 Diabetic mice exhibit delayed wound closure

The diabetic mice homozygous for the spontaneous mutation in the leptin receptor, or also known as the db/db mice, exhibit delayed wound healing and have been used by many as a model of this specific phenotype (183-185). The littermates that are heterozygous for the spontaneous mutation in the leptin receptor are the non-diabetic mice. However, one limitation of utilizing mouse models of chronic wound healing is that the skin of loosely-skinned rodents mainly close by wound contraction, rather than wound reepithelialization as observed mostly with human skin. In order to reduce contraction and promote reepithelialization in mice, the uses of splints and/or transparent dressings such as Tegaderm® have been widely utilized (182,186,187).

After wounding the backs of mice and letting the wounds heal with replacement of Tegaderm® every 3 days, we confirmed that diabetic mice exhibited delayed wound closure by tracing wound pictures that were taken every 3 days post-wounding and expressed as a percentage over the original wound area. By day 18, wounds of non-diabetic mice were fully closed as the mean percentage of the open wound was 0 ± 0 % whereas wounds of diabetic mice were only partially closed as the mean percentage of the open wound was 71.7 ± 6.6 % (Figure 7A and B). The weights of the diabetic mice were significantly greater than non-diabetic mice (Figure 7C; 40.7 ± 2.0 g versus 23.8 ± 1.2 g). In addition, the glucose levels in diabetic mice on the day of wound healing surgery were significantly higher than the levels found in non-diabetic mice (Figure 7D; 498.2 ± 29.8 mg/dL versus 160.4 ± 14.2 mg/dL). These results were consistent with current literature, thereby confirming the usage of diabetic mice as a model of delayed diabetic wound healing.

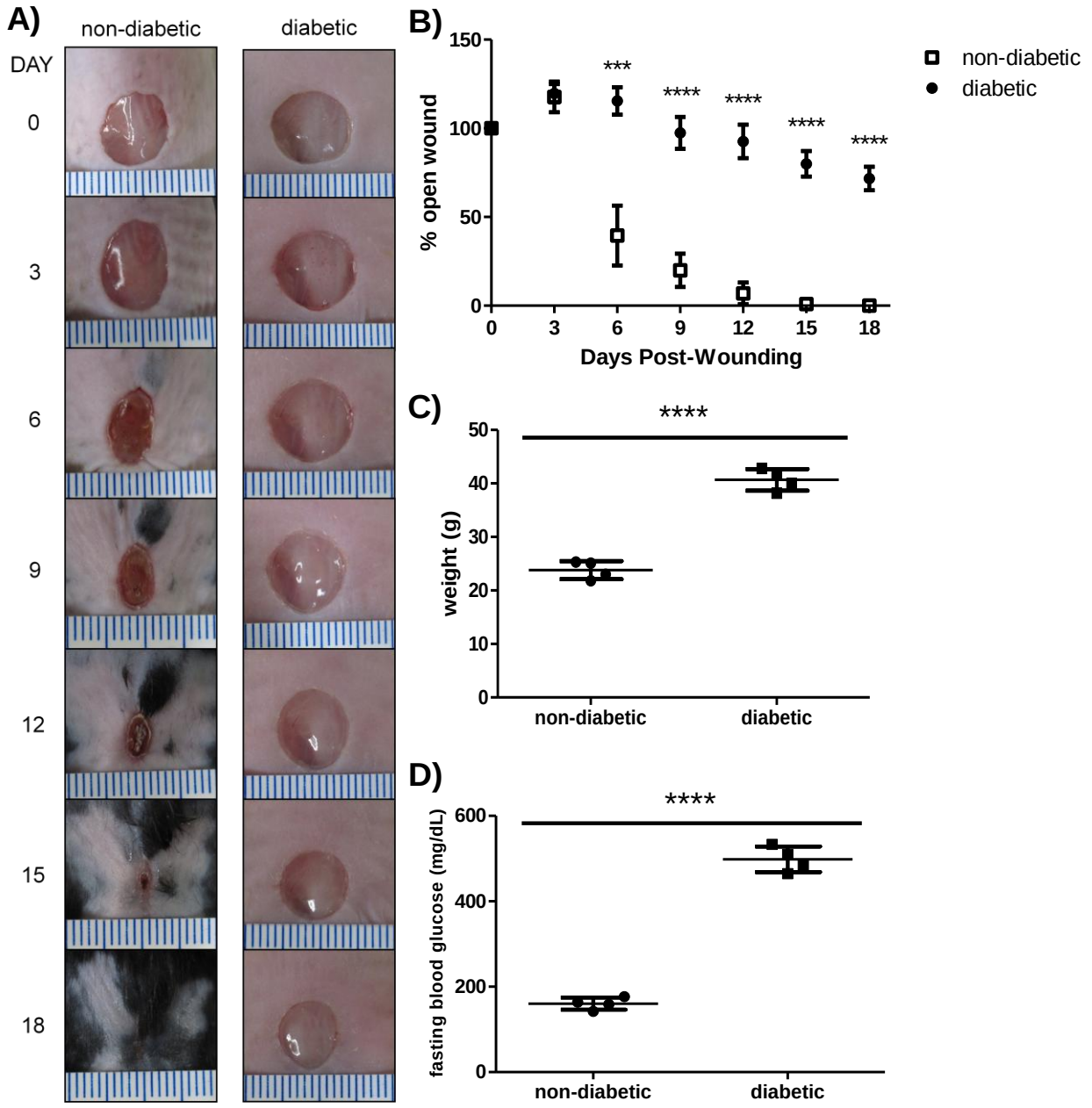

Figure 7 Obese, diabetic mice exhibit delayed wound closure. (A) Representative digital images of non-diabetic and diabetic mice wounds captured over 18 days wound healing period. **(B)** Comparison of the percentages of open wound over 18 days healing period between non-diabetic (n = 4) and diabetic mice (n = 4) showing that diabetic mice healed significantly slower than non-diabetic mice. **(C)** On the day of surgery, diabetic mice were significantly heavier than non-diabetic mice and **(D)** the fasting blood glucose levels of diabetic mice were significantly higher than that of non-diabetic mice. *[Error bars represent mean ± standard deviation. P-values were calculated using unpaired Student t-test. *** denotes p < 0.001 and **** denotes p < 0.0001.]*

4.2 Granzyme B is elevated and differentially expressed in the wound edges and granulation tissues of diabetic wounds

Since diabetic wounds feature chronic inflammation and GzmB is thought to accumulate in the ECM during chronic inflammation, we examined GzmB levels in wounded but fully reepithelialized tissues from non-diabetic and diabetic mice. By immunohistochemistry, the GzmB levels found in diabetic wounds were significantly higher than the levels found in non-diabetic wounds (percentage of positive GzmB per area in diabetic animals was $2.2 \pm 1.2\%$ and percentage in non-diabetic animals was $0.34 \pm 0.045\%$; Figure 8A andB).

We went on to investigate the spatial expression of GzmB in diabetic wounds by performing immunohistochemical analyses of wounded skin tissues at different healing stages. In an open wound (at day 12 post-wounding), GzmB expression was low and minimal GzmB was localized to wound edges (Figure 8C). In a partially reepithelialized wound (at day 18 post-wounding), GzmB expression was moderate and localized to mainly wound edges, but some were also minimally scattered throughout the granulation tissues (Figure 8C). In an entirely reepithelialized wound (at day 35 post-wounding), GzmB expression was high and scattered throughout the wound edges and granulation tissues (Figure 8C). These results confirmed GzmB's presence in the different phases of wound healing.

A)

non-diabetic wounded tissue

diabetic wounded tissue

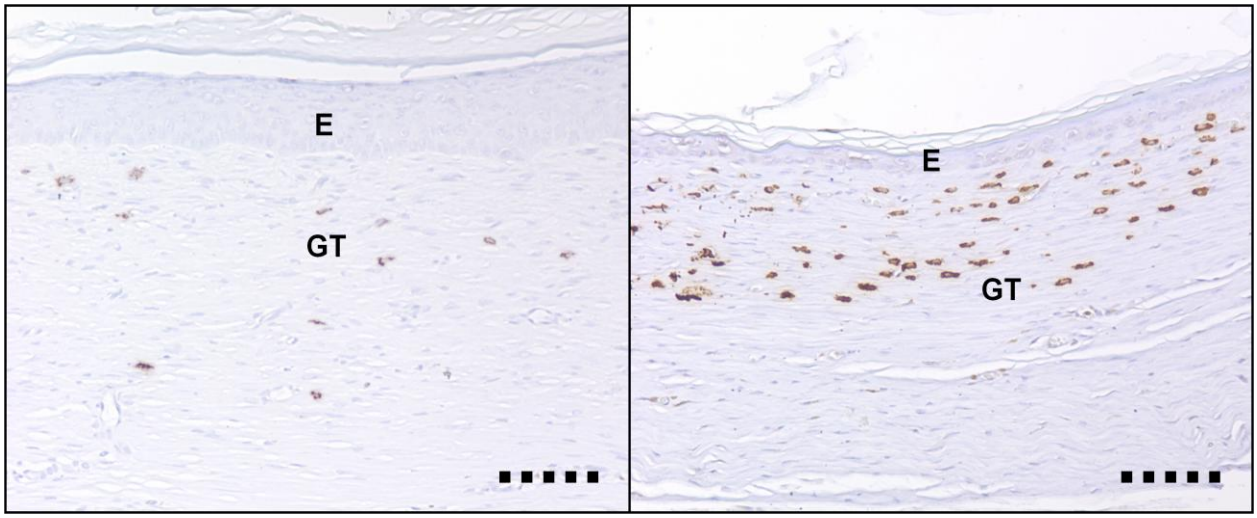

B)

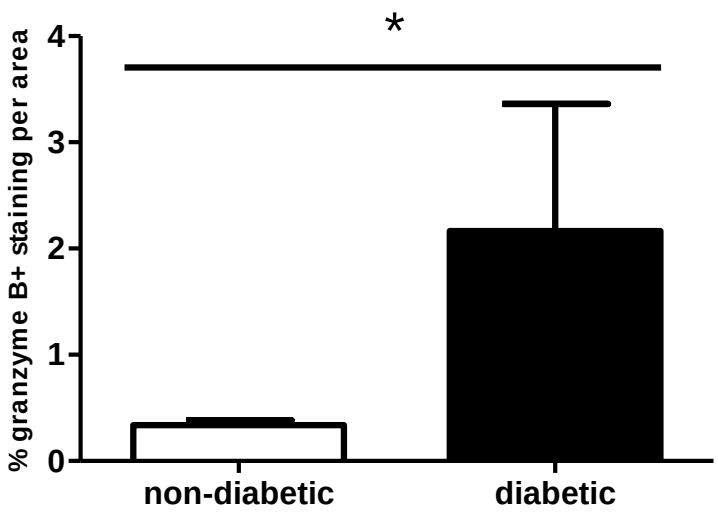

C) *Wound Edge* *Wound Middle*

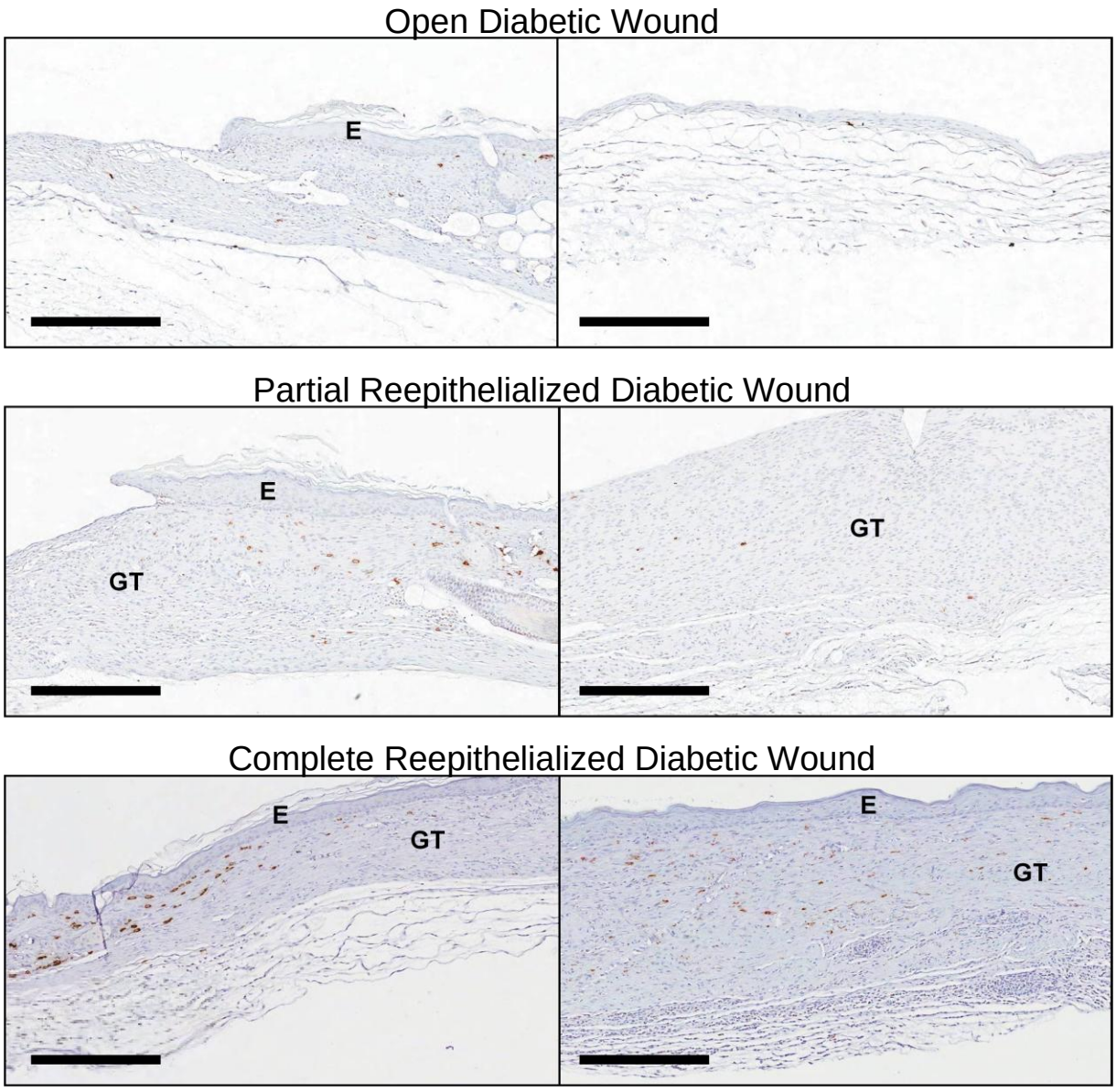

Figure 8 Expression of granzyme B in edges and middle of diabetic wounds. (A) and **(B)** Using immunohistochemistry, granzyme B expression, denoted by brown staining, was higher in completely reepithelialized diabetic wounds in comparison to non-diabetic wounds. **(C)** Granzyme B expression was found to be localized to wound edges and granulation tissues in open (at day 12), partially reepithelialized (at day 18) and completely reepithelialized (at day 35) diabetic wounds, respectively, as denoted by positive brown staining. *[E denotes epidermis and GT denotes granulation tissue. Error bars represent mean ± standard deviation. P-value was calculated using unpaired Student t-test. * denotes $p < 0.05$. Black scale bars = 300µm. Dotted scale bars = 50µm.]*

4.3 Granzyme B colocalizes with some mast cells in granulation tissues of diabetic wounds

As there are many immune and non-immune sources of GzmB, diabetic wound tissues were stained to determine the immune source(s) of GzmB. For quantifications, toluidine blue staining was used to detect mast cells, anti-F4/80 antibody was used as an immunohistochemical marker for macrophages, anti-CD3+ antibody was used as an immunohistochemical marker for CD3+ lymphocytes and hematoxylin and eosin (H&E) staining was used to detect polymorphonucleated neutrophils.

All of the immune cells that were probed for were present in the wounded tissues collected at day 18 (Figure 9A to D). However, there were very minimal neutrophils compared to macrophages, lymphocytes and mast cells. In particular, we noted that mast cells colocalized with positive GzmB staining (as denoted by black arrows in the red rectangular boxes of Figure 9D and E). The same tissue that was initially stained with toluidine blue for mast cells was stripped of the dye after scanning the slide, and it was observed that the sections remained intact. As such, immunohistochemical staining for GzmB was performed on the same tissue. As positive GzmB staining largely colocalized with granules of mast cells, we concluded that mast cells is one of the possible immune source of GzmB in the diabetic mice.

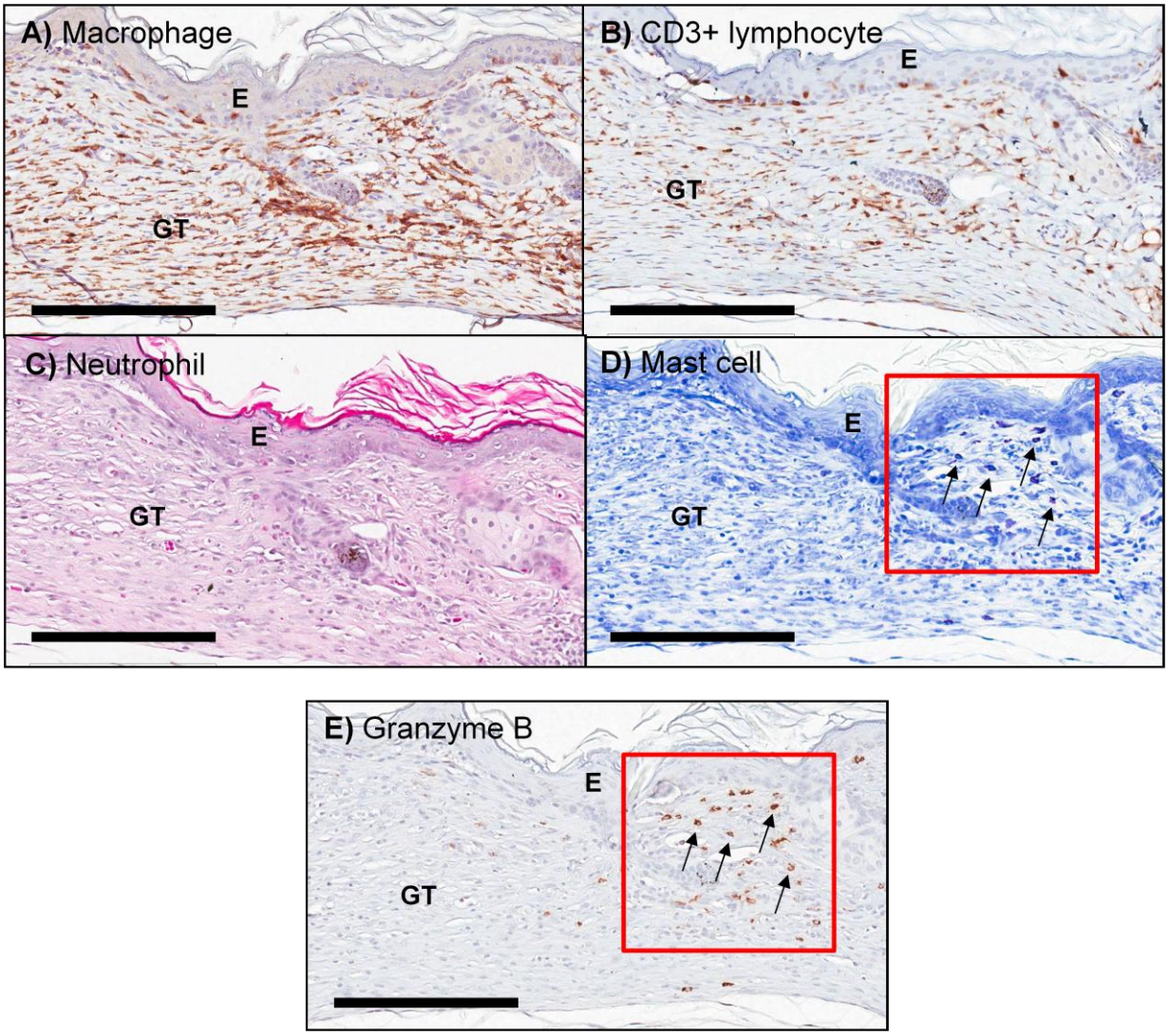

Figure 9 Granzyme B colocalizes with some mast cells in granulation tissues of diabetic wounds. Using F4/80 and CD3 immunohistochemical markers, hematoxylin and eosin staining and toluidine blue staining, **(A)** macrophages (brown coloured), **(B)** CD3+ lymphocytes (brown coloured), **(C)** neutrophils and **(D)** mast cells (dark red-purple coloured) were all detected in the diabetic wounds collected at day 18. **(E)** Notably, positive brown granzyme B staining largely colocalized with granules of mast cells as shown by red rectangular boxes and black arrows. *[E denotes epidermis and GT denotes granulation tissue. Scale bars = 200 µm.]*

4.4 Serpina3n inhibits mouse granzyme B *in vitro*

SA3N has previously been identified as a potent human and mouse GzmB inhibitor *in vitro* (161,162). Our laboratory has also previously demonstrated SA3N's efficacy as an *in vivo* mouse GzmB inhibitor in a mouse model of AAA (161). Since there are currently no GzmB inhibitors commercially available, we administered SA3N to wounds as a local GzmB inhibitor. We confirmed that the SA3N used in my thesis inhibits mouse GzmB *in vitro*. Specifically, fluorescence signals can be measured when the fluorogenic substrate, Ac-IEPD-AMC, is cleaved by mouse GzmB and that fluorescent signal should normally diminish with less substrate cleavage. This was confirmed as the activity of mouse GzmB decreased as concentration of SA3N increased (Figure 10). However, as SA3N is an irreversible inhibitor, the IC50 cannot be measured and the result from the assay can merely be interpreted as a qualitative indicator of SA3N's inhibitory activity.

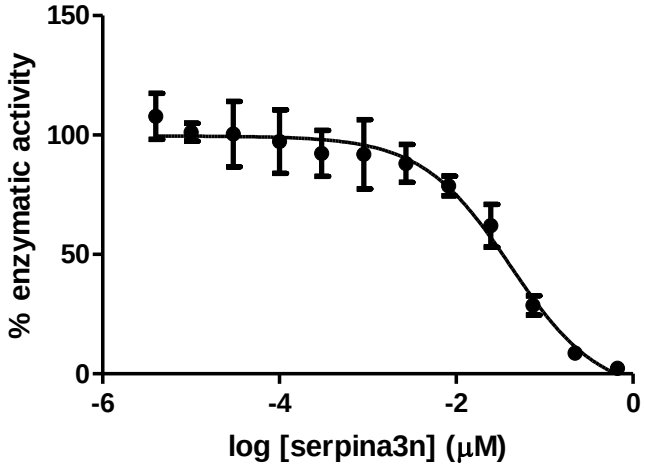

Figure 10 Serpina3n inhibits mouse granzyme B *in vitro*. The activity of mouse granzyme B after incubation with serpina3n was assessed by cleavage of the fluorogenic substrate, Ac-IEPD-AMC. Increasing concentrations of serpina3n inversely decreased the enzymatic activity of mouse granzyme B as demonstrated by the dose response curve. *[Error bars represent mean ± standard deviation.]*

4.5 Serpina3n inhibits fibronectin fragmentation *in vitro*

The fragmentation of FN is a hallmark of chronic wounds and has many pathophysiological implications as FN is one of the most abundant ECM proteins in granulation tissue, and regulates cell attachment, differentiation and migration during wound healing (42,44,45,188-191). Since GzmB is capable of cleaving FN and SA3N is capable of inhibiting GzmB, we examined whether SA3N can inhibit GzmB-mediated cleavage of FN *in vitro*. After coating wells with mouse FN, incubating them with GzmB in the presence or absence of SA3N and finally collecting the cleavage fragments of the supernatants, We demonstrated that in the wells with mouse FN only or with SA3N only, only full-length FN (denoted by #) was observed as shown in lanes 1, 2, 5 and 6 (Figure 11). We also confirmed that mouse GzmB does cleave mouse FN as observed in lanes 3 and 4 and the cleavage of mouse FN by mouse GzmB was inhibited by SA3N as there were fewer fragments (denoted by ##) observed in lanes 7 and 8 (Figure 11). We also stained for SA3N to confirm that SA3N was indeed added to the designated wells as this was denoted by ^^ in lanes 5, 6, 7, and 8 (Figure 11). In addition, the cleavage assay was also an indirect method of confirming the functional inhibitory activity of SA3N.

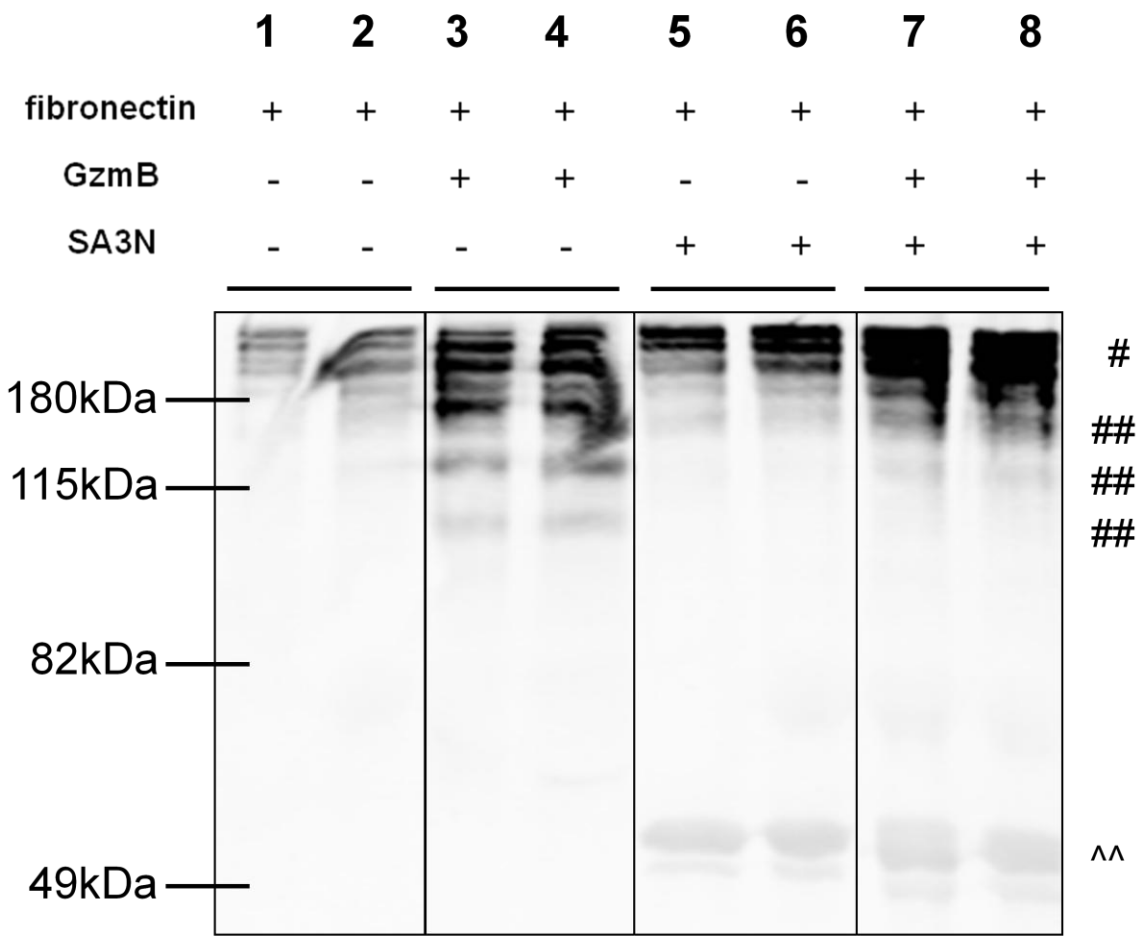

Figure 11 Cleavage profile of granzyme B-mediated fibronectin fragments. Wells were coated with fibronectin and incubated with granzyme B in the presence or absence of serpina3n. Supernatants were subsequently collected and cleavage fragments were assessed by western blot. In all lanes, the full-length fibronectin was observed and denoted by #. In lanes 3 and 4, granzyme B-mediated fibronectin fragments were observed and the resulting cleavage fragments were denoted by ##. Inhibition of mouse granzyme B with serpina3n resulted in fewer fragments as seen in lanes 7 and 8. The presence of serpina3n was denoted by ^^ in lanes 5, 6, 7, and 8.

4.6 Granzyme B promotes detachment of mouse embryonic fibroblasts

The presence of viable and mature fibroblasts in granulation tissue is crucial for proper wound healing as they synthesize much of the collagen and elastic fibers, as well as ECM proteins, to provide the structural and functional framework of the connective tissue in the dermis. Since GzmB is capable of cleaving ECM substrates that are important in cell attachment, ECM integrity and deposition, we investigated the effect of GzmB on the viability of fibroblasts *in vitro*. Upon exogenous GzmB treatment, fibroblasts appeared detached over the 7 hours time period as compared to control cells, which appeared well attached (Figure 12A). The effect of GzmB was abrogated via co-treatment with SA3N, with the attachment of cells comparable to those in the control group (Figure 12A). In addition to the qualitative assessment, we also quantified the relative percentage of adherent cells remaining after GzmB treatment by using a MTS viability assay. Treatment of GzmB led to a dose dependent decrease in adherent fibroblasts, whereas co-incubation with SA3N protected against cell detachment-mediated cell death (Figure 12B).

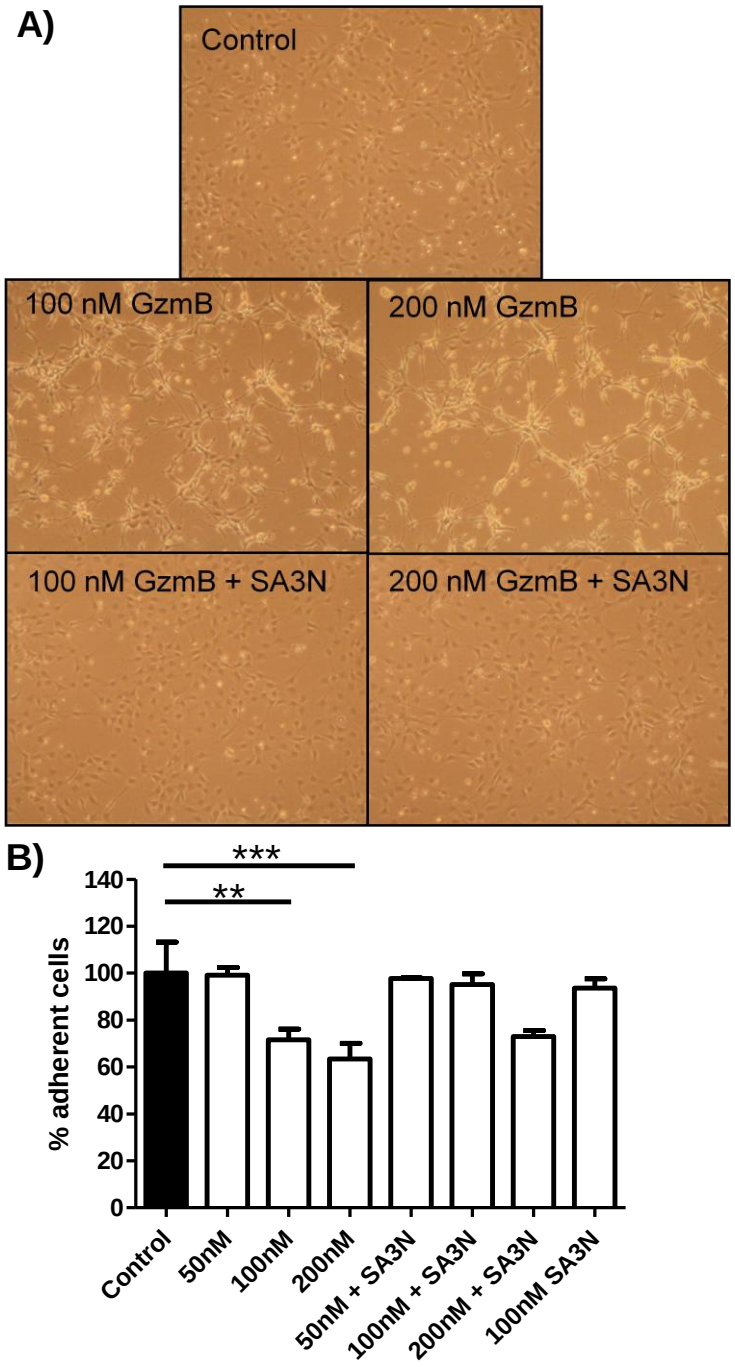

Figure 12 Granzyme B promotes detachment of mouse embryonic fibroblasts. (A) Representative images of mouse embryonic fibroblasts when treated with 50 and 100 nM granzyme B in the absence or presence of 100 nM serpina3n. In control and granzyme B with serpina3n wells, fibroblasts were well attached. In granzyme B only wells, fibroblasts appeared detached. **(B)** Granzyme B reduced adherence of mouse embryonic fibroblasts in a dose-dependent manner and co-treatment with serpina3n reversed the effect. *[Error bars represent mean ± standard deviation. P-values were calculated using one-way ANOVA Dunnett's multiple comparison test. ** denotes $p < 0.01$ and *** denotes $p < 0.001$.]*

4.7 Serpina3n accelerates diabetic wound closure

To investigate whether SA3N accelerates wound closure, digital images of wounds were captured every 3 days during dressing changes at a fixed distance and angle for planimetry measurements. SA3N significantly accelerated wound closure compared to saline vehicle control over the 35 days healing period (Figure 13A and B). In all the animals, wound sizes initially expanded (Figure 13B). The difference in wound closure between the two treatment groups was significantly different by day 12 as the SA3N-treated wounds began to reveal provisional matrix formation on top and surrounding the original wounds as they closed (Figure 13A). By day 18, the percentage of the open wound size was significantly reduced in SA3N-treated animals, with the mean percentage of the open wound size of saline-treated animals being 53.7 ± 28.7% and that of SA3N-treated animals being 16.4 ± 6.1% (Figure 13A and B). Furthermore, by day 35, the wounds from both treatment groups had largely healed as the mean percentage of the open wound size of saline-treated wounds was 16.3 ± 18.0 % and that of SA3N-treated wounds was 0 ± 0 % (Figure 13A and B). In addition, the healing rate of SA3N-treated diabetic animals was intermediate to that of non-diabetic animals and saline-treated diabetic animals as shown in Figure 13B. Prior to surgery, the weights and fasting blood glucose levels were similar in the mice between the two treatment groups (37.5 ± 4.1 g versus 37.2 ± 3.3 g and 345.2 ± 115.9 mg/dL versus 404.5 ± 98.24 mg/dL; Figure 13C and D).

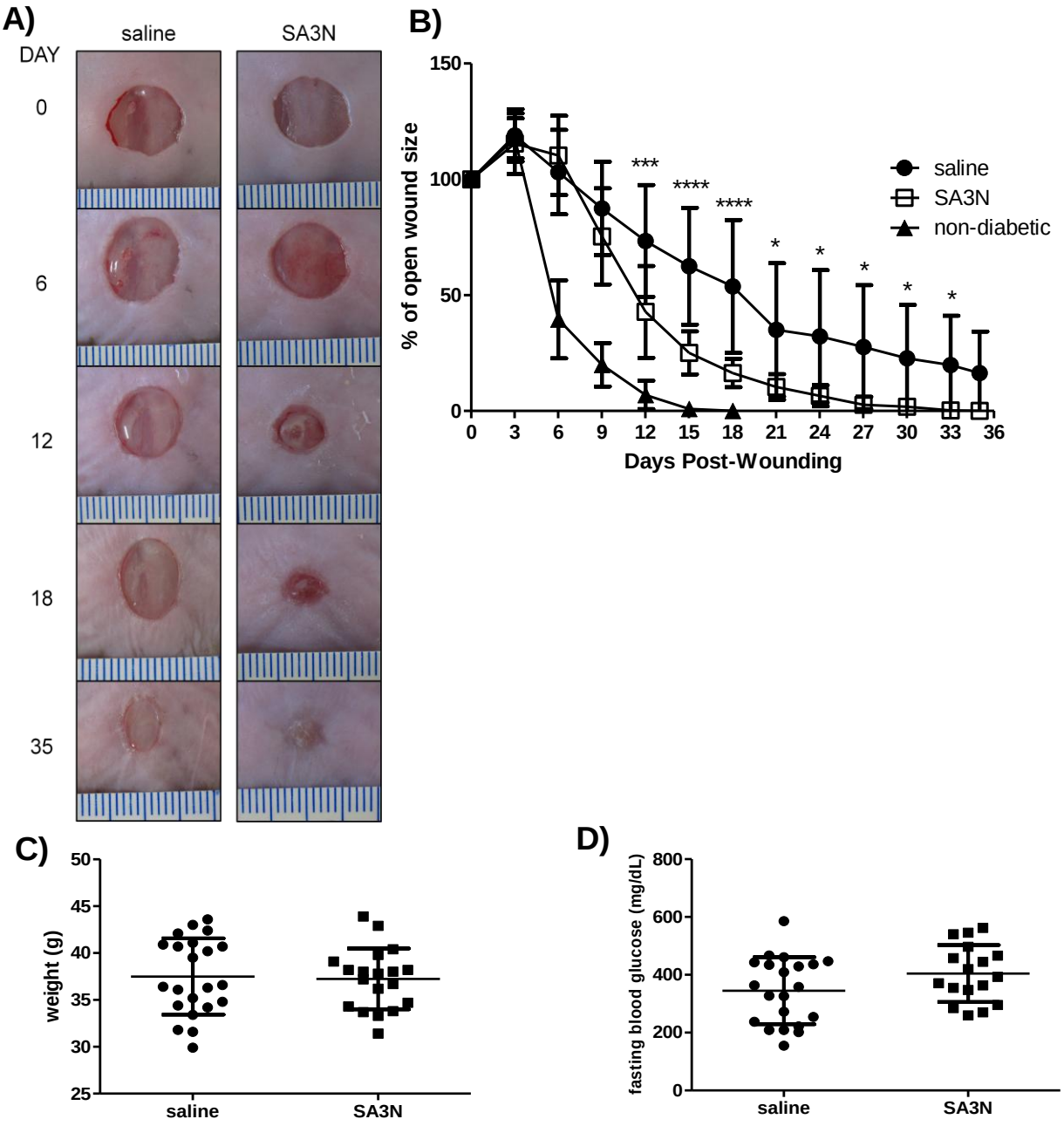

Figure 13 Serpina3n accelerates diabetic wound closure. (A) Representative digital images of non-diabetic and diabetic mice wounds captured over 35 days wound healing period. **(B)** Comparison of the percentages of the open wound size over 35 days healing period between saline- (n = 17), serpina3n-treated diabetic mice (n = 14) and non-diabetic mice (n = 4), showing that serpina3n-treated wounds healed significantly faster than saline-treated wounds and that the healing rate was similar to that of non-diabetic wounds. On the day of surgery, **(C)** there were no significant differences in body weights and **(D)** fasting blood glucose levels between the two groups. *[Error bars represent mean ± standard deviation. P-values were calculated using unpaired Student t-test. * denotes p < 0.05, *** denotes p < 0.001 and **** denotes p < 0.0001 between saline- and SA3N-treated wounds.]*

4.8 Serpina3n increases reepithelialization, contraction and granulation tissue formation in diabetic wounds

During the granulation tissue formation phase of wound healing, reepithelialization and contraction occur to close the wound. More specifically, keratinocytes at the wound edges migrate and hyperproliferate (leading to an increase in epithelial thickness that is eventually resolved) along the epithelial tongue, and fibroblasts differentiate into myofibroblasts in the newly formed granulation tissue to stimulate contraction of the wound. Bisected wound tissues harvested from all animals at days 12, 18 and 35 were sectioned and stained with H&E for histological analyses.

The distances between the leading edges of the epithelial margins (mean distance of saline-treated animals was 7964.1 ± 603.0 μm and that of SA3N-treated animals was 4196.0 ± 1017.8 μm) and the PC muscle layers (mean distance of saline-treated animals was 10151.1 ± 1161.4 μm and that of SA3N-treated animals was 7421.9 ± 875.5 μm) were both significantly shorter in the SA3N-treated animals by day 18 (Figure 14A and B). As such, it can be indirectly interpreted that the rate of reepithelialization was faster than the rate of contraction, which makes the use of Tegaderm® in this model more clinically relevant to human skin. At day 35, there was no difference in the distance of epithelial margins between the two groups; the mean distance of saline-treated animals was 2224.752 ± 3255.771 μm and that of SA3N-treated animals was 0 ± 0 μm (Figure 14B). However, the distance between PC muscle layers was still significantly shorter in the SA3N-treated animals; the mean distance of saline-treated animals was 8406.2 ± 1555.7 μm and that of SA3N-treated animals was 5804.2 ± 607.6 μm (Figure 14B). In both treatment groups, there was a time-dependent decrease of epithelial and PC margins over the 35 days healing period (Figure 14B).

In addition, by day 18, the epithelial thicknesses (mean thickness of saline-treated animals was 59.3 ± 14.7 μm and that of SA3N-treated animals was 89.0 ± 14.4 μm), granulation tissue thicknesses (mean thickness of saline-treated animals was 253.3 ± 57.3 μm and that of SA3N-treated animals was 672.6 ± 171.2 μm) and granulation tissue areas (mean area of saline-treated animals was 0.20 ± 0.02 mm^2 and that of SA3N-treated animals was 2.4 ± 0.9 mm^2) of SA3N-treated wounds was significantly greater than in saline-treated wounds (Figure 14C and D). We found that by day 35, the differences in epithelial and granulation tissue thicknesses, and granulation tissue areas between the saline- and SA3N-treated wounds were not significant (Figure 14D). Specifically, at day 35, the mean epithelial thickness of saline-treated animals was 51.7 ± 26.7 μm and that of SA3N-treated animals was 40.5 ± 8.0 μm, the mean granulation tissue thickness of saline-treated animals was 238.7 ± 112.4 μm and that of SA3N-treated animals was 299.5 ± 95.6 μm and the mean granulation tissue area of saline-treated animals was 0.63 ± 0.33 mm^2 and that of SA3N-treated animals was 0.96 ± 0.25 mm^2 (Figure 14D). Between days 12, 18 and 35, the values of epithelial and granulation tissue thicknesses, and granulation tissue areas, peaked at day 18 in the SA3N-treated wounds, whereas all three values were similar in the saline-treated wounds (Figure 14D).

A)

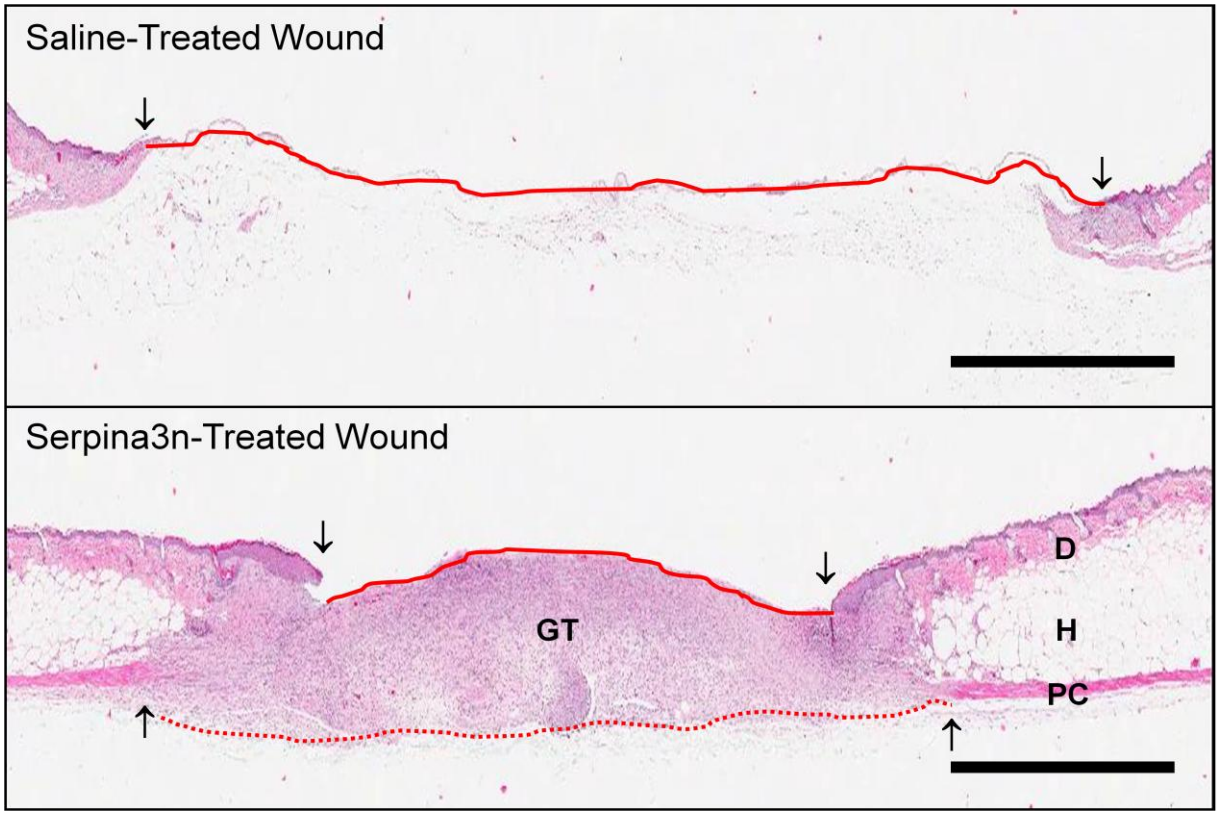
Saline-Treated Wound
Serpina3n-Treated Wound
GT
D
H
PC

B)

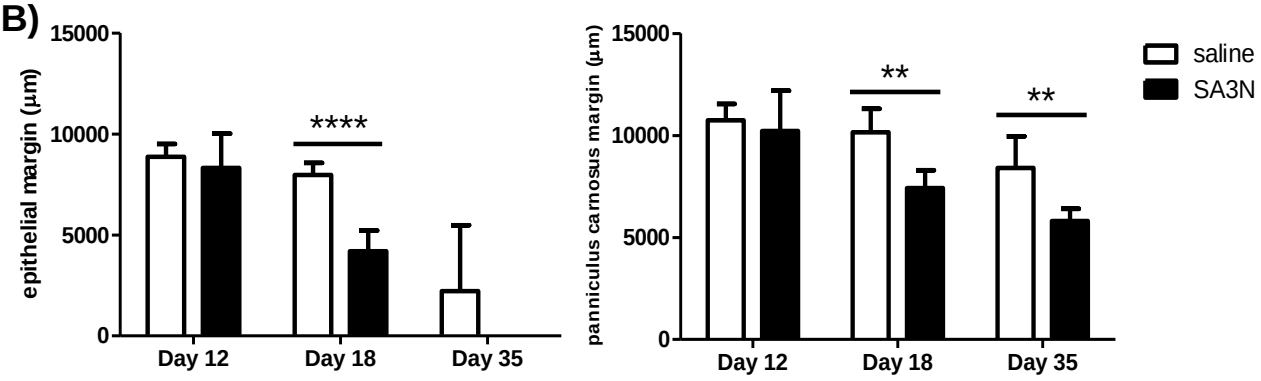
epithelial margin (µm)
15000
10000
5000
0
****
Day 12
Day 18
Day 35
panniculus carnosus margin (µm)
**
**
saline
SA3N

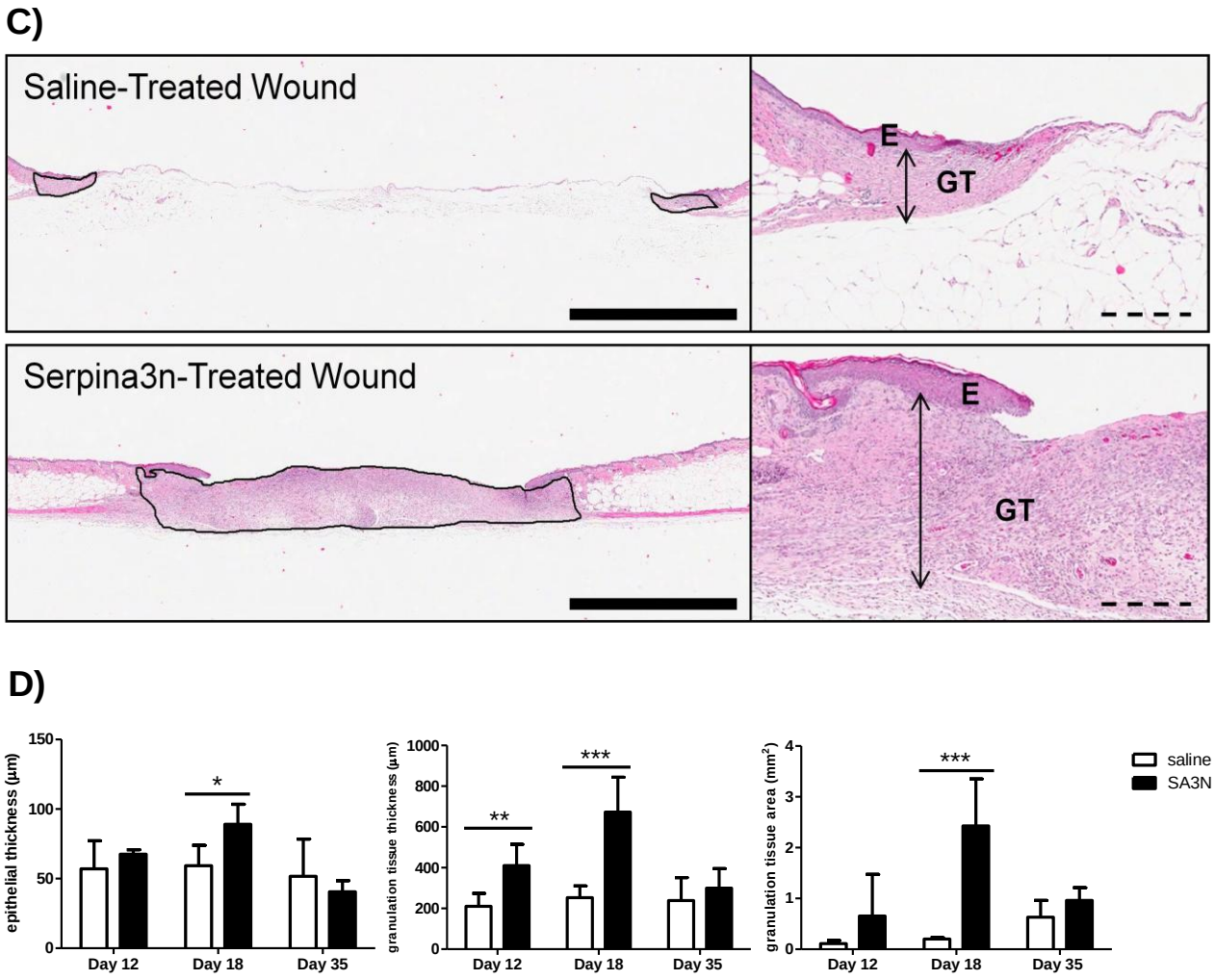

Figure 14 Serpina3n increases wound reepithelialization, contraction and granulation tissue formation in diabetic wounds. (A) Representative histological images of skin sections from day 18 wounds treated with saline and serpina3n. Downward arrows and red solid lines denoted ends of epithelial tongue. Upward arrows and red dotted lines denoted ends of panniculus carnosus layer. **(B)** The distances between the ends of the epidermis and/or the panniculus carnosus were significantly less in serpina3n-treated wounds at days 18 and 35. **(C)** Representative histological images of skin sections from day 18 wounds treated with saline and serpina3n. Black area represented granulation tissue, downward arrows represented epithelial thickness and double arrows represented granulation tissue thickness. **(D)** Increases in both epithelial and/or granulation tissue thicknesses, and overall granulation tissue areas, were observed in serpina3n-treated wounds at days 12 and 18. *[E denotes epidermis, D denotes dermis, H denotes hypodermis, PC denotes panniculus carnosus and GT denotes granulation tissue. Error bars represent mean ± standard deviation. P-values were calculated using unpaired Student t-test. * denotes $p < 0.05$, ** denotes $p < 0.01$, *** denotes $p < 0.001$ and **** denotes $p < 0.0001$. Black scale bars = 2mm. Dotted scale bars = 300µm.]*

4.9 Serpina3n promotes granulation tissue maturation and collagen deposition in the granulation tissues of diabetic wounds

The formation and maturation of granulation tissue is a highly active process. There are many different cell types and ECM proteins in the granulation tissue and their presence ensure that the newly deposited ECM is functional for wounds to resolve. The maturation of the granulation tissue can consequently affect collagen deposition during tissue remodeling in order to restore tensile strength of the wounded skin.

Using immunohistochemistry, skin sections from the middle of wounds were stained for Ki67, CD31, vimentin and α-SMA (Figure 15A). They are common markers for cellular proliferation, vasculature, mesenchymal cells and contractile myofibroblasts respectively. At day 18, the granulation tissues of SA3N-treated wounds exhibited significantly greater expression of Ki67 (the number of positive cells per area in saline-treated animals was 14.4 ± 4.9 cells and the number in SA3N-treated animals was 67.8 ± 34.2 cells), CD31 (percentage of positive staining per area in saline-treated animals was 0.3 ± 0.1% and percentage in SA3N-treated animals was 1.4 ± 0.5%) and α-SMA (percentage of positive staining per area in saline-treated animals was 2.1 ± 2.8% and percentage in SA3N-treated animals was 14.4 ± 2.7%) as shown by Figure 15B to D. There was no notable difference in the relative expression of vimentin (percentage of positive staining per area in saline-treated animals was 3.8 ± 1.6% and percentage in SA3N-treated animals was 5.3 ± 2.3%) when comparing the saline- and SA3N-treated wounds (Figure 15E). This was an indication of, overall, more mature granulation tissues by day 18 in the SA3N-treated wounds when the provisional matrices had largely formed.

Furthermore, we examined the wounded tissues at day 35 and noted that there was no difference in the immunohistochemical staining of Ki67, CD31, vimentin and α-SMA, which indicates that the proliferative activity and the number of blood vessels, mesenchymal cells and contractile myofibroblasts were similar between the saline- and SA3N-treated wounds by then. Specifically, the number of Ki67 positive cells per area in saline- and SA3N-treated animals was, respectively, 15.0 ± 18.0 cells and 19.3 ± 11.6 cell, and the percentage of CD31 positive staining per area in saline- and SA3N-treated animals was respectively, 3.0 ± 1.9 % and 1.8 ± 1.2% (Figure 15B and C). The percentage of vimentin positive staining per area in saline- and SA3N-treated animals was respectively, 2.6 ± 2.4% and 4.4 ± 3.4%, and the percentage of α-SMA positive staining per area in saline- and SA3N-treated animals was respectively, 0.42 ± 0.83% and 0.62 ± 0.62% (Figure 15D and E).

In the SA3N-treated wounds, we observed that the number of Ki67 positive cells, and the percentages of CD31 and α-SMA positive staining per area, peaked at day 18 and the values all gradually decreased by day 35 (Figure 15B to D). This trend is similar to that observed in wounded non-diabetic animals whereby we detected peaked values at day 12 and notably decreased values by day 31 (Figure 16A to C). In contrast, the saline-treated wounds did not exhibit the same trend as the values were similar across the three time points for the number of Ki67 positive cells, and the percentages of vimentin and α-SMA positive staining per area (Figure 15B to D).

As previously noted, fibroblasts and myofibroblasts are important in synthesizing collagen. Using Masson's trichrome staining for collagen, the SA3N-treated wounds had greater green-blue positive staining for collagen in comparison to saline-treated wounds on days 18 and

35. The percentage of collagen per area in saline-treated animals was respectively, 7.4 ± 2.0% and 25.0 ± 22.6%, and percentage in SA3N-treated animals was respectively, 24.8 ± 7.0% and 55.4 ± 18.0% (Figure 15F). In all the wounded diabetic and non-diabetic tissues, we observed that collagen content was highest at the latest time points, either day 35 or 31 (Figure 15F and 16E). We also specifically examined the levels of fibrillar collagen in the remodeling wounded tissues (at day 35) by using picrosirius red staining and found that the percentage of fibrillar collagen per area in saline- and SA3N-treated wounds was 6.7 ± 8.3% and 6.3 ± 4.6% (Figure 15G). The analyses of picrosirius red staining revealed that there was no difference in the percentage of fibrillar collagen per area between saline- and SA3N-treated diabetic wounds and that this value was also similar in non-diabetic wounds as the percentage of fibrillar collagen per area was 10.1 ± 5.5% at day 31 (Figure 15G).

A)

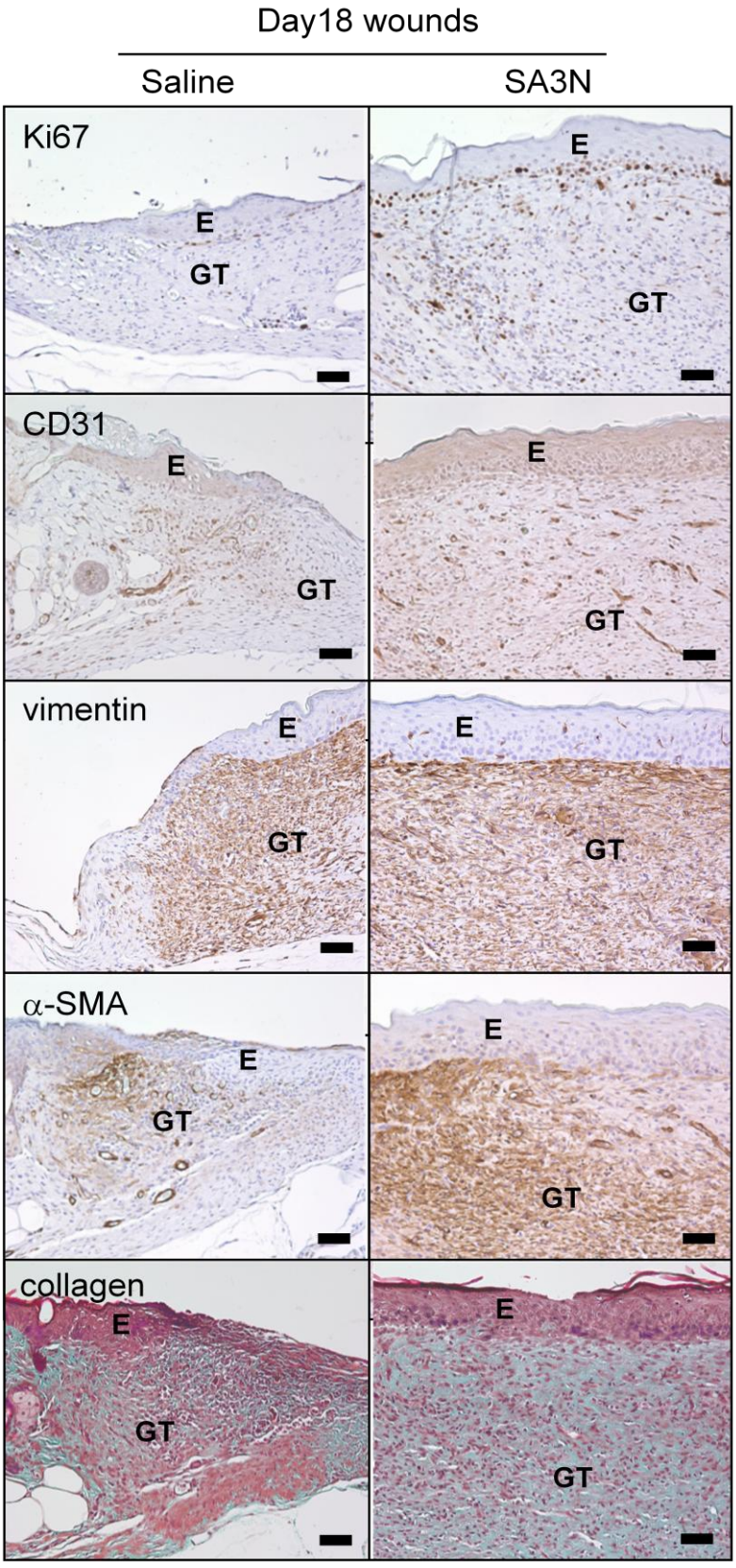
Day18 wounds
Saline
SA3N
Ki67
E
GT
E
GT
CD31
E
GT
E
GT
vimentin
E
GT
E
GT
α-SMA
E
GT
E
GT
collagen
E
GT
E
GT

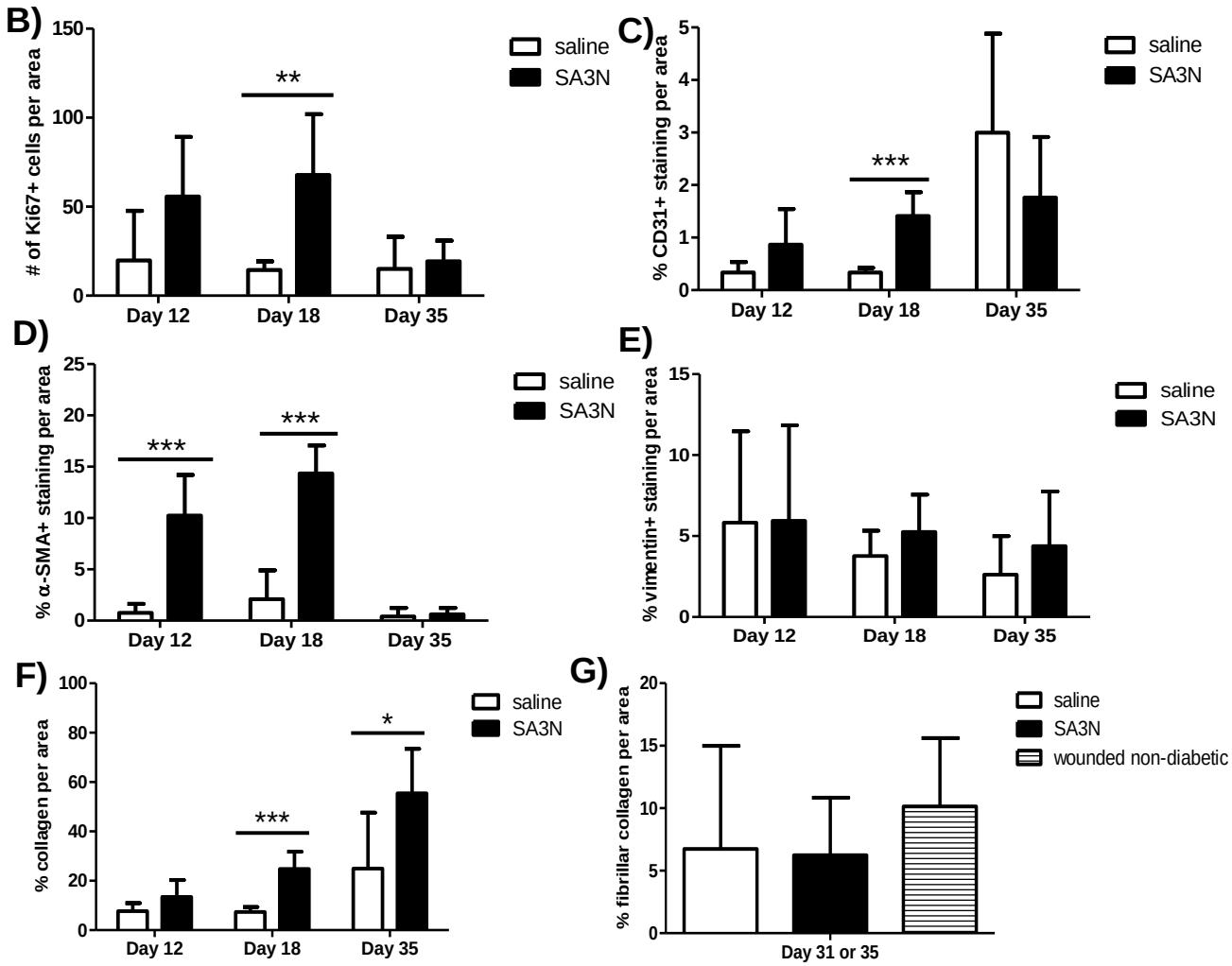

Figure 15 Serpina3n promotes granulation tissue maturation and collagen deposition in the granulation tissues of diabetic wounds. (A) The first 4 panels represented immunohistochemical staining of skin sections for Ki67 (a marker of proliferation cells), CD31 (a marker of vasculature), vimentin (a marker of mesenchymal cells) and α-smooth muscle actin (a marker of contractile myofibroblasts), where positive staining was coloured brown. The last row of panels represented Masson's trichrome staining of skin sections where keratin and muscle fibers appeared red and collagen appeared blue-green. Greater number and positive staining of **(B)** proliferating cells, **(C)** blood vessels and **(D)** myofibroblasts with contracting capability were observed in wounds treated with serpina3n at day 18. **(E)** There was no difference in levels of vimentin between the saline- and serpina3n-treated groups at all 3 time points. **(F)** Analyses of Masson's trichrome staining (left) revealed that there was increased percentage of collagen in SA3N-treated wounds at both days 18 and 35 when compared to saline-treated wounds. **(G)** Analyses of picrosirius red staining (right) revealed that there was no difference in percentage of fibrillar collagen between the two treatments at day 35 as well as when compared to wounded non-diabetic wounds at day 31. *[E denotes epidermis and GT denotes granulation tissue. Error bars represent mean ± standard deviation. P-values were calculated using unpaired Student t-test. * denotes $p < 0.05$, ** denotes $p < 0.01$ and *** denotes $p < 0.001$. Black scale bars = 50µm.]*

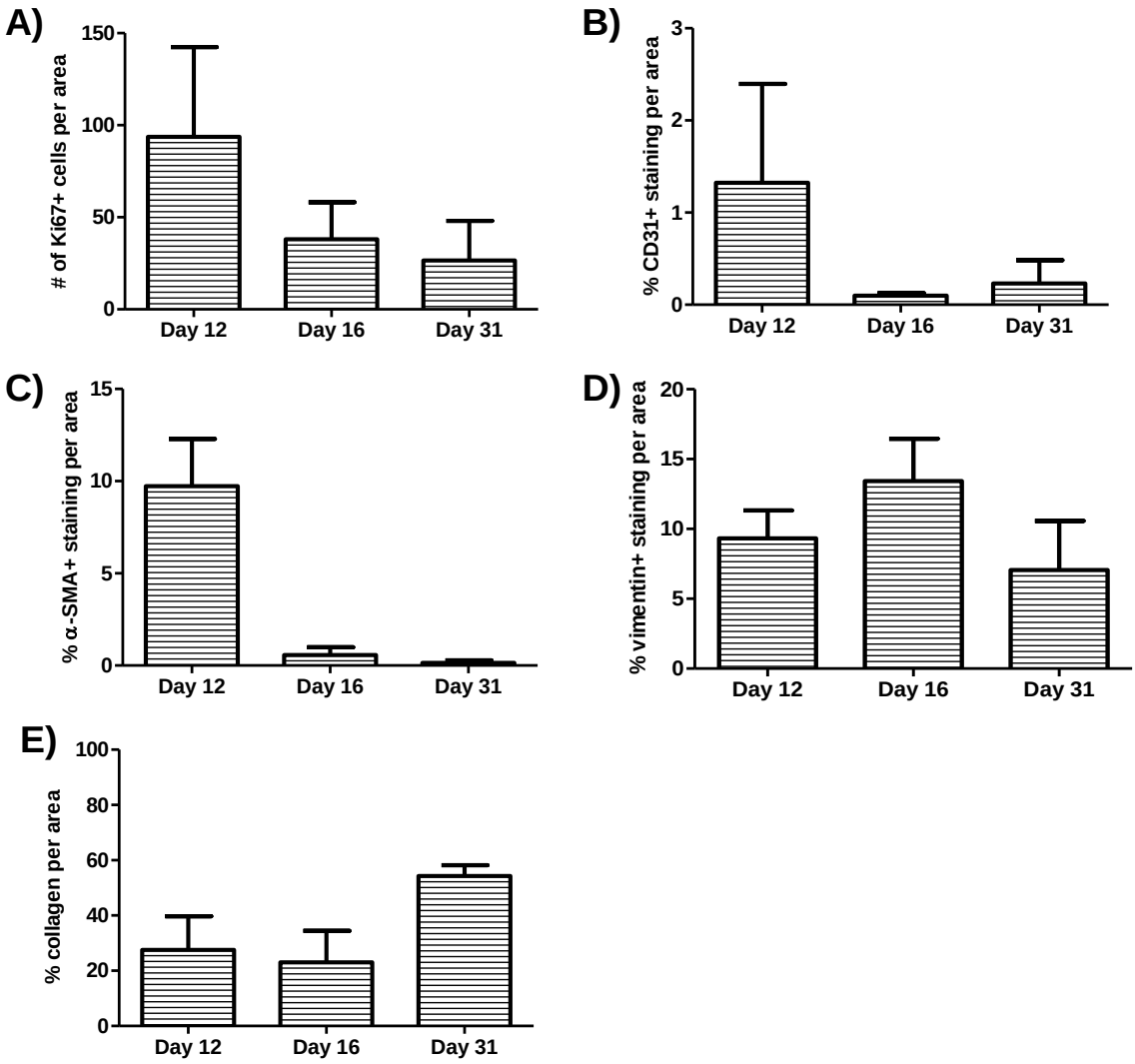

Figure 16 Immunohistochemical and staining profiles of granulation tissues in non-diabetic wounds. (A) The number of Ki67 positive cells, and **(B)** the percentages of CD31 and **(C)** alpha-smooth muscle actin positive staining per area ere highest at day 12 and decreased by days 16 and 31. **(D)** The percentage of vimentin positive staining per area was highest at day 16. **(E)** The percentage of collagen positive staining per area was highest at day 31. *[Error bars represent mean ± standard deviation.]*

4.10 Serpina3n inhibits the degradation of fibronectin in diabetic wounds

In the previous section, we showed that SA3N inhibited GzmB-mediated cleavage of FN *in vitro*. To examine FN content and possibly FN fragmentation *in vivo*, we homogenized wound tissues from saline- and SA3N-treated wounds, and subsequently, probed for FN by western immunoblotting. There was no difference in full-length FN content between the two treatment groups on day 12 (Figure 17). However, the SA3N-treated wounds were found to have significantly more full-length FN after normalizing to GAPDH when compared to saline-treated wounds at day 18 (a 44% increase in relative FN level), thereby indicating that SA3N protected the degradation of FN (Figure 17).

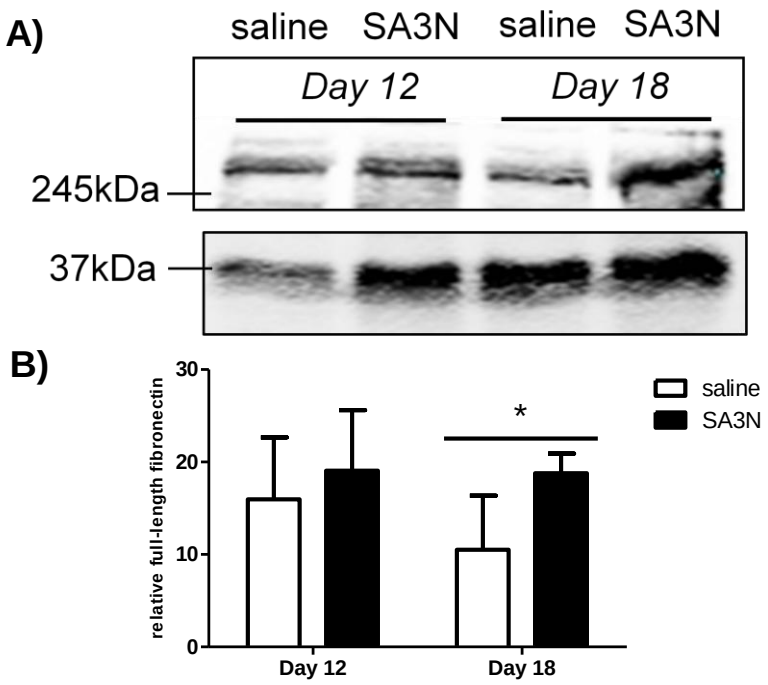

Figure 17 Serpina3n inhibits the degradation of fibronectin in diabetic wounds. (A) Representative western blot probing for fibronectin in skin homogenates collected from wounds treated with saline and serpina3n. The top band is full-length fibronectin and the bottom is loading control, GAPDH. **(B)** The full-length fibronectin content was significantly greater in homogenates of serpina3n-treated wounds, indicating less cleavage when normalized to GADPH and analyzed by densitometry. *[Error bars represent mean ± standard deviation. P-values were calculated using unpaired Student t-test. * denotes $p < 0.05$]*

Chapter 5: Discussion

The main purpose of this thesis was to determine whether GzmB contributes to the pathogenesis of chronic wound healing in individuals with diabetes. Specifically, we utilized a genetically-induced type II diabetic mouse model of delayed wound healing to mimic the underlying hyperglycemic condition associated with diabetic patients. Instead of a systemic knockout study, we investigated whether local inhibition of extracellular GzmB could accelerate wound healing in this model by using a potent GzmB inhibitor, SA3N.

Firstly, the delayed wound healing phenotype exhibited by the db/db mice that has been widely reported in current literature was confirmed (183,185,186). By day 18, all the wounds in the lean, normoglycemic non-diabetic mice were largely closed, whereas in comparison, the majority of the wounds in the obese, hyperglycemic diabetic mice closed by day 35 instead (Figure 7 and 13). Therefore, the wounds in the non-diabetic mice are considered acute models of wound closure, whereas the wounds in the diabetic mice are a model of chronic closure due to delayed wound healing. Mice are loosely-skinned, which means healing occurs predominantly due to the wound contraction, compared to humans where healing occurs due to both wound contraction and reepithelialization. We therefore employed a transparent Tegaderm® dressing in the procedures to reduce contraction and promote reepithelialization. This was successful, as the closure of epithelial margins was shorter than that of PC margins in all the treated diabetic mice (Figure 14). All of these results supported the usage of db/db mice and Tegaderm® dressing to mimic wound healing in humans.

The interaction between cells and the ECM is essential in creating a microenvironment that promotes normal acute wound healing (14). Abnormal levels of proteases can disrupt ECM integrity and disturb this microenvironment, leading to the development of chronic wounds. We

demonstrated that in comparison to non-diabetic wounds, diabetic wounds exhibited higher GzmB expression in mice (Figure 8). There have been various studies showing elevated levels and increased proteolytic activity of MMPs in human chronic wound fluid (37-44). In addition to MMPs, groups also reported elevated activity of plasmin, neutrophil elastase and cathepsin G in human chronic wound fluid, all of which are part of the same serine protease family as GzmB (42-44). It is therefore possible that GzmB also exhibits elevated activity in chronic human wounds, in addition to the chronic mouse wounds identified in this thesis. So far, there have been no reports of the quantification of GzmB in human samples. Our group is currently collecting diabetic wound fluid samples from patients to assess the levels and proteolytic activity of GzmB and to further support our experimental results with clinical evidence.

In support of my hypothesis, we demonstrated that wound healing, including both reepithelialization and contraction, was significantly accelerated in diabetic mice treated with SA3N, a GzmB inhibitor. Furthermore, we noted that SA3N-treated wounds healed significantly faster than saline-treated wounds beginning at day 12 and until day 33 (Figure 13 and 14). Based on the wound pictures captured, this was around the period when the initial hemostasis and inflammation phases had subdued as the wounds appeared less red, and the granulation tissue formation phase had begun with the formation of the white-coloured provisional matrix as observed in the SA3N-treated wounds (Figure 13). As such, we further examined how SA3N may be accelerating wound healing by harvesting skin tissues at three time points, days 12, 18 and 35, in an attempt to capture the latter two phases of wound healing.

During granulation tissue formation, non-contractile fibroblasts secrete ECM proteins, PGs and collagen. As wound healing progresses, these fibroblasts differentiate into contractile myofibroblasts that enable contraction. In earlier experiments of this thesis, we observed a

reduction in fibroblast attachment in cultured mouse fibroblasts treated with GzmB *in vitro*. Conversely, cultured mouse fibroblasts that were treated with both GzmB and SA3N were well-attached (Figure 12). Of relevance, we confirmed that FN was cleaved by GzmB and that this cleavage was inhibited when GzmB was incubated together with SA3N (Figure 11). In support of our *in vitro* findings, homogenized tissues from the SA3N-treated wounds exhibited a greater level of full-length FN when compared to saline-treated wounds (Figure 17). The observations associated with impaired fibroblasts and that FN fragmentation could be contributing to functional defects in fibroblasts are supported by studies reported in the literature (171,188,190). In particular, Stanley *et al*. noted that attachment efficiency and migration of primary human gingival fibroblasts and human fibrosarcoma cells decreased when coated on a matrix containing fragmented FN (188). They also observed that cells seeded on fragmented FN exhibited less filopodia spreading and formed more clusters than cells plated on full-length intact FN (188). Grinnell *et al*. also reported similar findings where they observed baby hamster kidney fibroblasts rounding up when the cells were treated with chronic wound fluid containing fragmented FN and vitronectin (190). In addition, Buzza *et al*. have also shown that GzmB is responsible for cell detachment and the reduced spreading and migration of many different cell lines, including primary human vascular endothelial and human breast adenocarcinoma cells (171). Therefore, when considering the results from the studies altogether, it is highly possible that FN fragmentation impairs the abilities of fibroblasts to properly attach and to mature. This is expected as FN is a scaffolding protein and the attachment of fibroblasts to FN is mostly mediated through integrins, including $\alpha 4\beta 1$, $\alpha 5\beta 1$ and fibrinogen (192). In addition, phosphorylation of focal adhesion kinase and activation of mitogen-activated kinase have been shown to induce adhesion in fibroblasts isolated from Balb/c mice as well as cultured rat embryonic fibroblasts (193,194).

Based on these previous studies done by others and from the results, it is possible that GzmB-mediated FN cleavage may impair fibroblasts and thus be contributing to the delayed wound closure in saline-treated wounds. However, we were unable to do an exact correlation study as the site of FN cleavage by GzmB is still currently unknown. Although the RGD integrin site on FN has been suggested as the possible cleavage site, it would still be useful to determine the exact cleavage site so that recombinant FN fragments can be synthesized. This would prompt further investigations into determining if, and which, GzmB-mediated FN fragments are responsible for defects in fibroblasts and pathophysiological implications in chronic wounds. Interestingly, FN fragmentation is also a hallmark of chronic wound fluid with fragment sizes ranging from 20 to 202 kDa as reported by previous studies (42,44,45,188-191). Rao *et al.*'s group incubated FN with serine, cysteine or acid protease inhibitors to chronic wound fluid samples which contained elevated levels of native proteases. They attributed serine proteases to be the main contributor of FN fragmentation in chronic wound fluid samples, but the specific serine protease has yet to be determined (189). Therefore, it is possible that GzmB may also be contributing to FN fragmentation.

We found that by day 18, there were more granulation tissues formed in SA3N-treated wounds and that these were also more active as suggested by increased cellular proliferation and blood vessel formation (Figure 14 and Figure 15). The increase in Ki67 expression highlighted the proliferative state of the granulation tissues. The granulation tissues should be highly proliferative and decreased proliferative capacity have been found in fibroblasts isolated from human chronic wound samples, indicating that many of the fibroblasts are in a senescent state even though Ki67 staining does not specifically stained for proliferation of fibroblasts (51-54). The increase in CD31 expression should also promote wound healing as angiogenesis provides oxygen and nutrients to

support proliferating cells. Previous studies have shown that GzmB-mediated FN cleavage contributes to impaired angiogenesis and vascular permeability through the disruption of the interaction between FN and endothelial cells, which leads to the release of VEGF (172,175). As such, inhibition of GzmB activity can be expected to promote vascularization in chronic wounds and augment healing.

We observed that the granulation tissues of SA3N-treated wounds featured elevated levels of contractile myofibroblasts and increased collagen deposition when compared to saline-treated wounds on days 12 and 18 (Figure 15). This was expected as the differentiation of fibroblasts to myofibroblasts and contraction is largely dependent on three factors: TGFβ-1, the ED-A domain of FN and mechanical tension (28,30). Typically, cellular FN is synthesized without an ED-A domain (34). However, during wound healing, endothelial cells and fibroblasts synthesize a splice variant of the cellular FN containing an extra ED-A domain (195). In order for proper differentiation of fibroblasts to occur, TGFβ-1 interacts with the ED-A domain of FN to trigger downstream signaling and induction to a myofibroblast-like phenotype by increasing expression of α-SMA (36,195). The increase in α-SMA expression supported the observation that wound closure was accelerated in SA3N-treated mice as wound contraction is one of the two means by which wound closes and myofibroblasts expressing α-SMA are largely responsible (Figure 13). In addition, it is possible that GzmB cleavage of FN may disrupt the interaction between TGFβ-1 and the ED-A domain, thus leading to the decreased contractile ability of myofibroblasts and collagen deposition that were observed in the granulation tissues of saline-treated wounds since saline-treated wounds also feature increased FN degradation (Figure 17).

The formation, maturation and deposition of the ECM in the granulation tissue ensure that there is proper functional tissue restoration during the subsequent remodeling phase as differentiation of fibroblasts to myofibroblasts is critical for wound contraction and for the production of collagen fibers. By day 35, the number of proliferating cells, blood vessels, mesenchymal cells and contractile myofibroblasts had decreased from day 18 in the SA3N-treated wounds and that there was no difference between the saline- and SA3N-treated wounds (Figure 17). This was expected as by the time the wound closed, granulation tissues had largely been formed and that collagen deposition was taking place to remodel the tissues, therefore requiring very minimal cells and blood vessels. The trend associated with changes in the granulation tissues was also observed in the non-diabetic wounds (Figure 15 and 16). However, the majority of the values peaked at day 12, a time point that was earlier than the SA3N-treated wounds, which peaked at day 18 (Figure 15 and 16). This was expected since the healing rate of the non-diabetic wounds were faster than the SA3N-treated wounds (Figure 14). A similar trend was not observed with the granulation tissues of the saline-treated wounds. This is probably because we did not collect the skin tissues at the appropriate time in the saline-treated wounds. As healing rate was slower in the saline-treated wounds but eventually caught up by day 35, we suspected that a trend in the saline-treated wounds may be established if I harvest tissues sometime between days 18 and 35. Vimentin is the major component of intermediate filaments and is expressed abundantly by cells of mesenchymal origin (196). Specifically, in the skin, cells of mesenchymal origin include fibroblasts and endothelial cells (196). As both fibroblasts and endothelial cells are important in orchestrating the granulation tissue formation phase, a surge in the levels of vimentin was expected. However, we found that the levels of vimentin were similar across all three time points for diabetic and non-diabetic wounds (Figure 15). This may be due to the fact that not all

fibroblasts are of mesenchymal origin and therefore, some may not express vimentin (25). It is possible that not all the fibroblasts that are in the granulation tissues was detected and additional fibroblast markers may need to be used since there is no single reliable fibroblast immunohistochemical marker.

The tissues collected at the last time point enabled the detection of collagen fibers in the remodeling tissues. When we examined collagen deposition by analysis of Masson's trichrome staining, there was a time-dependent increase in collagen in both treatment groups (Figure 15). This was expected as granulation tissue formation in the wounds eventually resolves and proceeds to collagen production during the final phase of tissue remodeling. We found that collagen content in SA3N-treated wounds was greater than in saline-treated wounds at day 35 (Figure 15). Conversely, analysis of picrosirius red staining revealed that the collagen content in SA3N-treated wounds was similar to the content in saline-treated wounds and also comparable to the content in wounded non-diabetic wounds (Figure 15 and 16). With Masson's trichrome staining, all types of collagen fibers appeared a blue-green colour that is considered positive in the analysis. In contrast, picrosirius red staining was more specific in its detections as only fibrillar collagen appeared the reddish color under polarized light that is considered positive in the analysis (197). Therefore, our results suggested that there was no difference between the fibrillar collagen that is in the remodeling diabetic tissues of saline- and SA3N-treated wounds but by day 35, the SA3N-treated wounds had greater amount of collagen. This may be of benefit as more collagen can subsequently contribute to an increase in tensile strength of the remodeled tissues. This is important as many chronic wounds are fragile and do not heal properly due to repeated tearing so treatment that allows for healing with greater tensile strength would be clinically relevant. However, collagen analysis using multi-photon microscopy and long-term studies need to be

conducted to determine whether the increase in collagen in SA3N-treated wounds would eventually resolve as continuous presence of excessive collagen in tissues can lead to fibrosis, and thus lead to impaired skin function.

In this thesis, we observed that GzmB expression was prominent in wound edges, granulation tissue and remodeling tissues during the latter phases of wound healing when the diabetic wounds have largely been reepithelialized (Figure 8). This coincidentally correlated with our other observation that full-length FN content differed in saline- and SA3N-treated wounds at day 18 but not day 12, supporting the proposed time line and the possibility that SA3N inhibition of GzmB activity prevented the degradation of FN in the latter stages (Figure 16). Furthermore, GzmB's cleavage of decorin has been implicated in mouse models of skin aging and AAA (139,161). As decorin is important in collagen fibrillogenesis and organization, both of which are most critical during granulation tissue formation and tissue remodeling, this is another line of evidence suggesting why GzmB expression may be highest then.

5.1 Limitations

Likewise with all animal models, there are some obvious shortfalls when drawing comparisons to humans. First of all, the manifestations of chronic wounds in mice and humans are different. In mice, all wounds eventually heal and chronic wounds are merely wounds that exhibit delayed healing as shown even though saline-treated wounds showed slower healing than SA3N-treated wounds, the former eventually caught up, and by day 35, wounds from both treatment groups were healed (Figure 13). In contrast, in humans, chronic wounds often do not heal and in turn become infected, which can result in amputations. However, the usage of db/db mice as a model of delayed wound healing is still extremely useful as the goal of human wound therapy is to

promote and accelerate wound healing such that an acute wound does not become a chronic wound.

In addition, it should be noted that the most common location for the development of diabetic skin ulcers in humans is the foot due to continuous pressure on the ulcerated sites. Since one of the treatments for diabetic ulcers is mechanical relief to offload foot pressure, our model mimics such an environment as wounds were created on the mid-lower backs of the mice where there is no obvious pressure pressing against the wounds.

Another caveat is that the db/db homozygous mice contain a spontaneous mutation in the leptin receptor which consequently leads to a complete loss of function. However, binding of leptin to the leptin receptor in the hypothalamus has been shown to be involved in the modulation of wound repair through promoting reepithelialization (198). As such, there may be some implications when the leptin receptor is impaired (199).

Finally, the db/db mice are a monogenic model of type II diabetes whereas type II diabetic patients confer a more polygenic profile. Even though some polygenic diabetic mice strains, including the TallyHo and NONcNZO10, have been developed recently, their usages still remain limited as they have, largely, not been fully characterized yet (200-202). It would be valuable if similar positive results can be demonstrated with the use of another type II diabetic mouse model, such as the ob/ob diabetic mice, as well as other type I diabetic mouse models that also exhibit delayed wound healing, such as the streptozotocin-induced diabetic mice (203,204)

5.2 Future studies

The focus of this thesis was to investigate the effect of inhibiting GzmB cleavage of ECM proteins in wound healing. However, we observed that GzmB colocalized with mast cells in this

model and that there were immune cells, notably macrophages, and CD3+ lymphocytes present in the diabetic wounds (Figure 9). As inflammation is an integral aspect of wound healing, it would be of significance to examine the role of extracellular GzmB in modulating the immune system, especially since the intracellular role of GzmB is closely related to CTLs and NK cells.

In addition, there have been no studies so far which have studied the effect of SA3N on GzmB-mediated apoptosis *in vivo*. Apoptosis is also an integral part of wound healing and has been shown to aid in the removal of cells, including inflammatory cells, fibroblasts and myofibroblasts, so that the phases of wound healing can proceed in an orderly manner (31,205). Since intracellular GzmB is involved in many apoptotic pathways, it is possible that inhibition by SA3N would also contribute to wound healing. In addition, apoptosis may be a reason why the cellular profile of remodeling tissues at day 35 decreased in comparison to granulation tissues at day 18, since apoptosis of myofibroblasts should be highly regulated to prevent excessive scar growth.

5.3 Therapeutic strategies

Of relevance, it is worthwhile to note that SA3N is a broad spectrum serine protease inhibitor. Although SA3N is a GzmB inhibitor, as shown in Figure 10 and 11, it can also inhibit chymotrypsin, neutrophil elastase and cathepsin G (154,161,162). However, as SA3N had previously been utilized in an animal model of AAA where the rupture rates and ECM remodeling was similar to that from a GzmB knockout study, it is highly plausible that SA3N's effect on GzmB is much more potent than on these other serine proteases (141,161). In addition, the human α1-antichymotrpysin, which is an orthologue of SA3N, does not inhibit GzmB. Therefore, when a

small molecule-specific GzmB inhibitor becomes available, it would be beneficial to use that to repeat some experiments from this thesis.

In this thesis, we administered SA3N every 3 days with the first administration being immediately after wounding. We observed a significant difference between the saline- and SA3N-treated wounds when the provisional matrix was forming at day 12 (Figure 13). It would be interesting to determine whether it is necessary to administer SA3N this early on and establish a time line by which inhibition of GzmB may be the most significant. This would further contribute to the therapeutic value of potential GzmB inhibitors.

Chapter 6: Conclusion

As current treatment strategies remain grossly inadequate, diabetic skin ulcers are a major public health problem and are the leading cause of lower limb amputations associated with diabetic patients. In diabetic patients, the normal continuum of wound healing is disrupted, and wounds enter a chronic, non-healing state characterized by persistent inflammation, enhanced proteolytic activity and impaired ECM deposition.

Even though MMPs were once believed to be the major culprits in impaired wound healing, it is now recognized that they are essential for normal wound healing. As it becomes difficult to appropriately tether the levels of MMPs in chronic wounds to maximize their beneficial effect in modulating the immune system while minimizing their detrimental effect in degrading growth factors, I proposed that inhibition of GzmB may be more effective at promoting acute wound healing.

GzmB has traditionally been studied as a serine protease that is released from CTLs and NK cells and induces apoptotic cell death intracellularly. However, many lines of evidence now suggest that GzmB can accumulate in the extracellular milieu and is capable of cleaving many ECM proteins that are important in wound healing.

In this thesis, using a genetically-induced type II diabetic model of delayed wound healing, elevated levels of GzmB were expressed throughout wound edges and newly-formed granulation tissues. We also observed that the majority of GzmB colocalized with mast cells. Furthermore, we demonstrated that the inhibition of GzmB by a serine protease inhibitor, SA3N, can accelerate wound healing by promoting maturation of granulation tissue, inhibition of GzmB-mediated FN cleavage and stimulation of collagen deposition in remodeling tissues. The results, as summarized in Figure 18, suggest that GzmB might be contributing to the pathogenesis of diabetic wound

healing, and offer preliminary evidence that a GzmB inhibitor may be a relevant therapeutic target in wound management therapy.

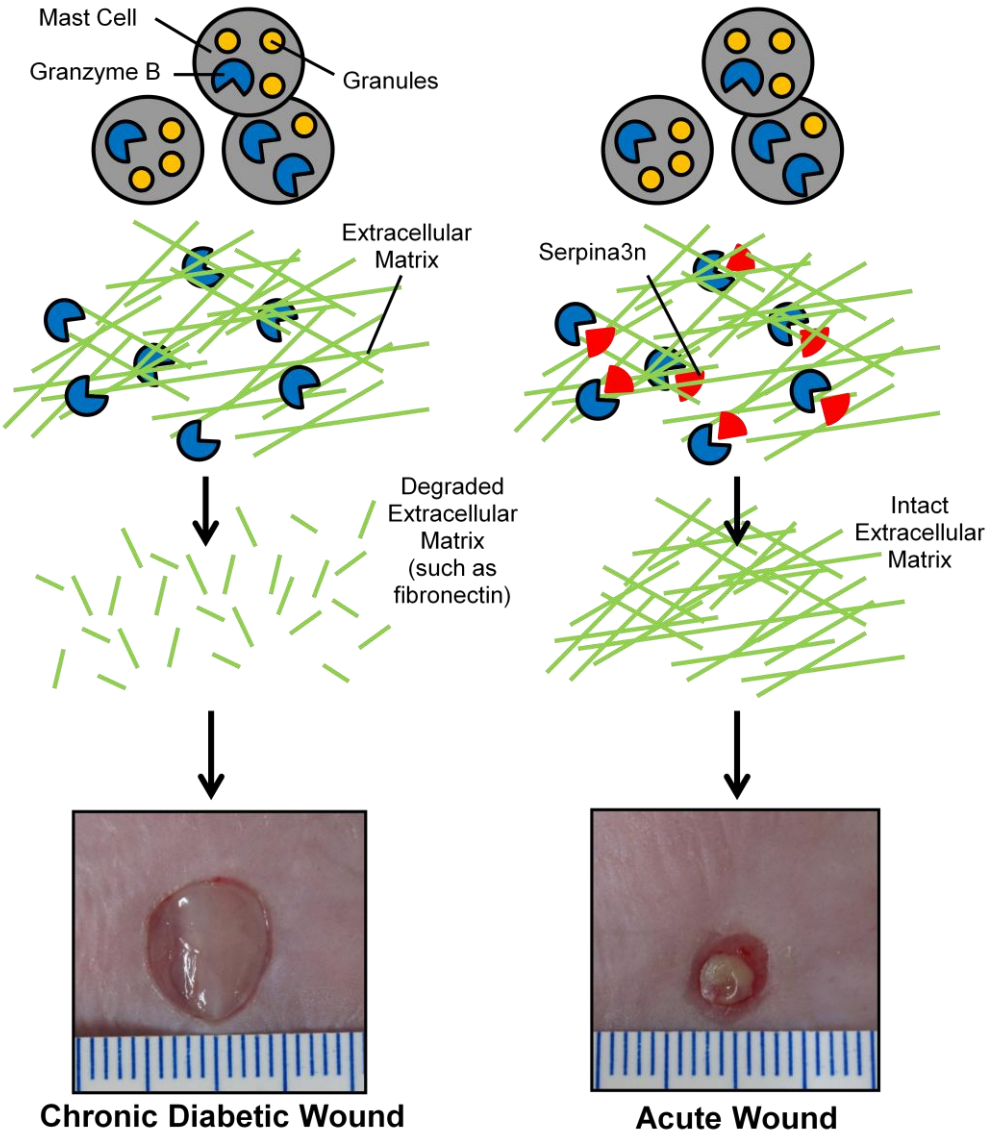

Figure 18 Possible mechanism by which serpina3n accelerates wound healing. We proposed that in chronic wounds, excessive granzyme B is secreted by mast cells and disrupts the integrity of the extracellular matrix. Specifically, granzyme B can alter fibroblast attachment and degrade fibronectin, leading to the development of chronic wounds due to impaired granulation tissue formation. In this thesis, we demonstrated that serpina3n's inhibition of granzyme B preserves the integrity of the extracellular matrix and enables maturation of granulation tissues and collagen deposition, thus preventing acute wounds from developing into chronic wounds.

Bibliography

(1) McLafferty E, Hendry C, Alistair F. The integumentary system: anatomy, physiology and function of skin. Nurs Stand 2012 Sep 19-25;27(3):35-42.

(2) Burgeson R, Christiano A. The dermal-epidermal junction. Curr Opin Cell Biol 1997 OCT;9(5):651-658.

(3) Gudjonsson JE, Johnston A, Dyson M, Valdimarsson H, Elder JT. Mouse models of psoriasis. J Invest Dermatol 2007 JUN;127(6):1292-1308.

(4) Uitto J, Olsen D, Fazio M. Extracellular-Matrix of the Skin - 50 Years of Progress. J Invest Dermatol 1989 APR;92(4):S61-S77.

(5) Frantz C, Stewart KM, Weaver VM. The extracellular matrix at a glance. J Cell Sci 2010 DEC 15;123(24):4195-4200.

(6) Sakai L, Keene D, Engvall E. Fibrillin, a New 350-Kd Glycoprotein, is a Component of Extracellular Microfibrils. J Cell Biol 1986 DEC;103(6):2499-2509.

(7) Pankov R, Yamada K. Fibronectin at a glance. J Cell Sci 2002 OCT 15;115(20):3861-3863.

(8) Schaefer L, Schaefer RM. Proteoglycans: from structural compounds to signaling molecules. Cell Tissue Res 2010 JAN;339(1):237-246.

(9) Hildebrand A, Romaris M, Rasmussen L, Heinegard D, Twardzik D, Border W, et al. Interaction of the Small Interstitial Proteoglycans Biglycan, Decorin and Fibromodulin with Transforming Growth-Factor-Beta. Biochem J 1994 SEP 1;302:527-534.

(10) Lopezcasillas F, Cheifetz S, Doody J, Andres J, Lane W, Massague J. Structure and Expression of the Membrane Proteoglycan Betaglycan, a Component of the Tgf-Beta Receptor System. Cell 1991 NOV 15;67(4):785-795.

(11) Kolset SO, Tveit H. Serglycin - Structure and biology. Cell Mol Life Sci 2008 APR;65(7-8):1073-1085.

(12) Bernfield M, Gotte M, Park P, Reizes O, Fitzgerald M, Lincecum J, et al. Functions of cell surface heparan sulfate proteoglycans. Annu Rev Biochem 1999;68:729-777.

(13) Mott J, Werb Z. Regulation of matrix biology by matrix metalloproteinases. Curr Opin Cell Biol 2004 OCT;16(5):558-564.

(14) Schultz GS, Davidson JM, Kirsner RS, Bornstein P, Herman IM. Dynamic reciprocity in the wound microenvironment. Wound Repair Regen 2011 MAR-APR;19(2):134-148.

(15) Schultz GS, Wysocki A. Interactions between extracellular matrix and growth factors in wound healing. Wound Repair Regen 2009 MAR-APR;17(2):153-162.

(16) Visse R, Nagase H. Matrix metalloproteinases and tissue inhibitors of metalloproteinases - Structure, function, and biochemistry. Circ Res 2003 MAY 2;92(8):827-839.

(17) Baker A, Edwards D, Murphy G. Metalloproteinase inhibitors: biological actions and therapeutic opportunities. J Cell Sci 2002 OCT 1;115(19):3719-3727.

(18) Yannas I. Similarities and differences between induced organ regeneration in adults and early foetal regeneration. J R Soc Interface 2005 DEC 22;2(5):403-417.

(19) Laurens N, Koolwijk P, De Maat M. Fibrin structure and wound healing. J Thromb Haemost 2006 MAY;4(5):932-939.

(20) Schultz G, Rotatori D, Clark W. Egf and Tgf-Alpha in Wound-Healing and Repair. J Cell Biochem 1991 APR;45(4):346-352.

(21) Pierce G, Mustoe T, Altrock B, Deuel T, Thomason A. Role of Platelet-Derived Growth-Factor in Wound-Healing. J Cell Biochem 1991 APR;45(4):319-326.

(22) Eming SA, Krieg T, Davidson JM. Inflammation in wound repair: Molecular and cellular mechanisms. J Invest Dermatol 2007 MAR;127(3):514-525.

(23) Rodero MP, Khosrotehrani K. Skin wound healing modulation by macrophages. Int J Clin Exp Pathol 2010;3(7):643-653.

(24) Artuc M, Hermes B, Steckelings U, Grutzkau A, Henz B. Mast cells and their mediators in cutaneous wound healing active participants or innocent bystanders? Exp Dermatol 1999 FEB;8(1):1-16.

(25) McAnulty RJ. Fibroblasts and myofibroblasts: Their source, function and role in disease. Int J Biochem Cell Biol 2007;39(4):666-671.

(26) Haase I, Evans R, Pofahl R, Watt F. Regulation of keratinocyte shape, migration and wound epithelialization by IGF-1- and EGF-dependent signalling pathways. J Cell Sci 2003 AUG 1;116(15):3227-3238.

(27) Shibata S, Tada Y, Asano Y, Hau CS, Kato T, Saeki H, et al. Adiponectin Regulates Cutaneous Wound Healing by Promoting Keratinocyte Proliferation and Migration via the ERK Signaling Pathway. J Immunol 2012 SEP 15;189(6):3231-3241.

(28) Desmouliere A, Geinoz A, Gabbiani F, Gabbiani G. Transforming Growth-Factor-Beta-1 Induces Alpha-Smooth Muscle Actin Expression in Granulation-Tissue Myofibroblasts and in Quiescent and Growing Cultured Fibroblasts. J Cell Biol 1993 JUL;122(1):103-111.

(29) Hinz B. Formation and function of the myofibroblast during tissue repair. J Invest Dermatol 2007 MAR;127(3):526-537.

(30) Desmouliere A, Chaponnier C, Gabbiani G. Tissue repair, contraction, and the myofibroblast. Wound Repair Regen 2005 JAN-FEB;13(1):7-12.

(31) Desmouliere A, Redard M, Darby I, Gabbiani G. Apoptosis Mediates the Decrease in Cellularity during the Transition between Granulation-Tissue and Scar. Am J Pathol 1995 JAN;146(1):56-66.

(32) Clark R. Cutaneous Tissue-Repair - Basic Biologic Considerations .1. J Am Acad Dermatol 1985;13(5):701-725.

(33) Mustoe T, O'Shaughnessy K, Kloeters O. Chronic wound pathogenesis and current treatment strategies: A unifying hypothesis. Plast Reconstr Surg 2006 JUN;117(7):35S-41S.

(34) To WS, Midwood KS. Plasma and cellular fibronectin: distinct and independent functions during tissue repair. Fibrogenesis Tissue Repair 2011 Sep 16;4:21-1536-4-21.

(35) Grinnell F. Fibronectin and wound healing. J Cell Biochem 1984;26(2):107-116.

(36) Serini G, Bochaton-Piallat M, Ropraz P, Geinoz A, Borsi L, Zardi L, et al. The fibronectin domain ED-A is crucial for myofibroblastic phenotype induction by transforming growth factor-beta 1. J Cell Biol 1998 AUG 10;142(3):873-881.

(37) Moor AN, Vachon DJ, Gould LJ. Proteolytic activity in wound fluids and tissues derived from chronic venous leg ulcers. Wound Repair Regen 2009 NOV-DEC;17(6):832-839.

(38) Trengove N, Stacey M, Macauley S, Bennett N, Gibson J, Burslem F, et al. Analysis of the acute and chronic wound environments: the role of proteases and their inhibitors. Wound Repair Regen 1999 NOV-DEC;7(6):442-452.

(39) Wysocki A, Staianocoico L, Grinnell F. Wound Fluid from Chronic Leg Ulcers Contains Elevated Levels of Metalloproteinases Mmp-2 and Mmp-9. J Invest Dermatol 1993 JUL;101(1):64-68.

(40) Muller M, Trocme C, Lardy B, Morel F, Halimi S, Benhamou PY. Matrix metalloproteinases and diabetic foot ulcers: the ratio of MMP-1 to TIMP-1 is a predictor of wound healing. Diabetic Med 2008 APR;25(4):419-426.

(41) Ladwig G, Robson M, Liu R, Kuhn M, Muir D, Schultz G. Ratios of activated matrix metalloproteinase-9 to tissue inhibitor of matrix metalloproteinase-1 in wound fluids are inversely correlated with healing of pressure ulcers. Wound Repair Regen 2002 JAN-FEB;10(1):26-37.

(42) Palolahti M, Lauharanta J, Stephens RW, Kuusela P, Vaheri A. Proteolytic activity in leg ulcer exudate. Exp Dermatol 1993 Feb;2(1):29-37.

(43) Cullen B, Smith R, McCulloch E, Silcock D, Morrison L. Mechanism of action of PROMOGRAN, a protease modulating matrix, for the treatment of diabetic foot ulcers. Wound Repair Regen 2002 JAN-FEB;10(1):16-25.

(44) Grinnell F, Zhu M. Fibronectin degradation in chronic wounds depends on the relative levels of elastase, alpha 1-proteinase inhibitor, and alpha 2-macroglobulin. J Invest Dermatol 1996 FEB;106(2):335-341.

(45) Schmidtchen A. Degradation of antiproteinases, complement and fibronectin in chronic leg ulcers. Acta Derm Venereol 2000 MAY;80(3):179-184.

(46) Gohel MS, Windhaber RAJ, Tarlton JF, Whyman MR, Poskitt KR. The relationship between cytokine concentrations and wound healing in chronic venous ulceration. J Vasc Surg 2008 NOV;48(5):1272-1277.

(47) Barone E, Yager D, Pozez A, Olutoye O, Crossland M, Diegelmann R, et al. Interleukin-1 alpha and collagenase activity are elevated in chronic wounds. Plast Reconstr Surg 1998 SEP;102(4):1023-1027.

(48) Trengove N, Bielefeldt-Ohmann H, Stacey M. Mitogenic activity and cytokine levels in non-healing and healing chronic leg ulcers. Wound Repair Regen 2000 JAN-FEB;8(1):13-25.

(49) James T, Hughes M, Cherry G, Taylor R. Evidence of oxidative stress in chronic venous ulcers. Wound Repair Regen 2003 MAY-JUN;11(3):172-176.

(50) Wlaschek M, Scharffetter-Kochanek K. Oxidative stress in chronic venous leg ulcers. Wound Repair Regen 2005 SEP-OCT;13(5):452-461.

(51) Stanley A, Park H, Phillips T, Russakovsky V, Menzoian J. Reduced growth of dermal fibroblasts from chronic venous ulcers can be stimulated with growth factors. J Vasc Surg 1997 DEC;26(6):994-999.

(52) Raffetto J, Mendez M, Phillips T, Park H, Menzoian J. The effect of passage number on fibroblast cellular senescence in patients with chronic venous insufficiency with and without ulcer. Am J Surg 1999 AUG;178(2):107-112.

(53) Agren M, Steenfos H, Dabelsteen S, Hansen J, Dabelsteen E. Proliferation and mitogenic response to PDGF-BB of fibroblasts isolated from chronic venous leg ulcers is ulcer-age dependent. J Invest Dermatol 1999 APR;112(4):463-469.

(54) Vande Berg J, Rose M, Haywood-Reid P, Rudolph R, Payne W, Robson M. Cultured pressure ulcer fibroblasts show replicative senescence with elevated production of plasmin,

plasminogen activator inhibitor-1, and transforming growth factor-beta 1. Wound Repair Regen 2005 JAN-FEB;13(1):76-83.

(55) Lerman O, Galiano R, Armour M, Levine J, Gurtner G. Cellular dysfunction in the diabetic fibroblast - Impairment in migration, vascular endothelial growth factor production, and response to hypoxia. Am J Pathol 2003 JAN;162(1):303-312.

(56) Galkowska H, Olszewski W, Wojewodzka U. Keratinocyte and dermal vascular endothelial cell capacities remain unimpaired in the margin of chronic venous ulcer. Arch Dermatol Res 2005 JAN;296(7):286-295.

(57) Andriessen M, VanBergen B, Spruijt K, Go I, Schalkwijk J, VandeKerkhof P. Epidermal proliferation is not impaired in chronic venous ulcers. Acta Derm Venereol 1995 NOV;75(6):459-462.

(58) Galkowska H, Olszewski W, Wojewodzka U, Mijal J, Filipiuk E. Expression of apoptosis- and cell cycle-related proteins in epidermis of venous leg and diabetic foot ulcers. Surgery 2003 AUG;134(2):213-220.

(59) Usui ML, Mansbridge JN, Carter WG, Fujita M, Olerud JE. Keratinocyte migration, proliferation, and differentiation in chronic ulcers from patients with diabetes and normal wounds. J Histochem Cytochem 2008 JUL;56(7):687-696.

(60) Hinz B, Phan SH, Thannickal VJ, Prunotto M, Desmouliere A, Varga J, et al. Recent Developments in Myofibroblast Biology Paradigms for Connective Tissue Remodeling. Am J Pathol 2012 APR;180(4):1340-1355.

(61) Ishihara H, Yoshimoto H, Fujioka M, Murakami R, Hirano A, Fujii T, et al. Keloid fibroblasts resist ceramide-induced apoptosis by overexpression of insulin-like growth factor I receptor. J Invest Dermatol 2000 DEC;115(6):1065-1071.

(62) Jelaska A, Korn J. Role of apoptosis and transforming growth factor beta 1 in fibroblast selection and activation in systemic sclerosis. Arthritis Rheum 2000 OCT;43(10):2230-2239.

(63) Ramsey S, Sandhu N, Newton K, Reiber G, Blough D, Wagner E, et al. Incidence, outcomes, and cost of foot ulcers in patients with diabetes. Diabetes Care 1999 MAR;22(3):382-387.

(64) Singh N, Armstrong D, Lipsky B. Preventing foot ulcers in patients with diabetes. JAMA-J Am Med Assoc 2005 JAN 12;293(2):217-228.

(65) Bharara M, Schoess J, Armstrong DG. Coming events cast their shadows before: detecting inflammation in the acute diabetic foot and the foot in remission. Diabetes-Metab Res Rev 2012 FEB;28:15-20.

(66) Falanga V. Wound healing and its impairment in the diabetic foot. Lancet 2005 NOV 12;366(9498):1736-1743.

(67) Marston W, Hanft J, Norwood P, Pollak R, Dermagraft Diabet Foot Ulcer Study. The efficacy and safety of Dermagraft in improving the healing of chronic diabetic foot ulcers - Results of a prospective randomized trial. Diabetes Care 2003 JUN;26(6):1701-1705.

(68) Gentzkow G, Iwasaki S, Hershon K, Mengel M, Prendergast J, Ricotta J, et al. Use of dermagraft, a cultured human dermis, to treat diabetic root ulcers. Diabetes Care 1996 APR;19(4):350-354.

(69) Wieman T, Smiell J, Su Y. Efficacy and safety of a topical gel formulation of recombinant human platelet-derived growth factor-BB (becaplermin) in patients with chronic neuropathic diabetic ulcers - A phase III randomized placebo-controlled double-blind study. Diabetes Care 1998 MAY;21(5):822-827.

(70) Steed D, Webster M, Ricotta J, Luterman A, Brown S, Comerota A, et al. Clinical-Evaluation of Recombinant Human Platelet-Derived Growth-Factor for the Treatment of Lower-Extremity Diabetic Ulcers. J Vasc Surg 1995 JAN;21(1):71-81.

(71) Blume PA, Walters J, Payne W, Ayala J, Lantis J. Comparison of negative pressure wound therapy using vacuum-assisted closure with advanced moist wound therapy in the treatment of diabetic foot ulcers: A multicenter randomized controlled trial. Diabetes Care 2008 APR;31(4):631-636.

(72) Bus SA, Valk GD, van Deursen RW, Armstrong DG, Caravaggi C, Hlavacek P, et al. The effectiveness of footwear and offloading interventions to prevent and heal foot ulcers and reduce plantar pressure in diabetes: a systematic review. Diabetes-Metab Res Rev 2008 MAY-JUN;24:S162-S180.

(73) Wunderlich R, Peters E, Lavery L. Systemic hyperbaric oxygen therapy - Lower-extremity wound healing and the diabetic foot. Diabetes Care 2000 OCT;23(10):1551-1555.

(74) Pierce G, Tarpley J, Yanagihara D, Mustoe T, Fox G, Thomason A. Platelet-Derived Growth-Factor (Bb Homodimer), Transforming Growth Factor-Beta-1, and Basic Fibroblast Growth-Factor in Dermal Wound-Healing - Neovessel and Matrix Formation and Cessation of Repair. Am J Pathol 1992 JUN;140(6):1375-1388.

(75) Trapani JA. Granzymes: a family of lymphocyte granule serine proteases. Genome Biol 2001;2(12):3014.1.

(76) Smyth M, OConnor M, Trapani J. Granzymes: A variety of serine protease specificities encoded by genetically distinct subfamilies. J Leukoc Biol 1996 NOV;60(5):555-562.

(77) Ewen CL, Kane KP, Bleackley RC. A quarter century of granzymes. Cell Death Differ 2012 JAN;19(1):28-35.

(78) Simon M, Hoschutzky H, Fruth U, Simon H, Kramer M. Purification and Characterization of a T-Cell Specific Serine Proteinase (Tsp-1) from Cloned Cytolytic Lymphocytes-T. EMBO J 1986 DEC;5(12):3267-3274.

(79) Bleackley RC, Duggan B, Ehrman N, Lobe CG. Isolation of two cDNA sequences which encode cytotoxic cell proteases. FEBS Lett 1988 Jul 4;234(1):153-159.

(80) Masson D, Nabholz M, Estrade C, Tschopp J. Granules of cytolytic T-lymphocytes contain two serine esterases. EMBO J 1986 Jul;5(7):1595-1600.

(81) Young JD, Leong LG, Liu CC, Damiano A, Wall DA, Cohn ZA. Isolation and characterization of a serine esterase from cytolytic T cell granules. Cell 1986 Oct 24;47(2):183-194.

(82) Pasternack MS, Eisen HN. A novel serine esterase expressed by cytotoxic T lymphocytes. Nature 1985 Apr 25-May 1;314(6013):743-745.

(83) Brunet JF, Dosseto M, Denizot F, Mattei MG, Clark WR, Haqqi TM, et al. The inducible cytotoxic T-lymphocyte-associated gene transcript CTLA-1 sequence and gene localization to mouse chromosome 14. Nature 1986 Jul 17-23;322(6076):268-271.

(84) Barry M, Bleackley R. Cytotoxic T lymphocytes: All roads lead to death. Nat Rev Immunol 2002 JUN;2(6):401-409.

(85) Smyth M, Trapani J. Granzymes - Exogenous Proteinases that Induce Target-Cell Apoptosis. Immunol Today 1995 APR;16(4):202-206.

(86) Susanto O, Trapani JA, Brasacchio D. Controversies in granzyme biology. Tissue Antigens 2012 DEC;80(6):477-487.

(87) Sower L, Klimpel G, Hanna W, Froelich C. Extracellular activities of human granzymes .1. Granzyme a induces IL6 and IL8 production in fibroblast and epithelial cell lines. Cell Immunol 1996 JUL 10;171(1):159-163.

(88) Metkar SS, Menaa C, Pardo J, Wang B, Wallich R, Freudenberg M, et al. Human and Mouse Granzyme A Induce a Proinflammatory Cytokine Response. Immunity 2008 NOV 14;29(5):720-733.

(89) Hendel A, Ang LS, Granville DJ. Inflammaging and Proteases in Abdominal Aortic Aneurysm. Curr Vasc Pharmacol 2012 Jun 22.

(90) Hiebert PR, Granville DJ. Granzyme B in injury, inflammation, and repair. Trends Mol Med 2012 DEC;18(12):732-741.

(91) Boivin WA, Cooper DM, Hiebert PR, Granville DJ. Intracellular versus extracellular granzyme B in immunity and disease: challenging the dogma. Lab Invest 2009 NOV;89(11):1195-1220.

(92) Hendel A, Hiebert PR, Boivin WA, Williams SJ, Granville DJ. Granzymes in age-related cardiovascular and pulmonary diseases. Cell Death Differ 2010 APR;17(4):596-606.

(93) Heusel J, Wesselschmidt R, Shresta S, Russell J, Ley T. Cytotoxic Lymphocytes Require Granzyme-B for the Rapid Induction of Dna Fragmentation and Apoptosis in Allogeneic Target-Cells. Cell 1994 MAR 25;76(6):977-987.

(94) Hatcher VB, Oberman MS, Lazarus GS, Grayzel AI. A cytotoxic proteinase isolated from human lymphocytes. J Immunol 1978 Feb;120(2):665-670.

(95) Klein J, Shows T, Dupont B, Trapani J. Genomic Organization and Chromosomal Assignment for a Serine Protease Gene (Cspb) Expressed by Human Cyto-Toxic Lymphocytes. Genomics 1989 JUL;5(1):110-117.

(96) Waugh S, Harris J, Fletterick R, Craik C. The structure of the pro-apoptotic protease granzyme B reveals the molecular determinants of its specificity. Nat Struct Biol 2000 SEP;7(9):762-765.

(97) Kim W, Kim H, Suk K, Lee W. Macrophages express granzyme B in the lesion areas of atherosclerosis and rheumatoid arthritis. Immunol Lett 2007 JUL 31;111(1):57-65.

(98) Baba T, Ishizu A, Iwasaki S, Suzuki A, Tomaru U, Ikeda H, et al. CD4(+)/CD8(+) macrophages infiltrating at inflammatory sites: a population of monocytes/macrophages with a cytotoxic phenotype. Blood 2006 MAR 1;107(5):2004-2012.

(99) Hagn M, Schwesinger E, Ebel V, Sontheimer K, Maier J, Beyer T, et al. Human B Cells Secrete Granzyme B When Recognizing Viral Antigens in the Context of the Acute Phase Cytokine IL-21. J Immunol 2009 AUG 1;183(3):1838-1845.

(100) Grossman W, Verbsky J, Tollefsen B, Kemper C, Atkinson J, Ley T. Differential expression of granzymes A and B in human cytotoxic lymphocyte subsets and T regulatory cells. Blood 2004 NOV 1;104(9):2840-2848.

(101) Rissoan MC, Duhen T, Bridon JM, Bendriss-Vermare N, Peronne C, de Saint Vis B, et al. Subtractive hybridization reveals the expression of immunoglobulin-like transcript 7, Eph-B1, granzyme B, and 3 novel transcripts in human plasmacytoid dendritic cells. Blood 2002 Nov 1;100(9):3295-3303.

(102) Pardo J, Wallich R, Ebnet K, Iden S, Zentgraf H, Martin P, et al. Granzyme B is expressed in mouse mast cells in vivo and in vitro and causes delayed cell death independent of perforin. Cell Death Differ 2007 OCT;14(10):1768-1779.

(103) Strik MCM, de Koning PJA, Kleijmeer MJ, Bladergroen BA, Wolbink AM, Griffith JM, et al. Human mast cells produce and release the cytotoxic lymphocyte associated protease granzyme B upon activation. Mol Immunol 2007 JUL;44(14):3462-3472.

(104) Wagner C, Iking-Konert C, Denefleh B, Stegmaier S, Hug F, Hansch G. Granzyme B and perforin: constitutive expression in human polymorphonuclear neutrophils. Blood 2004 FEB 1;103(3):1099-1104.

(105) Tschopp CM, Spiegl N, Didichenko S, Lutmann W, Julius P, Virchow JC, et al. Granzyme B, a novel mediator of allergic inflammation: its induction and release in blood basophils and human asthma. Blood 2006 OCT 1;108(7):2290-2299.

(106) Horiuchi K, Saito S, Sasaki R, Tomatsu T, Toyama Y. Expression of granzyme B in human articular chondrocytes. J Rheumatol 2003 AUG;30(8):1799-1810.

(107) Sasson R, Dantes A, Tajima K, Amsterdam A. Novel genes modulated by FSH in normal and immortalized FSH-responsive cells: new insights into the mechanism of FSH action. FASEB J 2003 JUL;17(10):1256-1266.

(108) Hernandez-Pigeon H, Jean C, Charruyer A, Haure M, Titeux M, Tonasso L, et al. Human keratinocytes acquire cellular cytotoxicity under UV-B irradiation - Implication of granzyme B and perforin. J Biol Chem 2006 MAY 12;281(19):13525-13532.

(109) Hirst C, Buzza M, Sutton V, Trapani J, Loveland K, Bird P. Perforin-independent expression of granzyme B and proteinase inhibitor 9 in human testis and placenta suggests a role for granzyme B-mediated proteolysis in reproduction. Mol Hum Reprod 2001 DEC;7(12):1133-1142.

(110) Choy J, McDonald P, Suarez A, Hung V, Wilson J, McManus B, et al. Granzyme B in atherosclerosis and transplant vascular disease: Association with cell death and atherosclerotic disease severity. Mod Pathol 2003 MAY;16(5):460-470.

(111) Vernooy JHJ, Moeller GM, van Suylen RJ, van Spijk MP, Cloots RHE, Hoet PH, et al. Increased granzyme A expression in type II pneumocytes of patients with severe chronic obstructive pulmonary disease. Am J Respir Crit Care Med 2007 MAR 1;175(5):464-472.

(112) Babichuk C, Duggan B, Bleackley R. In vivo regulation of murine granzyme B gene transcription in activated primary T cells. J Biol Chem 1996 JUL 12;271(28):16485-16493.

(113) Wargnier A, Lafaurie C, Legros-Maida S, Bourge J, Sigaux F, Sasportes M, et al. Down-regulation of human granzyme B expression by glucocorticoids - Dexamethasone inhibits

binding to the Ikaros and AP-1 regulatory elements of the granzyme B promoter. J Biol Chem 1998 DEC 25;273(52):35326-35331.

(114) Fregeau C, Bleackley R. Transcription of 2 Cytotoxic-Cell Protease Genes is Under the Control of Different Regulatory Elements. Nucleic Acids Res 1991 OCT 25;19(20):5583-5590.

(115) Haddad P, Wargnier A, Bourge J, Sasportes M, Paul P. A Promoter Element of the Human Serine Esterase Granzyme-B Gene Controls Specific Transcription in Activated T-Cells. Eur J Immunol 1993 MAR;23(3):625-629.

(116) Chowdhury D, Lieberman J. Death by a thousand cuts: Granzyme pathways of programmed cell death. Annu Rev Immunol 2008;26:389-420.

(117) Russell J, Ley T. Lymphocyte-mediated cytotoxicity. Annu Rev Immunol 2002;20:323-370.

(118) Griffiths G, Isaaz S. Granzymes-a and Granzymes-B are Targeted to the Lytic Granules of Lymphocytes by the Mannose-6-Phosphate Receptor. J Cell Biol 1993 FEB;120(4):885-896.

(119) Smyth M, McGuire M, Thia K. Expression of Recombinant Human Granzyme-B - a Processing and Activation Role for Dipeptidyl Peptidase-i. J Immunol 1995 JUN 15;154(12):6299-6305.

(120) Grujic M, Braga T, Lukinius A, Eloranta M, Knight S, Pejler G, et al. Serglycin-deficient cytotoxic T lymphocytes display defective secretory granule maturation and granzyme B storage. J Biol Chem 2005 SEP 30;280(39):33411-33418.

(121) Grakoui A, Bromley S, Sumen C, Davis M, Shaw A, Allen P, et al. The immunological synapse: A molecular machine controlling T cell activation. Science 1999 JUL 9;285(5425):221-227.

(122) Froelich C, Orth K, Turbov J, Seth P, Gottlieb R, Babior B, et al. New paradigm for lymphocyte granule-mediated cytotoxicity - Target cells bind and internalize granzyme B, but an endosomolytic agent is necessary for cytosolic delivery and subsequent apoptosis. J Biol Chem 1996 NOV 15;271(46):29073-29079.

(123) Shi L, Mai S, Israels S, Browne K, Trapani J, Greenberg A. Granzyme B (GraB) autonomously crosses the cell membrane and perforin initiates apoptosis and GraB nuclear localization. J Exp Med 1997 MAR 3;185(5):855-866.

(124) Sauer H, Pratsch L, Tschopp J, Bhakdi S, Peters R. Functional Size of Complement and Perforin Pores Compared by Confocal Laser Scanning Microscopy and Fluorescence Microphotolysis. Biochim Biophys Acta 1991 MAR 18;1063(1):137-146.

(125) Adrain C, Murphy B, Martin S. Molecular ordering of the caspase activation cascade initiated by the cytotoxic T lymphocyte/natural killer (CTL/NK) protease granzyme B. J Biol Chem 2005 FEB 11;280(6):4663-4673.

(126) Sutton V, Davis J, Cancilla M, Johnstone R, Ruefli A, Sedelies K, et al. Initiation of apoptosis by granzyme B requires direct cleavage of Bid, but not direct granzyme B-mediated caspase activation. J Exp Med 2000 NOV 20;192(10):1403-1413.

(127) Heibein J, Goping I, Barry M, Pinkoski M, Shore G, Green D, et al. Granzyme B-mediated cytochrome c release is regulated by the Bcl-2 family members Bid and Bax. J Exp Med 2000 NOV 20;192(10):1391-1401.

(128) Pinkoski M, Waterhouse N, Heibein J, Wolf B, Kuwana T, Goldstein J, et al. Granzyme B-mediated apoptosis proceeds predominantly through a Bcl-2-inhibitable mitochondrial pathway. J Biol Chem 2001 APR 13;276(15):12060-12067.

(129) Han J, Goldstein L, Gastman B, Froelich C, Yin X, Rabinowich H. Degradation of Mcl-1 by granzyme B - Implications for Bim-mediated mitochondrial apoptotic events. J Biol Chem 2004 MAY 21;279(21):22020-22029.

(130) Jiang X, Wang X. Cytochrome c promotes caspase-9 activation by inducing nucleotide binding to Apaf-1. J Biol Chem 2000 OCT 6;275(40):31199-31203.

(131) Li P, Nijhawan D, Budihardjo I, Srinivasula S, Ahmad M, Alnemri E, et al. Cytochrome c and dATP-dependent formation of Apaf-1/caspase-9 complex initiates an apoptotic protease cascade. Cell 1997 NOV 14;91(4):479-489.

(132) Cullen SP, Martin SJ. Mechanisms of granule-dependent killing. Cell Death Differ 2008 FEB;15(2):251-262.

(133) Masson D, Tschopp J. A Family of Serine Esterases in Lytic Granules of Cytolytic Lymphocytes-T. Cell 1987 JUN 5;49(5):679-685.

(134) Afonina IS, Cullen SP, Martin SJ. Cytotoxic and non-cytotoxic roles of the CTL/NK protease granzyme B. Immunol Rev 2010 MAY;235:105-116.

(135) Kurschus F, Kleinschmidt M, Fellows E, Dornmair K, Rudolph R, Lilie H, et al. Killing of target cells by redirected granzyme B in the absence of perforin. FEBS Lett 2004 MAR 26;562(1-3):87-92.

(136) Kramer M, Simon M. Are Proteinases Functional Molecules of Lymphocytes-T. Immunol Today 1987 MAY;8(5):140-142.

(137) Isaaz S, Baetz K, Olsen K, Podack E, Griffiths G. Serial Killing by Cytotoxic T-Lymphocytes - T-Cell Receptor Triggers Degranulation, Re-Filling of the Lytic Granules and

Secretion of Lytic Proteins Via a Non-Granule Pathway. Eur J Immunol 1995 APR;25(4):1071-1079.

(138) Prakash MD, Bird CH, Bird PI. Active and zymogen forms of granzyme B are constitutively released from cytotoxic lymphocytes in the absence of target cell engagement. Immunol Cell Biol 2009 MAR-APR;87(3):249-254.

(139) Hiebert PR, Boivin WA, Abraham T, Pazooki S, Zhao H, Granville DJ. Granzyme B contributes to extracellular matrix remodeling and skin aging in apolipoprotein E knockout mice. Exp Gerontol 2011 JUN;46(6):489-499.

(140) Hiebert PR, Boivin WA, Zhao H, McManus BM, Granville DJ. Perforin and Granzyme B Have Separate and Distinct Roles during Atherosclerotic Plaque Development in Apolipoprotein E Knockout Mice. PLoS One 2013 OCT 24;8(10):e78939.

(141) Chamberlain CM, Ang LS, Boivin WA, Cooper DM, Williams SJ, Zhao H, et al. Perforin-Independent Extracellular Granzyme B Activity Contributes to Abdominal Aortic Aneurysm. Am J Pathol 2010 FEB;176(2):1038-1049.

(142) Spaeny-Dekking E, Hanna W, Wolbink A, Wever P, Kummer A, Swaak A, et al. Extracellular granzymes A and B in humans: Detection of native species during CTL responses in vitro and in vivo. J Immunol 1998 APR 1;160(7):3610-3616.

(143) Buzza MS, Bird PI. Extracellular granzymes: current perspectives. Biol Chem 2006 JUL;387(7):827-837.

(144) Young L, Joag S, Lin P, Luo S, Zheng L, Liu C, et al. Expression of Cytolytic Mediators by Synovial-Fluid Lymphocytes in Rheumatoid-Arthritis. Am J Pathol 1992 MAY;140(5):1261-1268.

(145) Tak P, Spaeny-Dekking L, Kraan M, Breedveld F, Froelich C, Hack C. The levels of soluble granzyme A and B are elevated in plasma and synovial fluid of patients with rheumatoid arthritis (RA). Clin Exp Immunol 1999 MAY;116(2):366-370.

(146) Kim JY, Shin E, Kim H, Park K. Expression of Epstein-Barr Virus and Granzyme B in Cytologic Smears of Histiocytic Necrotizing Lymphadenitis. Diagn Cytopathol 2012 SEP;40(9):792-797.

(147) Malmestrom C, Lycke J, Haghighi S, Andersen O, Carlsson L, Wadenvik H, et al. Relapses in multiple sclerosis are associated with increased CD8(+) T-cell mediated cytotoxicity in CSF. J Neuroimmunol 2008 MAY 30;196(1-2):159-165.

(148) Schneider R, Mohebiany AN, Ifergan I, Beauseigle D, Duquette P, Prat A, et al. B Cell-Derived IL-15 Enhances CD8 T Cell Cytotoxicity and Is Increased in Multiple Sclerosis Patients. J Immunol 2011 OCT 15;187(8):4119-4128.

(149) Omoto Y, Yamanaka K, Tokime K, Kitano S, Kakeda M, Akeda T, et al. Granzyme B is a novel interleukin-18 converting enzyme. J Dermatol Sci 2010 AUG;59(2):129-135.

(150) Takahashi Y, Mine J, Kubota Y, Yamazaki E, Fujiwara T. A substantial number of Rasmussen syndrome patients have increased IgG, CD4(+) T cells, TNF alpha, and Granzyme B in CSF. Epilepsia 2009 JUN;50(6):1419-1431.

(151) Bratke K, Bottcher B, Leeder K, Schmidt S, Kupper M, Virchow J, et al. Increase in granzyme B+ lymphocytes and soluble granzyme B in bronchoalveolar lavage of allergen challenged patients with atopic asthma. Clin Exp Immunol 2004 JUN;136(3):542-548.

(152) Silverman G, Bird P, Carrell R, Church F, Coughlin P, Gettins P, et al. The serpins are an expanding superfamily of structurally similar but functionally diverse proteins - Evolution, mechanism of inhibition, novel functions, and a revised nomenclature. J Biol Chem 2001 SEP 7;276(36):33293-33296.

(153) Forsyth S, Horvath A, Coughlin P. A review and comparison of the murine alpha(1)-antitrypsin and alpha(1)-antichymotrypsin multigene clusters with the human clade A serpins. Genomics 2003 MAR;81(3):336-345.

(154) Horvath A, Irving J, Rossjohn J, Law R, Bottomley S, Quinsey N, et al. The murine orthologue of human antichymotrypsin - A structural paradigm for CLADE A3 serpins. J Biol Chem 2005 DEC 30;280(52):43168-43178.

(155) Kaiserman D, Bird PI. Control of granzymes by serpins. Cell Death Differ 2010 APR;17(4):586-595.

(156) Sun J, Bird C, Sutton V, McDonald L, Coughlin P, DeJong T, et al. A cytosolic granzyme B inhibitor related to the viral apoptotic regulator cytokine response modifier a is present in cytotoxic lymphocytes. J Biol Chem 1996 NOV 1;271(44):27802-27809.

(157) Hirst C, Buzza M, Bird C, Warren H, Cameron P, Zhang M, et al. The intracellular granzyme B inhibitor, proteinase inhibitor 9, is up-regulated during accessory cell maturation and effector cell degranulation, and its overexpression enhances CTL potency. J Immunol 2003 JAN 15;170(2):805-815.

(158) Buzza M, Hirst C, Bird C, Hosking P, McKendrick J, Bird P. The granzyme B inhibitor, PI-9, is present in endothelial and mesothelial cells, suggesting that it protects bystander cells during immune responses. Cell Immunol 2001 MAY 25;210(1):21-29.

(159) Young J, Sukhova G, Foster D, Kisiel W, Libby P, Schonbeck U. The serpin proteinase inhibitor 9 is an endogenous inhibitor of interleukin 1 beta-converting enzyme (caspase-1) activity in human vascular smooth muscle cells. J Exp Med 2000 MAY 1;191(9):1535-1544.

(160) Rowshani A, Strik M, Molenaar R, Yong S, Wolbink A, Bemelman F, et al. The granzyme B inhibitor SERPINB9 (protease inhibitor 9) circulates in blood and increases on primary cytomegalovirus infection after renal transplantation. J Infect Dis 2005 DEC 1;192(11):1908-1911.

(161) Ang LS, Boivin WA, Williams SJ, Zhao H, Abraham T, Carmine-Simmen K, et al. Serpina3n attenuates granzyme B-mediated decorin cleavage and rupture in a murine model of aortic aneurysm. Cell Death Dis 2011 SEP;2:e209.

(162) Sipione S, Simmen KC, Lord SJ, Motyka B, Ewen C, Shostak I, et al. Identification of a novel human granzyme B inhibitor secreted by cultured Sertoli cells. J Immunol 2006 OCT 15;177(8):5051-5058.

(163) Mulligan-Kehoe MJ, Drinane MC, Mollmark J, Casciola-Rosen L, Hummers LK, Hall A, et al. Antiangiogenic plasma activity in patients with systemic sclerosis. Arthritis Rheum 2007 OCT;56(10):3448-3458.

(164) Buzza MS, Dyson JM, Choi H, Gardiner EE, Andrews RK, Kaiserman D, et al. Antihemostatic activity of human granzyme B mediated by cleavage of von Willebrand factor. J Biol Chem 2008 AUG 15;283(33):22498-22504.

(165) Savage B, Saldivar E, Ruggeri Z. Initiation of platelet adhesion by arrest onto fibrinogen or translocation on von Willebrand factor. Cell 1996 JAN 26;84(2):289-297.

(166) Castellino F, Ploplis V. Structure and function of the plasminogen/plasmin system. Thromb Haemost 2005 APR;93(4):647-654.

(167) Hanford H, Wong C, Kassan H, Cundiff D, Chandel N, Underwood S, et al. Angiostatin(4.5)-mediated apoptosis of vascular endothelial cells. Cancer Res 2003 JUL 15;63(14):4275-4280.

(168) Reading PC, Whitney PG, Barr DP, Wojtasiak M, Mintern JD, Waithman J, et al. IL-18, but not IL-12, regulates NK cell activity following intranasal herpes simplex virus type 1 infection. J Immunol 2007 Sep 1;179(5):3214-3221.

(169) Shao X, Feng L, Gu L, Wu L, Feng T, Yang Y, et al. Expression of interleukin-18, IL-18BP, and IL-18R in serum, synovial fluid, and synovial tissue in patients with rheumatoid arthritis. Clin Exper Med 2009 SEP;9(3):215-221.

(170) Afonina IS, Tynan GA, Logue SE, Cullen SP, Bots M, Luethi AU, et al. Granzyme B-Dependent Proteolysis Acts as a Switch to Enhance the Proinflammatory Activity of IL-1 alpha. Mol Cell 2011 OCT 21;44(2):265-278.

(171) Buzza M, Zamurs L, Sun J, Bird C, Smith A, Trapani J, et al. Extracellular matrix remodeling by human granzyme B via cleavage of vitronectin, fibronectin, and laminin. J Biol Chem 2005 JUN 24;280(25):23549-23558.

(172) Hendel A, Granville DJ. Granzyme B cleavage of fibronectin disrupts endothelial cell adhesion, migration and capillary tube formation. Matrix Biol 2013 JAN;32(1):14-22.

(173) Hiebert PR, Wu D, Granville DJ. Granzyme B degrades extracellular matrix and contributes to delayed wound closure in apolipoprotein E knockout mice. Cell Death Differ 2013 OCT;20(10):1404-1414.

(174) Choy J, Hung V, Hunter A, Cheung P, Motyka B, Goping I, et al. Granzyme B induces smooth muscle cell apoptosis in the absence of perforin - Involvement of extracellular matrix degradation. Arterioscler Thromb Vasc Biol 2004 DEC;24(12):2245-2250.

(175) Hendel A, Hsu I, Granville DJ. Granzyme B releases vascular endothelial growth factor from extracellular matrix and induces vascular permeability. Lab Invest 2014 May 5.

(176) Boivin WA, Shackleford M, Vanden Hoek A, Zhao H, Hackett TL, Knight DA, et al. Granzyme B Cleaves Decorin, Biglycan and Soluble Betaglycan, Releasing Active Transforming Growth Factor-beta 1. PLoS One 2012 MAR 30;7(3):e33163.

(177) Reed C, Iozzo R. The role of decorin in collagen fibrillogenesis and skin homeostasis. Glycoconj J 2002 MAY-JUN;19(4-5):249-255.

(178) Gahring L, Carlson N, Meyer E, Rogers S. Cutting edge: Granzyme B proteolysis of a neuronal glutamate receptor generates an autoantigen and is modulated by glycosylation. J Immunol 2001 FEB 1;166(3):1433-1438.

(179) Loeb CRK, Harris JL, Craik CS. Granzyme B proteolyzes receptors important to proliferation and survival, tipping the balance toward apoptosis. J Biol Chem 2006 SEP 22;281(38):28326-28335.

(180) Casciola-Rosen L, Miagkov A, Nagaraju K, Askin F, Jacobson L, Rosen A, et al. Granzyme B: Evidence for a role in the origin of myasthenia gravis. J Neuroimmunol 2008 SEP 15;201:33-40.

(181) Sen CK, Gordillo GM, Roy S, Kirsner R, Lambert L, Hunt TK, et al. Human skin wounds: A major and snowballing threat to public health and the economy. Wound Repair Regen 2009 NOV-DEC;17(6):763-771.

(182) Peplow PV, Chung T, Ryan B, Baxter GD. Laser Photobiostimulation of Wound Healing: Reciprocity of Irradiance and Exposure Time on Energy Density for Splinted Wounds in Diabetic Mice. Lasers Surg Med 2011 SEP;43(8):843-850.

(183) Obara K, Ishihara M, Ishizuka T, Fujita M, Ozeki Y, Maehara T, et al. Photocrosslinkable chitosan hydrogel containing fibroblast growth factor-2 stimulates wound healing in healing-impaired db/db mice. Biomaterials 2003 SEP;24(20):3437-3444.

(184) Altavilla D, Saitta A, Cucinotta D, Galeano M, Deodato B, Colonna M, et al. Inhibition of lipid peroxidation restores impaired vascular endothelial growth factor expression and stimulates wound healing and angiogenesis in the genetically diabetic mouse. Diabetes 2001 MAR;50(3):667-674.

(185) Galiano R, Tepper O, Pelo C, Bhatt K, Callaghan M, Bastidas N, et al. Topical vascular endothelial growth factor accelerates diabetic wound healing through increased angiogenesis and by mobilizing and recruiting bone marrow-derived cells. Am J Pathol 2004 JUN;164(6):1935-1947.

(186) Michaels J, Churgin SS, Blechman KM, Greives MR, Aarabi S, Galiano RD, et al. Db/db Mice Exhibit Severe Wound-Healing Impairments Compared with Other Murine Diabetic Strains in a Silicone-Splinted Excisional Wound Model. Wound Repair Regen 2007 SEP-OCT;15(5):665-670.

(187) Galiano R, Michaels J, Dobryansky M, Levine J, Gurtner G. Quantitative and reproducible murine model of excisional wound healing. Wound Repair Regen 2004 JUL-AUG;12(4):485-492.

(188) Stanley CM, Wang Y, Pal S, Klebe RJ, Harkless LB, Xu X, et al. Fibronectin fragmentation is a feature of periodontal disease sites and diabetic foot and leg wounds and modifies cell behavior. J Periodontol 2008 MAY;79(5):861-875.

(189) Rao CN, Ladin DA, Liu YY, Chilukuri K, Hou ZZ, Woodley DT. Alpha 1-antitrypsin is degraded and non-functional in chronic wounds but intact and functional in acute wounds: the inhibitor protects fibronectin from degradation by chronic wound fluid enzymes. J Invest Dermatol 1995 Oct;105(4):572-578.

(190) Grinnell F, Ho C, Wysocki A. Degradation of Fibronectin and Vitronectin in Chronic Wound Fluid - Analysis by Cell Blotting, Immunoblotting, and Cell-Adhesion Assays. J Invest Dermatol 1992 APR;98(4):410-416.

(191) Wysocki A, Grinnell F. Fibronectin Profiles in Normal and Chronic Wound Fluid. Lab Invest 1990 DEC;63(6):825-831.

(192) Gailit J, Clark R. Studies in vitro on the role of alpha v and beta 1 integrins in the adhesion of human dermal fibroblasts to provisional matrix proteins fibronectin, vibronectin, and fibrinogen. J Invest Dermatol 1996 JAN;106(1):102-108.

(193) Hanks S, Calalb M, Harper M, Patel S. Focal Adhesion Protein-Tyrosine Kinase Phosphorylated in Response to Cell Attachment to Fibronectin. Proc Natl Acad Sci U S A 1992 SEP 15;89(18):8487-8491.

(194) Chen Q, Kinch M, Lin T, Burridge K, Juliano R. Integrin-Mediated Cell-Adhesion Activates Mitogen-Activated Protein-Kinases. J Biol Chem 1994 OCT 28;269(43):26602-26605.

(195) Darby I, Skalli O, Gabbiani G. Alpha-Smooth Muscle Actin is Transiently Expressed by Myofibroblasts during Experimental Wound-Healing. Lab Invest 1990 JUL;63(1):21-29.

(196) Eckes B, Colucci-Guyon E, Smola H, Nodder S, Babinet C, Krieg T, et al. Impaired wound healing in embryonic and adult mice lacking vimentin. J Cell Sci 2000 JUL;113(13):2455-2462.

(197) Dayan D, Hiss Y, Hirshberg A, Bubis JJ, Wolman M. Are the polarization colors of picrosirius red-stained collagen determined only by the diameter of the fibers? Histochemistry 1989;93(1):27-29.

(198) Frank S, Stallmeyer B, Kampfer H, Kolb N, Pfeilschifter J. Leptin enhances wound re-epithelialization and constitutes a direct function of leptin in skin repair. J Clin Invest 2000 AUG;106(4):501-509.

(199) Ring B, Scully S, Davis C, Baker M, Cullen M, Pelleymounter M, et al. Systemically and topically administered leptin both accelerate wound healing in diabetic ob/ob mice. Endocrinology 2000 JAN;141(1):446-449.

(200) Leiter EH, Strobel M, O'Neill A, Schultz D, Schile A, Reifsnyder PC. Comparison of Two New Mouse Models of Polygenic Type 2 Diabetes at the Jackson Laboratory, NONcNZO10Lt/J and TALLYHO/JngJ. J Diabetes Res 2013.

(201) Buck,Donald W.,,II, Jin DP, Geringer M, Hong SJ, Galiano RD, Mustoe TA. The TallyHo Polygenic Mouse Model of Diabetes: Implications in Wound Healing. Plast Reconstr Surg 2011 NOV;128(5):427E-437E.

(202) Fang RC, Kryger ZB, Buck,Donald W.,,II, De La Garza M, Galiano RD, Mustoe TA. Limitations of the db/db mouse in translational wound healing research: Is the NONcNZO10 polygenic mouse model superior? Wound Repair Regen 2010 NOV-DEC;18(6):605-613.

(203) Goren I, Muller E, Pfeilschifter J, Frank S. Severely impaired insulin signaling in chronic wounds of diabetic ob/ob mice - A potential role of tumor necrosis factor-alpha. Am J Pathol 2006 MAR;168(3):765-777.

(204) Siqueira MF, Li J, Chehab L, Desta T, Chino T, Krothpali N, et al. Impaired wound healing in mouse models of diabetes is mediated by TNF-alpha dysregulation and associated with enhanced activation of forkhead box O1 (FOXO1). Diabetologia 2010 FEB;53(2):378-388.

(205) Greenhalgh D. The role of apoptosis in wound healing. Int J Biochem Cell Biol 1998 SEP;30(9):1019-1030.